On Evil Twins and Their Absent Friends

Müller, Carola

2015

On Evil Twins and Their Absent Friends

Ternary Intermetallic Ni_2In Type Superstructures

Carola Jutta Müller

Doctoral Thesis

2015

LUND UNIVERSITY

Polymer & Materials Chemistry
Centre for Analysis and Synthesis
Sweden

Centre for Analysis and Synthesis
Lunds Tekniska Högskola
Lund University
SE-22100 Lund, Sweden

ISBN 978-91-7422-400-9

Printed in Sweden by Mediatryck, Lund 2015

Für Pete und Jakse
und uns, die wir überlebt haben
So jung kommen wir nicht mehr zusammen

Abstract

Knowledge on intermetallic compounds and alloys is essential for technology leaps. The latest of these, the so-called digital revolution, started the period of the information age which is characterized by fast information transfer. The constant development of faster and smaller electronic devices comes with the drawback of increased amounts of waste, meaning products that used to by high-end technology. Unsurprisingly, not all parts of an electronic device are recyclable, and some of the intermetallic compounds and alloys are in fact hazardous to the environment. For this reason, bans and restrictions on hazardous materials in electronic devices have been put into legislation in some countries over the past ten years, also in the European Union.
The direct consequence of these regulations is that the substitution of the affected metals with others created new interdisciplinary research fields as traditional materials like lead-containing solders are not allowed any longer. The here presented work is not directed towards finding new solder or semiconductor materials. The idea behind is to find and characterize ternary intermetallic compounds that are formed when metal-metal contacts are present in electronic devices. Besides chemical characterization techniques, crystallographic methods such as X-ray diffraction are employed to determine the crystal structure of the novel compounds. This is of particular importance for technical applications as the properties of any given intermetallic compound can neither be understood nor predicted without the knowledge on its crystal structure.

List of Publications

This thesis is based on the following papers, which will be referred to in the text by Roman numerals.

I C. J. Müller, S. Lidin, S. Ramos de Debiaggi, C. E. Deluque Toro, A. F. Guillermet, Synthesis, structural characterization and ab initio study of $Cu_{5+\delta}In_{2+x}Sb_{2-x}$ a new B8 related structure type, *Inorganic Chemistry* **2012**, *20*, 10787-10792.

II C. J. Müller, S. Lidin, Cu_3Sn understanding the systematic absences, *Acta Crystallographica Section B* **2014**, *70*, 879-887.

III C. J. Müller, S. Ramos de Debiaggi, C. Ritter, S. Lidin, HT-$Cu_{5+\delta}In_{2+x}Sb_{2-x}$ - A New Modulated Ni_2In Type Superstructure, Manuscript.

IV C. J. Müller, V. Bushlya, M. Ghasemi, S. Lidin, M. Valldor, F. Wang, Ternary intermetallic compounds in Au-Sn soldering systems structure and properties, Manuscript.

V C. J. Müller, S. Lidin, $Cu_{11}In_9$ Revised structure and its (physicochemical) relation to $Cu_{10}In_7$, *Journal of Alloys and Compounds* **2015**, *638*, 393-397.

VI C. J. Müller, S. Lidin, On Squaring the Triangle, Manuscript.

My contributions

I I synthesized the samples, and characterized them with PXRD and SC-XRD. EDXS was performed with help of Gunnel Karlsson. I was the main author of the paper.

II I synthesized the samples, and characterized them with PXRD, SC-XRD and EDXS. I was the main author of the paper.

III I synthesized the samples, and characterized them with PXRD, SC-XRD and EDXS, as well as TG-DSC. I was the main proposer for the PND experiments that I performed at beamline D2B@ILL with help of Clemens Ritter. I was the main author of the paper.

IV I synthesized the samples, and characterized them with PXRD, SC-XRD and EDXS, as well as TG-DSC. I was the main proposer for the PND experiments that I performed at beamline HRPT@SINQ with help of Vladimir Pomjakushin. I was the main author of the paper.

V I synthesized the samples, and characterized them with PXRD, SC-XRD and EDXS, as well as TG-DSC. I was the main author of the paper.

VI I synthesized the samples, and characterized them with PXRD, SC-XRD and EDXS. I was the main proposer for the PND experiments that I performed at beamline D2B@ILL with help of Clemens Ritter. I was the main author of the paper.

Publications not included in the thesis

I contributed to the following publications which are outside the scope of this thesis.

VII C. J. Müller, U. Schwarz, P. Schmidt, W. Schnelle, Th. Doert: High-pressure Synthesis, Crystal Structure, and Properties of GdS_2 with Thermodynamic Investigations in the Phase Diagram Gd-S, *Zeitschrift für Anorganische und Allgemeine Chemie* **2010**, *636*, 947-953.

VIII C. J. Müller, U. Schwarz, Th. Doert, High-pressure synthesis of rare-earth metal disulfides and diselenides LnX_2 (Ln = Sm, Gd, Tb, Dy, Ho, Er and Tm; X = S, Se), *Zeitschrift für Kristallographie* **2011**, *226*, 646-650.

IX C. J. Müller, U. Schwarz, Th. Doert, High Pressure Synthesis of Lanthanide Polysulfides and Polyselenides $LnX_{1.9}$ (Ln = Gd-Tm; X=S,Se), *Zeitschrift für Anorganische und Allgemeine Chemie* **2012**, *638*, 2477-2484.

X K. Guo, D. Rau, L. Toffoletti, C.J. Müller, U. Burkhardt, W. Schnelle, R. Niewa, U. Schwarz, The ternary metastable nitrides ϵ-Fe_2TMN (TM = Co, Ni): high-pressure high-temperature synthesis, crystal structure, thermal stability and magnetic properties, *Chemistry of Materials* **2012**, *24*, 4600-4606

XI U. Schwarz, A. Wosylus, H. Rosner, W. Schnelle, A. Ormeci, K. Meier, A. Baranov, M. Niklas, S. Leipe, C.J. Müller, J. Grin, Dumbbells of five-connected silicon atoms and superconductivity in the binary silicides MSi_3 (M = Ca, Y, Lu), *Journal of the American Chemical Society* **2012**, *134*, 13558-13561.

Abbreviations

bcc	body centered cubic
ccp	cubic close packed
EBS	electron backscattering
EDXS	energy dispersive X-Ray spectroscopy
epf	η phase field
epfc	compound from the η phase field with Ni_2In type (super)structure
hcp	hexagonal close packed
HT	high temperature
LN	lanthanide metal
LT	low temperature
P	(half)metallic p-block element
PND	powder neutron diffraction
PXRD	powder X-ray diffraction
RoHS	Restriction of Hazardous Substances Directive
RT	room temperature, 293 - 300 K
SC-XRD	single crystal X-Ray diffraction
SEM	scanning electron microscopy
TG-DSC	simultaneous thermogravimetry and differential scanning calorimetry
TM	transition metal element

Contents

1. Introduction **1**
1.1. Intermetallic Compounds in Electronic Devices 2
1.2. Intermetallic Compounds of Interest and Their Crystal Structures 3

2. Used Techniques **5**
2.1. Syntheses of the Intermetallic Compounds 5
2.2. Structural Analysis 6
2.3. Chemical Analysis 8
2.4. Thermal Analysis 8

3. Finding Ternary Intermetallic Compounds **11**
3.1. Binary Compounds 11
3.2. Guided Syntheses of Ternary Intermetallic Compounds - A Case Study . . 13

4. The Structure Chemistry of the Compounds **25**
4.1. The Ni_2In Structure Type - Review of its Description 25
4.2. Superstructure Formation in the Ternary Intermetallic Compounds 30
4.3. Hexagonal Structure Motifs in Coloured Cubic bcc Superstructures 48

5. Conclusions **51**

6. Populärvetenskaplig sammanfattning **53**

7. Acknowledgements **55**

Bibliography **57**

A. Experimental Details **69**

B. Crystallographic Background Information **71**
B.1. Supporting Information on Coloured bcc Structures 71
B.2. Binary Compounds TM-P 77
B.3. Ternary Compounds TM1-TM2-P with Ni_2In Type Structures 84
B.4. Ternary Compounds TM-P1-P2 with Ni_2In Type Structures 89
B.5. Compounds with Different Type Structures 93

1. Introduction

Intermetallic compounds and alloys have been of extraordinary importance for humankind. When the humans learnt how to handle and employ fire, they were able to obtain and work on metal-containing raw materials. In the beginning, only solid gold, silver and copper were used to make simple tools and jewellery. Unfortunately, the pure metals were not suited to manufacture more advanced tools, and humans had to rely on stone for axes, chisels and spears.[1] Hence, the discovery of the first copper alloys was the the starting shot for the development of technologies.[2] Through the ages, the constant improvement of the knowledge on intermetallic compounds and alloys guaranteed that technology leaps were possible in the first place. This is also the case for the latest of these, the so-called digital revolution that started the period of the information age.

Computers, servers and the internet are the foundation for the fast information transfer that characterizes our time. Unsurprisingly, speed is not the only challenge for modern engineers. Miniaturization, energy efficiency and at a progressive rate mobility are just some keywords within this context. The drawback of solving these problems is the creation of an increasing amount of waste of what used to be high-end technical products just a few years ago. Trying to burn old computers has never been an option as they contain too many precious resources, such as noble metals. Hence, the recycling of high-tech scrap is an equally fast developing business segment, but, not everything is retrievable in a profitable way. Moreover, some of the metals and their compounds are hazardous to the environment and as such classified as special waste.

One result of the steeply rising amount of tech waste is that restrictions and bans on hazardous materials in electronic devices have been put into legislation in some countries over the past ten years. One example is the European Union "Directive on the restriction of the use of certain hazardous substances in electrical and electronic equipment" (2002/95/EC) which is also referred to as Restriction of Hazardous Substances Directive (RoHS).[3] It restricts the utilization of cadmium, lead and mercury, and is closely related to additional directives concerning their waste (2002/96/EC)[4] as well as batteries (2006/66/EC)[5]. To exclude exemptions and to fill loopholes, the scope of the directives is increasing with time, e.g. the semiconductors GaAs and InP are currently evaluated.[6]

The direct consequence of these regulations is that the substitution of the affected metals with others created new interdisciplinary research fields as traditional materials like lead-containing solders are not allowed any longer. The here presented work is not directed towards finding new solder or semiconductor materials. The idea behind this thesis is to find and characterize intermetallic compounds that are formed when metal-metal contacts are present in electronic devices. Besides chemical characterization techniques,

crystallographic methods such as X-ray diffraction are employed to determine the crystal structure of the novel compounds. This is of particular importance for technical applications as the properties of any given intermetallic compound can neither be understood nor predicted without the knowledge of its crystal structure.

1.1. Intermetallic Compounds in Electronic Devices

A prominent example for a potentially reactive metal-metal contact in every electronic device are solders. They are crucial as they interconnect for instance wires with components on circuit boards, as shown in Fig. 1.1. Hence, the requirements on the long-time stability of these interconnections are high, and the classical Pb-Sn solders have been outstanding in fulfilling those.

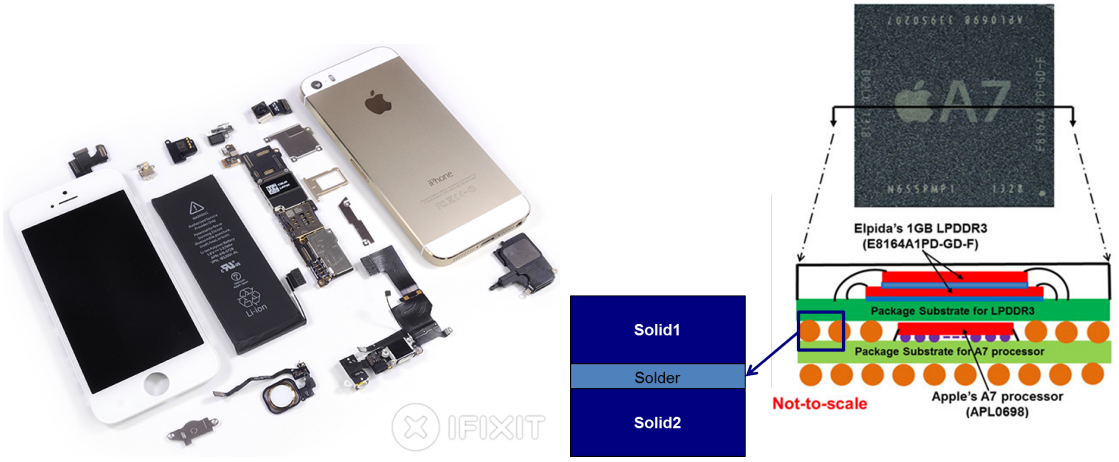

(a) iPhone 5S parts after teardown by iFixit [7]

(b) Solder Joints in an iPhone 5S, image after *Lau* [8]

Figure 1.1.: Solder Joints in electronic devices such as smart phones represent classical research questions for solid state chemists. For instance, the questions which intermetallic compounds are formed.

One of the advantages of the Pb-Sn system is that it can be used both for high-temperature (523 K to 623 K or higher) and low-temperature applications (below 523 K). There is no other combination of two metallic elements providing such a large range of working temperatures. For this reason, modern commercial Pb-free solders are complex mixtures of three elements, at least. Most of the new Pb-free solders contain Sn as one of constituents, but different base elements are discussed, such as In-Sn, Bi-Ag, Zn-Al or Au-Sn. [9] Further alloying additives are Sb, Mg, Ge, Ga and Cu. The scope of applications for these Pb-free solders, however, is limited as they are high-optimized products for specific purposes, and will fail for other terms of use.

Despite the challenge of finding suitable replacements for the Pb-solders, the demands for the solder joints are constantly increasing since the electronic devices are becoming smaller and smaller. One aspect of this miniaturization is an increase of the microjoint densities, which is implemented by decreased solder joint volumes, for example. As a result, many initially promising Pb-free soldering systems do not pass the indispensable mechanical, thermal and power cycling tests.[10] Reasons for their failures are dissolution processes, problems with filler components or board finishers and many more. Remarkably, every list of possible failures names intermetallic compounds as one of the key problems, and one may wonder why.
Any of these solders is composed of at least two different metals. Consequently, intermetallic compounds and alloys are constituting components of every solidified solder. Additionally, different intermetallic compounds can form in the early stages of the solidification or upon aging of the solder when the device is used. For instance, the Sn-rich Au-Sn solders are mixtures of AuSn and $AuSn_4$ first, but thermodynamically stable solders consists of the compound $AuSn_2$ and $AuSn_4$.[11] When the solder is then attached to a substrate, such as semiconducting or metallic materials, a chemical reaction has to occur. Without the formation of an intermetallic compound layer at the interface of solder and substrate, the desired permanent contact between the two components is impossible. Many of the new Pb-free solder materials form such layers with all kinds of substrates, but they also fail in tests because of them. The reasons are manifold, and just a few of them can be mentioned here. Intermetallic compound layers can grow, either into the substrate or into the thin solder layer. They can further transform to different compounds due to a chemical reaction or induced by changed conditions such as temperature or pressure. The solder joint may then become brittle, contain voids, break or creep. Moreover, an altered phase distribution can affect the resistivity or produce short circuits in the device upon whisker growth or oxidation. By these means, the intermetallic compounds and their (chemical) stability influence the mechanical, electrical and thermal performance of the whole interconnection significantly.

1.2. Intermetallic Compounds of Interest and Their Crystal Structures

The number of considerable intermetallic compounds is large, as they are formed not only in the Pb-free solders and solder joints but also when metallic protective coatings are attached on the interconnections. The selection of a limited number of constituting elements and composition ranges is unavoidable to obtain meaningful results within the chosen scope. Therefore, this study concentrates on ternary intermetallic compounds that are formed by group 10 and group 11 transition metal element (TM) with Sn as well as its neighbours In and Sb from the (half)metallic p-block element (P). Regarding the composition, the content of the TM is limited to the range from 50 to 72 at-% in systems with general formulae TM-P1-P2 and TM1-TM2-P. This also restricts the number of possible atomic arrangements, namely the crystal structures, significantly.

Many binary compounds TM-P (50 to 72 at-%) crystallize in structures that are related to the Ni_2In structure type; and it is not mere wildcatting to expect the ternary compounds to do the same. However, it is a novel approach to base the working hypothesis on the membership to a family of structures. This means that intermetallic compounds of interest were not only synthesized with respect to their relevance for soldering systems but also considering that their crystal structures may belong to the family of Ni_2In type structures. In fact, this approach is a consistent way to uncover hidden structure-property relationships in a systematic fashion.

The Ni_2In structure type is one of the most prominent hexagonal structure types of inorganic compounds, and therefore, mentioned in every text book on the structure chemistry of these compounds. The widely accepted description is that it is a stuffed version of the NiAs structure type. In general, the NiAs structure is understood as a distorted hexagonal close packed (hcp) arrangement of the As atoms wherein all octahedral interstices are occupied by Ni atoms. The stuffing refers to an additional occupation of trigonal bipyramidal interstices that consist of two face-sharing tetrahedra and are large enough to host a TM like Ni. Hence, there are three building blocks in these structures. The (pseudo)hexagonal network is formed by metallic elements from the p-block (group 13 to 15) whereas the octahedral and the trigonal bipyramidal interstices are occupied by TM elements. The hereby applied narrow elemental range is not arbitrary as it is the result of including compounds with allowed c/a ratios only.[12] Notably, these metric parameters can be used to measure the degree of network distortion, and thus, to delimit one isopointal structure type from another. Another comparison that is usually made is that the NiAs structure type is the hexagonal relative of the cubic NaCl structure type, a cubic close packed (ccp) arrangement of Cl^- ions wherein all octahedral interstices are occupied by Na^+ ions. These relations will be discussed in detail in chapter 4. Just as a remark, neither the compound NiAs nor the high temperature (HT) phase of Ni_2In crystallize in these idealized type structures.[13;14]

Besides this new approach, a number of ternary phases with higher TM content (up to 80 at-%) was studied in more detail in case of their presence as minor components in the samples. Further, the crystal structures of some binary compounds were re-investigated due to inconsistencies between experimental and theoretical data. An overview over the results will be discussed in detail in chapter 3.

2. Used Techniques

2.1. Syntheses of the Intermetallic Compounds

The binary and ternary intermetallic compounds in this study were synthesised from their constituting elements. The metallic pieces were reacted in evacuated silica ampoules (static vacuum $1{\cdot}10^{-4}$ mbar) that were positioned vertically in muffle furnaces at temperatures between 1023 K and 1323 K for a period of three to seven days. After oven cooling, the ampoules were either opened or annealed at temperatures between 373 K and 723 K before quenching them in cold water. For selected samples, the formation of superstructures has been investigated via heat treatments at higher temperatures. The experimental details of samples that are not covered within the attached manuscripts are given in appendix A.
At the first glance, this synthesis procedure is outdated and not useful to achieve either well grown single crystals or phase pure samples. Both of these approaches are very common, because the first is useful for crystal structure determinations, and the latter is preferred for subsequent physical property evaluations. Controversially, this "poor" choice was made on purpose.
Many engineering studies on potential lead-free soldering systems are not aiming towards reliable information on the compound stability for a period of time that is longer than one month. This is surprising, as the minimum warranty of electronic devices is at least one year. Additionally, the compounds or solder joints are very often studied at temperatures that are significantly higher than the temperatures which are present around or created by the waste heat inside of electronic equipment. Unsurprisingly, it has been criticized that these studies are irrelevant with respect to thermodynamic equilibrium states at pertinent temperatures.[15] A subsequent problem is that ternary phase diagrams for potentially interesting soldering systems are unknown, or calculated by extrapolation from insufficient data on the binary phase diagrams. For this reason, phase purity was not a relevant goal for the syntheses. And heat treatments of the samples were performed at temperatures that are in the range of working temperatures for the solders as well as the electronic devices. More importantly, the tempering was conducted in the way that the annealing time was increased when the annealing temperature was decreased.
The clear advantage of this procedure is that crystallographic as well as thermodynamic information can be extracted by characterization of the specimens. These are necessary for any judgement concerning the formation and stability of intermetallic compounds in solder joints within the time frame of the warranty of an electronic device. The obvious drawbacks are ungovernable crystal growth conditions as well as a limited possibility of

further studies regarding the mechanical and physical properties of the compounds.

Alternative synthesis strategies

Experiments using the centrifuge method were made to circumvent some of the described problems without changing the desired temperature-time regime.[16] The major problem was the choice of a suitable metallic flux that is liquid at the desired heat treatment temperatures and does not form intermetallic compounds outside the composition range. Metals with reasonable low melting temperatures are Ga, In, Bi, Sn and Hg. Only the first four were tested as the use of Hg is highly restricted in Sweden.[17] Independent from starting with the pure elements or from pre-synthesized compounds, either binary TM-flux compounds or phases that contained all present elements were formed. This means that elemental flux was neither useful for the phase-pure synthesis of the desired ternary intermetallic compounds nor controlled growth of single crystals. Moreover, In-Sn alloys were tested as flux agents for the growth of single crystals in Cu-In-Sn. The accessible temperature range is however limited, and superstructure formation takes place below the solidus temperature of the alloy flux. As a conclusion, it was not reasonable to rely on this method within the time-frame and the scope of this study, but it may be useful to grow larger single crystals of known compounds in the future.

2.2. Structural Analysis

All samples were characterized with powder X-ray diffraction (PXRD) to identify the intermetallic compounds present in the sample. For this purpose, the specimens where crushed and ground to fine powders. The PXRD experiments were performed on a Stoe Stadi MP diffractometer in transmission mode using Cu $K\alpha_1$ radiation, Ge monochromator (Johan geometry) and a Mythen or a linear position sensitive detector. The zero point of the instrument was calibrated against Si as standard, and the program suite WinXPow was employed for instrument control and data analysis.[18] For lattice parameter determinations with Jana2006[19], either Si was added or well defined compounds within the sample have been used as reference.
In studies on lead-free solders, single crystal X-Ray diffraction (SC-XRD) experiments are not a commonly used structure analysis technique as the phase identification is usually done with microscopic methods, and PXRD is used as an additional method to verify these results. There is however a risk that weak and overlapping reflections are overlooked or misinterpreted in the data analysis of PXRD patterns of Ni_2In type superstructures.[12] Suitable pieces with clean surfaces and metallic lustre were mounted on silica fibres with two-component glue. In-house SC-XRD experiments where performed on an Oxford Diffraction XCalibur3 or an Agilent XCaliburE four circle diffractometer, equipped with Mo $K\alpha$ radiation, graphite monochromators and an Saphire3 or EOS detector, respectively. Additional experiments using synchrotron radiation, were performed on crystals from Ni-Cu-In samples at the experimental station 1 at beamline I19 (Diamond Light Source, Didcot, UK)[20] as well as the four-circle diffractometer

at beamline CRISTAL (Soleil, Saint-Aubin, France). Data reduction, numerical absorption correction [21] and data integration were performed with CrysAlisPro [22] for all single crystal diffraction experiments. The charge flipping algorithm [23–25], as implemented in Superflip [26;27], was used for structure solution whereas structure refinements were performed with Jana2006. [19]

Many of the studied intermetallic compounds consist of elements that are neighbours in the periodic table. As a consequence, the occupation of different crystallographic sites in the structures cannot be resolved in X-ray diffraction experiments; mainly because a difference in the number of electrons of one or two makes it difficult to interpret the electron density maps. Unfortunately, electron diffraction suffers from the same problem as the electrons in the beam are interacting with the electrostatic field of the atoms. As sketched in Fig. 2.1, neutron scattering is not dependent on the number of electrons as neutrons interact with atoms via nuclear rather than electrical forces. [28] For example, the X-Ray scattering lengths of In, Sn and Sb are very similar, but different for neutrons with 4.06 fm, 6.225 fm and 5.57 fm. Cu and Ni have neutron scattering lengths of 7.72 fm and 10.3 fm. [29] This contrast is clearly sufficient. Neutron diffraction on powder samples is the method of choice to reveal site-specific ordering, because the growth of adequately large single crystals in these ternary systems in complicated.

A typical powder neutron diffraction (PND) instrument is very similar to a PXRD in-

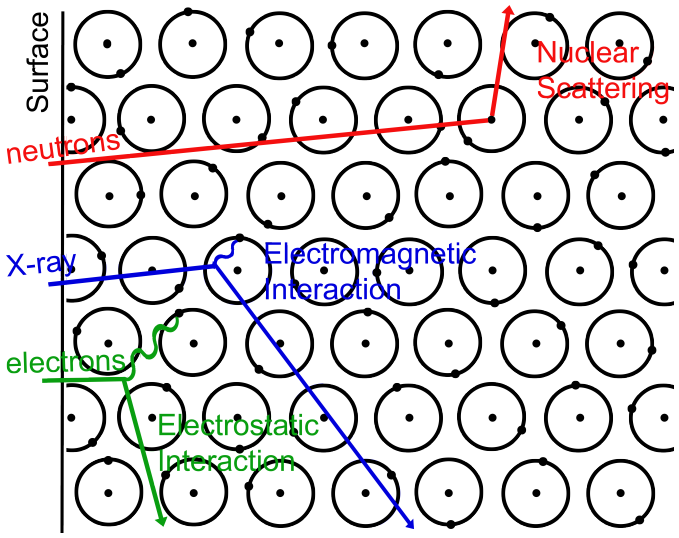

Figure 2.1.: Interactions of neutron, electron and X-ray radiation with matter. Image depicted after *Pynn* [28].

strument in terms of the present parts and their function. In contrary to PXRD experiments on thin films where only a few milligrams or less material is needed, high-resolution PND studies require samples of at least one gram. The reason is that neutron scattering is a signal-limited technique. [28] Hence, only high flux instruments were considered for beamline applications to ensure the detection of the weak superstructure reflections.

Notably, a room-temperature measurement takes four to six hours at least in order to further resolve these reflections from the background noise. PND experiments with a constant wavelength were performed at the beamlines D2B (Institute Laue-Langevin, Grenoble, France)[30], HRPT (Paul Scherrer Institute, Villigen, Switzerland)[31] and SPODI (FRM-II, Garching, Germany)[32] whereas a time-of-flight instrument was used at beamline POWGEN(Oak Ridge National Laboratory, Oak Ridge, USA)[33]. To reduce absorption effects, the powders were loaded in circular vandadium containers (cuvettes, ∅=6 mm) for the measurements.[34] The structure models from SC-XRD were used as starting models for the refinements from PND data. Only with a combination of both methods, detailed atomic ordering schemes are accessible.

2.3. Chemical Analysis

For an experimental determination of the compositions of the intermetallic compounds, pieces (20 - 50 mm^3) of selected samples were embedded in epoxy. The resin and the embedding method were chosen in dependence on the annealing temperature of the sample to preserve its microstructure. For samples whose heat treatment temperatures were between 373 K and 523 K , cold-embedding with Epofix resin (Streurs) was used whereas warm-embedding in PolyFast (Streurs) was the preferred method for all other specimens as this resin is already conductive. After embedding, the samples were ground with SiC papers of different grain sizes, and polished with diamond suspension (1 μm or 1/4 μ, Streurs) as final step.
The microstructure of planar specimens was investigated by scanning electron microscopy (SEM) on a JSM-6700F microscope equipped with an electron backscattering (EBS) detector. The composition of the observed phases was determined by means of energy dispersive X-Ray spectroscopy (EDXS). The collected spectra or elemental maps were analysed with the program AZtec.[35]

2.4. Thermal Analysis

The calculation of phase diagrams (Calphad) can be an alternative to the expensive experimental studies of ternary phase diagrams. It is a powerful method for the prediction of thermodynamic properties of any given composition, which is of great interest not only for industrial research. Its strength is the use of experimental data points to model the state of the system at different temperatures, pressures and phase constitutions. But this is also its weakness, as phases with an insufficient number of reliable data points or unknown stable constituents are difficult or impossible to assess.
For the purpose of including the ternary intermetallic compounds of Cu-In-Sb in an updated calculated ternary phase diagram, simultaneous thermogravimetry and differential scanning calorimetry (TG-DSC) measurements have been performed with a Netzsch STA449 Jupiter F3.[36] A series of standard metals was used for the temperature and sensitivity calibration of the machine. The temperature program was measured with empty sample and reference alumina crucibles first, to correct for the buoyancy of the

gas inside the chamber that is changing in the heating and cooling cycles. Afterwards, the sample was inserted and the experiment repeated under identical conditions. Observed thermal events are evaluated by using their onset temperatures instead of the temperatures of the peak maxima.[37]

3. Finding Ternary Intermetallic Compounds

3.1. Binary Compounds

A consequence of the selection criteria presented in section 1.2 is that all planning has to start from a review of the binary intermetallic compounds whose structure is related to the Ni_2In structure type. The underlying idea is to find and apply simple chemical principles to avoid a tremendous number of experiments. This is necessary as the presence of the Ni_2In type structures cannot be predicted by using empirical rules such as the various electron counting rules or geometry-driven approaches.

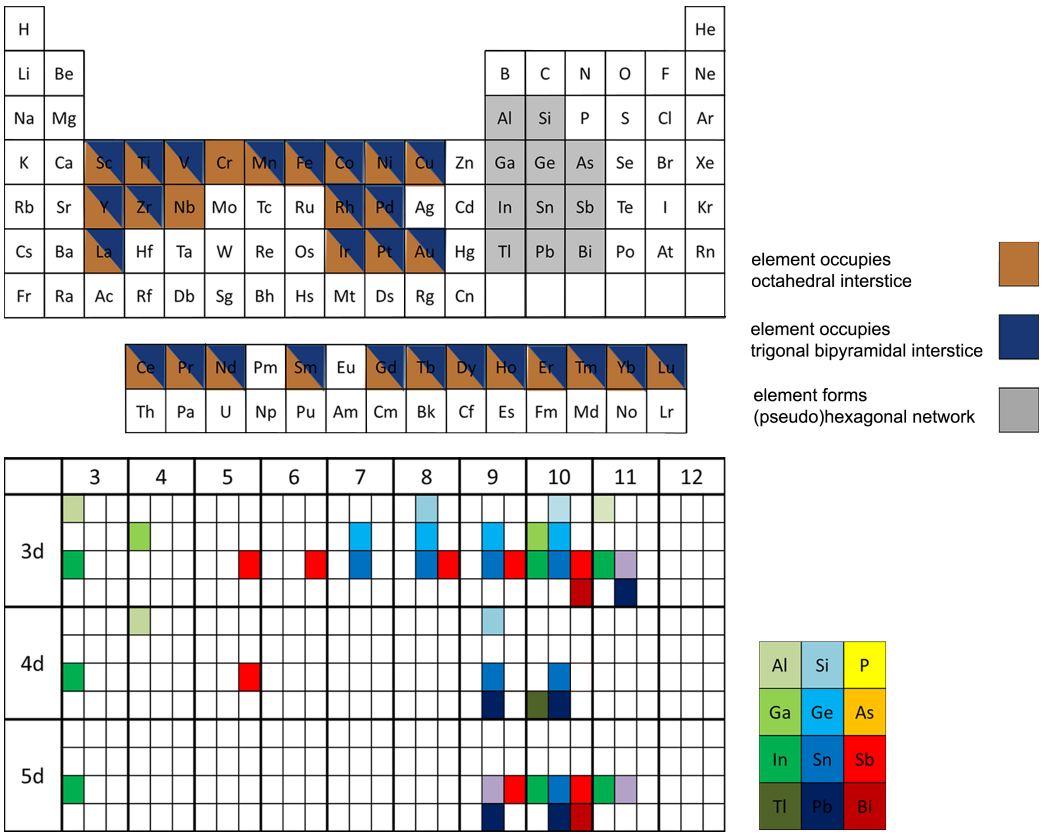

Figure 3.1.: Periodic tables of the elements for the occurrence of binary compounds TM-P with Ni_2In type (super)structures; references are given in Appendix B.2.

A very powerful tool is the critical evaluation of the presence or absence of the structure type for potential combinations of TM and P metals. As shown in Fig. 3.1, the number of present combinations is rather limited. Compounds of group 12 elements are not known in this structure type, and there is a general trend that 4d and 5d TM elements crystallize in different structure types in combination with these P metals. Within the elemental combinations of interest, it surprises that binary compounds have been described for all TM elements of group 10 and 11 but Ag. Using this knowledge base and some commonly accepted facts about structure formation, a decision tree can be outlined that guides the syntheses of ternary intermetallic compounds with crystal structures in the Ni_2In structure type (Confer Fig. 3.2).

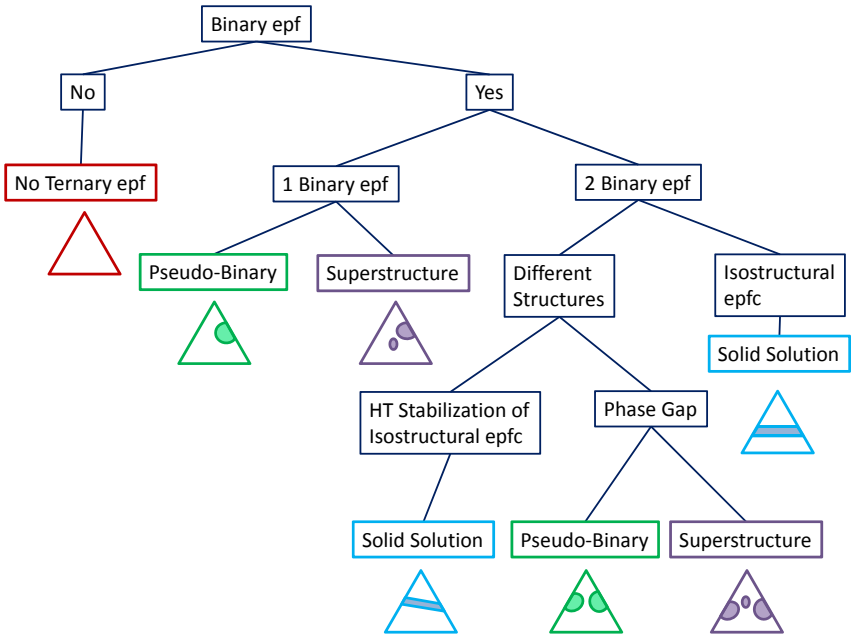

Figure 3.2.: Decision tree for the occurrence of ternary intermetallic compounds that crystallize in a Ni_2In type (super)structure. These compounds are denoted as epfc. The expected ternary phase diagrams for all cases are depicted schematically.

3.2. Guided Syntheses of Ternary Intermetallic Compounds - A Case Study

In order to increase the readability of the next paragraphs, the presence of at least one compound with a Ni_2In type (super)structure in the binary phase diagram will be addressed as *binary η phase field (epf)*, in general. A *ternary epf* refers to the presence of at least one pseudo-binary and one ternary compound whose structures are related to the Ni_2In aristotype structure. Notably, miscibility gaps have to be part of these epfs as the term incorporates a compositional range of 50 to 72 at-% of the TM content. The extension of a ternary epf is dependent on the number of binary epfs.

Case 1: No binary compound with a Ni_2In type (super)structure

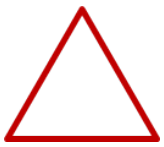

It appears that ternary intermetallic compounds are rarely crystallizing in structures that are unrelated to those of the neighbouring binary phases in the ternary phase diagram. The reason is that local atomic arrangements (structure motifs) have proven to be energetically and geometrically favourable in the stable binary phases. Hence, there is a driving force to preserve these structural motifs on the substitution of one of the elements, either in the network or on the interstitial sites, in a ternary compound (section 4.2).
The absence of binary compounds TM-P with Ni_2In type (super)structures indicates that the Ni_2In structure motifs are not stable enough for their appearance in crystal structures of a ternary compound, both energetically and geometrically. Notably, this absence does not imply a general absence of ternary compounds within the compositional range of the Ni_2In type (super)structures. It only means that other structure motifs are preferred, either energetically or geometrically. This is the case for ternary compounds in the systems Ag-In-Sn[38], Ag-In-Sb[39] and Ag-Sn-Sb[40], and all attempts to disprove the above stated within this study failed.
One compound that contradicts the here presented hypothesis is $Au_{10}In_7Sb_3$ with a AuSn type structure.[41] However, quenching samples from temperatures above 673 K, as described in the original publication by *Kubiak and Schubert*, lead to mixtures of the neighbouring compounds $AuIn_{0.9}Sb_{0.1}$[41], Au_3In_2 and $AuSb_2$[42]; the compound $Au_{10}In_7Sb_3$ was not found. This result corroborates the hypothesis that no ternary compounds with Ni_2In type (super)structures can be obtained when binary epfs are absent in the ternary phase diagram.

Case 2: One binary η phase field

The number of binary compounds within a given binary epf has an impact on the number of ternary compounds with Ni_2In type (super)structures. If there is only one binary compound, a pseudo-binary compound is formed in the fashion of a solid solution. In the case of more phases in the binary epf, the evolution of a ternary epf is probable.

Pseudo-binary compounds result from phase broadening that is very common in intermetallic compounds. They form easily by adding a third element to a binary compound from the binary epf. Hence, they substitute either network or interstitial elements in its Ni_2In type (super)structure. The substitution implies that the crystal structure of the ternary phase is isostructural to that of the binary, as lattice parameters change dependent on the size of the third element. Instances are the pseudo-binary phase Au_6Sn_5Sb, a solid solution of about 8 at-% Sb in AuSn (Paper IV), and $Cu_{4.8}Sn_{3.84}Sb_{0.16}$ [43]. The latter is interesting as the three different phases in the epf of Cu-Sn [44;45] are, in fact, one polymorphic compound. Only the HT modification is stabilized on the substitution of Sn with Sb, and not any of the low temperature (LT) modifications.

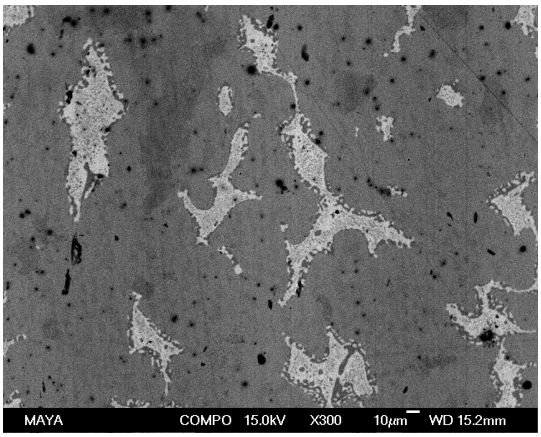

(a) LT-$Cu_5In_2Sb_2$-InSb-Sb-doped Cu_7In_3, 573 K

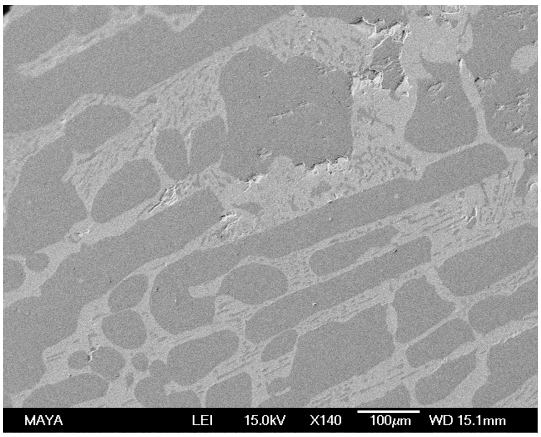

(b) Cu_2Sb-InSb, 573 K

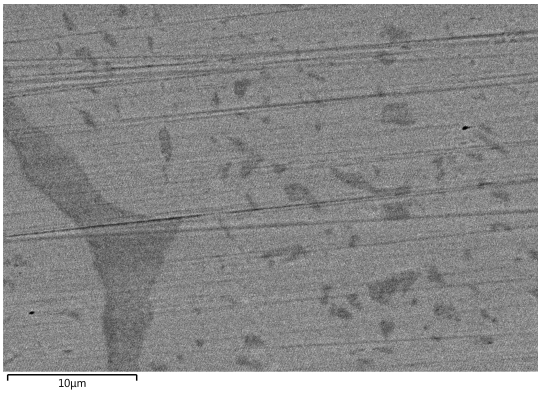

(c) Sb-doped Cu_7In_3 and $Cu_{3-3.5}In_xSb_{1-x}$, 523 K

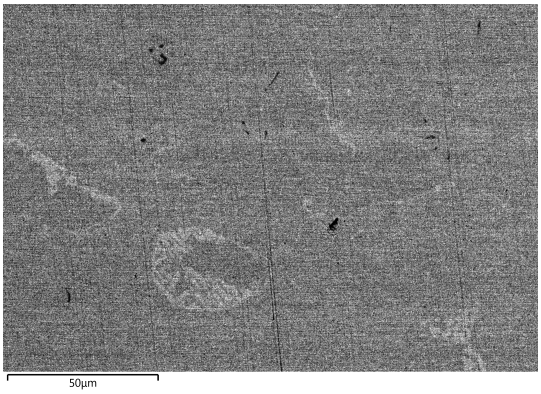

(d) Sb-doped Cu_4In and $Cu_{3-3.5}In_xSb_{1-x}$, 523 K

Figure 3.3.: Miscibility gaps in the ternary phase diagram Cu-In-Sb. Depicted are images that were taken with the EBS detector: The darker phases are Cu-rich whereas brighter phases are P-rich.

Real, ternary intermetallic compounds crystallize in crystal structures that are not isostructural to any of the neighbouring (pseudo)binary compounds. In general, the amount of substitute is larger than in pseudo-binary compounds, and thus, the influence of the third element on the structure and the properties is higher. Different compounds in the binary epf of Cu-In, could form various pseudo-binary compounds on addition of Sb. Experimental evidence has been found only for a solid solution of Sb in Cu_7In_3, the Cu-rich border of the binary epf, and not for Cu_2In, Cu_7In_4 or $Cu_{10}In_7$. As discussed in Paper VI, the crystal structure of $Cu_7In_{2.5}Sb_{0.5}$ is not really isostructural to that of Cu_7In_3, as its triclinic angles are obtuse instead of acute, although their structural motifs are alike. Moreover, two real ternary compounds have been found in the ternary epf in the Cu-In-Sb phase diagram, the dimorphic $Cu_5In_2Sb_2$ (Paper I,III) and $Cu_2In_{0.75}Sb_{0.25}$ (2:1 phase, Paper VI). The maximal extension of the ternary epf is reached in $Cu_5In_2Sb_2$, where up to half of the In positions in the network are substituted by Sb atoms. Higher amounts of Sb lead to the formation of Cu_2Sb, whose ionic bonding does not allow for a solid solution of In in the compound. On the Cu-poor side, the ternary epf is delimited by the semiconductor InSb, because Cu atoms can only diffuse into vacancies in the crystal structure of InSb. Above a critical concentration, interstitial Cu and InSb react to the compound $Cu_5In_2Sb_2$. On the Cu-rich side, Sb-doped Cu_4In and $Cu_{3-3.5}In_xSb_{1-x}$ ($0 \leq x \leq 0.5$) are the neighbouring phase fields (Confer Fig. 3.3).

Case 3.1: Two binary isostructural compounds with Ni_2In type (super)structures

A well-known principle within solid state chemistry is that isostructural compounds can form solid solutions that obey Vegard's law.[46] Consequently, only isostructural Ni_2In type (super)structures can form solid solutions. This situation is rather uncommon, and thus, it was not observed for any of the ternary phase diagrams that were experimentally evaluated within this project. For instance, the isostructural compounds Cu_7In_3 and Ni_7In_3 as well as $Ni_{13}In_9$ and $Pt_{13}In_9$ do not form continuous solid solutions, details on their superstructures are discussed in section 4.2.
An existing example from literature is the solid solution between the AuSn type structures PtSn and PtSb[47]. Further potential ternary combinations are: AuSn[48]-PtSn, NiSb[49]-VSb[50] or lanthanide metal (LN) indides $LN1_{2-x}LN2_xIn$. Therefore, one may ask whether only simple, highly symmetric compounds form solid solutions within the family of Ni_2In type superstructures. By this, compounds that crystallize in space group $P6_3/mmc$ are meant where random atomic order of atoms with similar metallic radii prevents symmetry reduction.

Despite the different metallic radii, SEM micrographs (Fig. 3.4) and determined compositions indicate that there is a solid solution between the Au-rich side of the Au_3In_2 epf and the Cu_7In_4 A-phase at 673 K and 523 K. (Confer Fig. 3.4) Unsurprisingly, Au and Cu atoms occupy the interstitial sites in the hexagonal In atom network randomly in alloys $Au_{3-x}Cu_xIn_2$. The observed solid solubility should be re-investigated with more data points and at temperatures lower than 523 K in continuative studies.

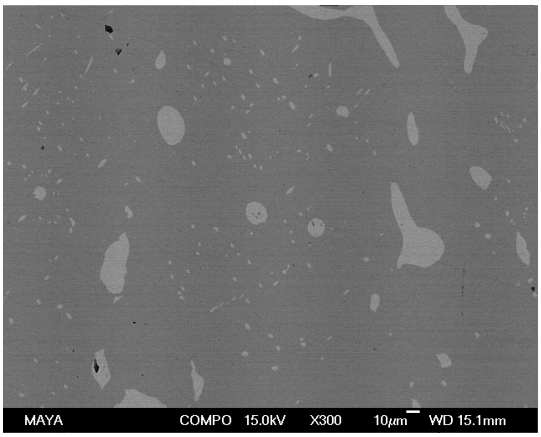

(a) nominal composition $AuCu_2In_2$

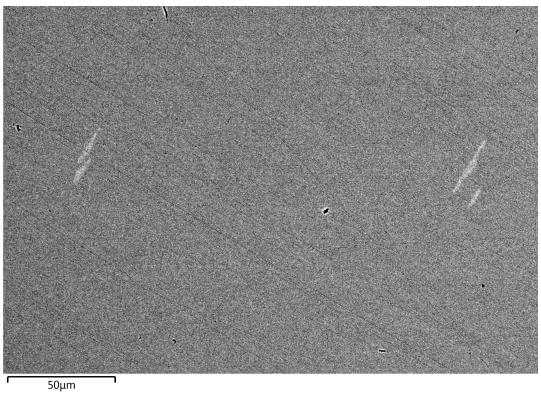

(b) nominal composition $Au_{1.5}Cu_{1.5}In_2$

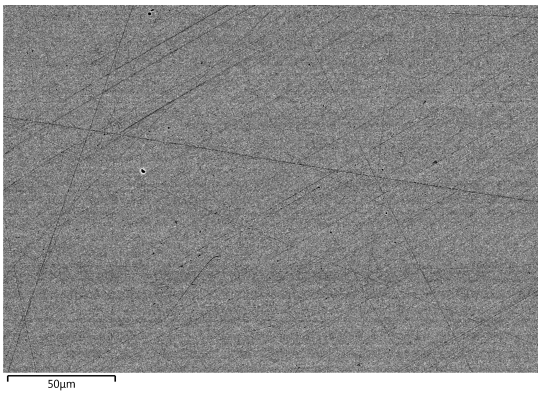

(c) nominal composition Au_2CuIn_2

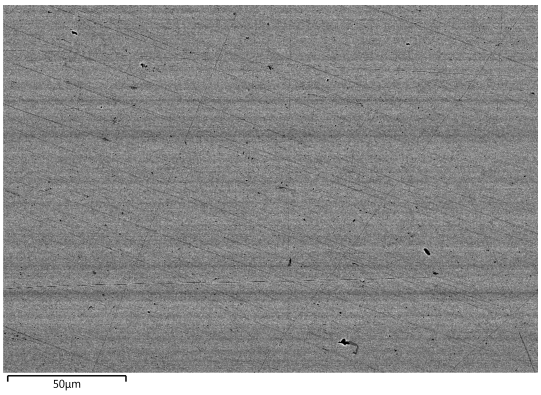

(d) nominal composition $Au_{4.7}Cu_{2.3}In_3$

Figure 3.4.: Observed solid solution in the ternary phase diagram Au-Cu-In at 673 K, minor phase in samples $Au_{3-x}Cu_xIn_2$ is (Cu-doped) $AuIn_2$. Picture (d) shows one alloy from the solid solution between Au_9In_4 and Cu_9In_4.

An indication for a corroboration of the high symmetry hypothesis is that solid solutions are also possible between AuSn type structures and compounds whose HT modifications are Ni_2In type structures which are stabilized on addition of the third element. Between these two isopointal structures, the lattice parameters of the ternary alloys change as the content of the TM in the trigonal bipyramidal interstices increases. An example is the solid solution between NiSb and HT-Ni_3Sn_2 [51], which are miscible even at 473 K. [52;53] Notably, the same is not true for AuSn and the HT phase Au_3In_2 as the latter is not a polymorphic compound. (Paper IV)
Now, think about a situation where the HT modifications of both binary border compounds adopt Ni_2In type structures with partial occupation of the trigonal bipyramidal interstices; i.e. Ni_2In and HT Ni_3Sn_2. (Confer Fig. 3.5) Above 673 K, a solid solution is observable between the two, isopointal compounds [54], wherein the occupation of the trigonal bipyramidal interstices as well as the lattice parameters of ternary phases change in dependence of their compositions. Below this temperature, electronic and geometric restraints lead to the formation of ternary compounds with different local atomic environments, and several miscibility gaps are formed in the ternary epf. Other instances of this gap formation are the solid solutions HT-Cu_2In-HT-Cu_5Sn_4, HT-Ni_3Sn_2-HT-Cu_5Sn_4 [55], and as mentioned above Ni_2In-HT-Cu_2In. (Confer Fig. 3.6)

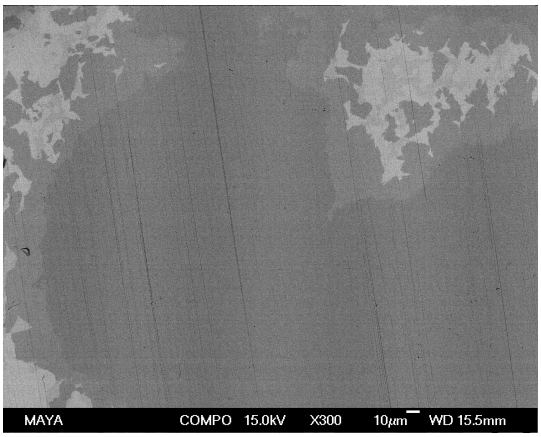

(a) Sn-doped Ni_3In_7, NiInSn, and $Ni_{1.68}In_{0.33}Sn_{0.67}$ (dark)

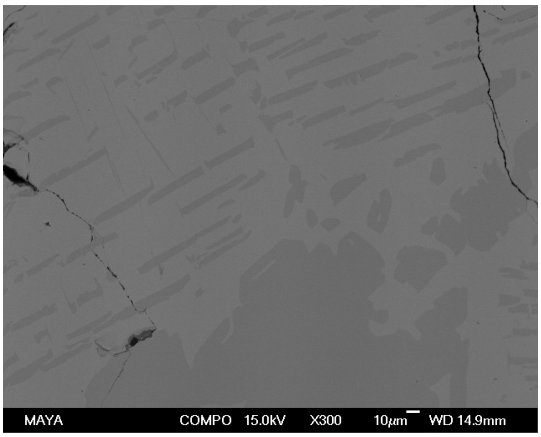

(b) Dark phase field of $Ni_3In_{1-x}Sn_x$ and the bright ternary epf, Ni_5In_2Sn and $Ni_{1.68}In_{0.33}Sn_{0.67}$

Figure 3.5.: Miscibility gaps in the ternary phase diagram Ni-In-Sn: Samples of nominal compositions $Ni_6In_2Sn_3$ and $Ni_7In_{1.5}Sn_{1.5}$, quenched from 573 K. The structures of the TM-poor phases (below 50 at.-%) were not further investigated whereas the miscibility gap between Ni_5In_2Sn and $Ni_{1.68}In_{0.33}Sn_{0.67}$ is not resolved in the image.

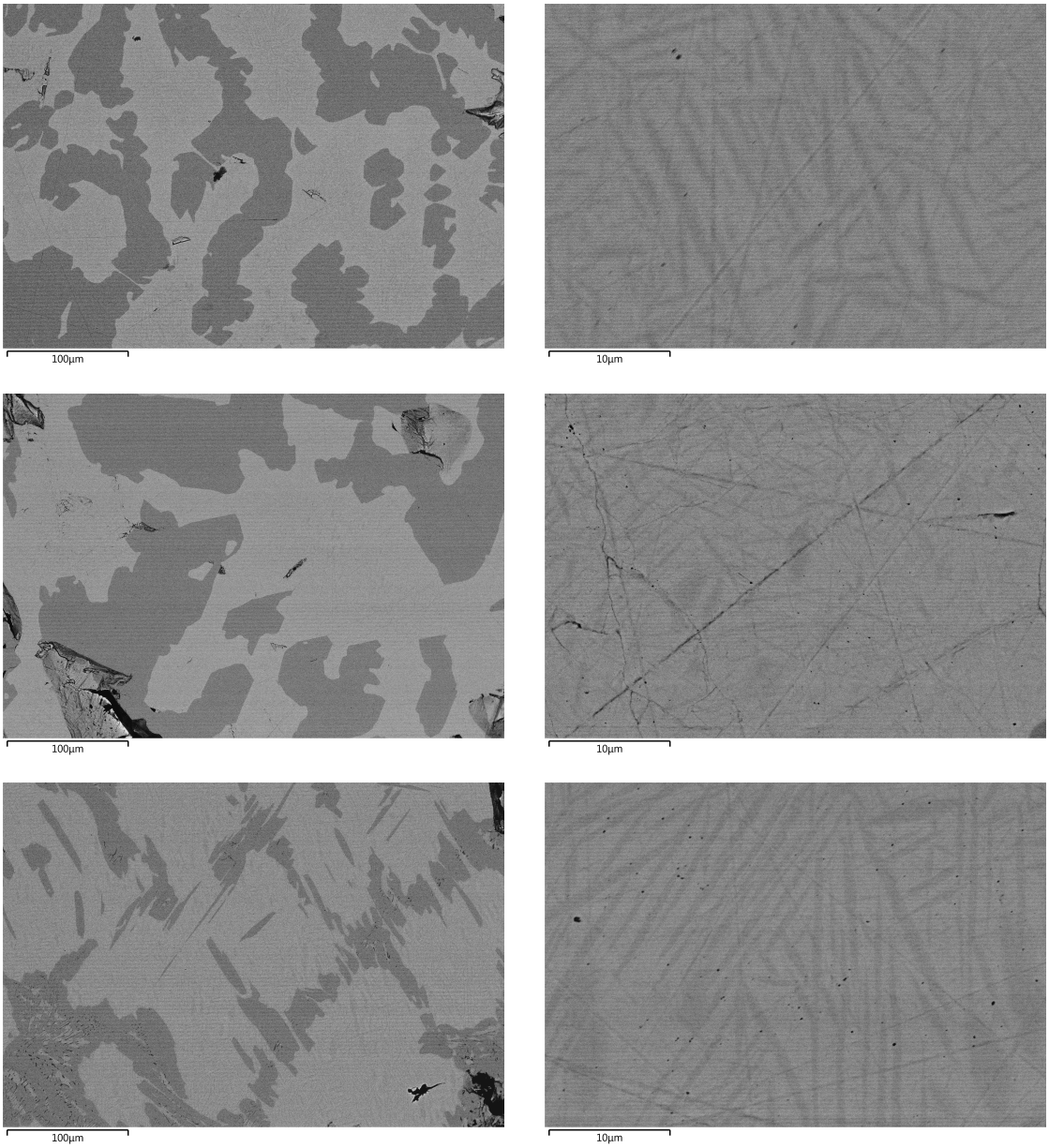

Figure 3.6.: Miscibility gaps in the ternary phase diagram Ni-Cu-In at the line from Ni_7In_3 to Cu_7In_3, quenched from 573 K: Overview electron micrographs (left) show that there is a general miscibility gap between the dark $Ni_{3-x}Cu_xIn$ and the bright ternary epf with an average In content of 30 at.-%. Fine structure images (right) reveal that small domains of slightly different compositions dominate the ternary epf, indicating a separation into phases with an In content of about 28 at.-% and 33 at.-%, respectively. Depicted are nominal compositions $Ni_6Cu_1In_3$ (upper), $Ni_4Cu_3In_3$ (middle) and $Ni_3Cu_4In_3$ (lower).

Case 3.2: Two binary epf with different Ni_2In type (super)structures

Following the above argumentation, the formation of miscibility gaps is expected to be very common in ternary epf, and the probability of ternary compounds is dependent on the number of compounds with Ni_2In type (super)structures in the neighbouring binary epf. Having this in mind, ternary phases were found even in systems like Au-Ni-In or Ni-Pt-In that had neither been experimentally evaluated nor accessed by the using the Calphad method prior to this study.

The ternary phase diagram of Au-Ni-In contains two binary epf. The compounds $Ni_{13}In_9$ and Ni_7In_3, whose HT modification is Ni_2In[56], are forming the binary epf of Ni-In. In contrast to that, the HT phase Au_3In_2 is the only compound in the binary epf of Au-In, indicating that the structure motifs of the Ni_2In structure type are local atomic arrangements that are not stable at temperatures as low as room temperature, 293 - 300 K (RT). As a result, pseudobinary compounds with Ni_2In type superstructures are surrounded by temperature dependent phase gaps that dominate the area of the ternary phase diagram where one would expect to find ternary compounds. (Confer Fig. 3.8) Notably, the miscibility gap spans from $Ni_{13}In_9$ to Ni_3In as Ni_7In_3 does not form a pseudo-binary compound with Au. There is however only a small solubility of Ni in Au_3In_2 of about 8 at.-%, whereas up to 17 at.-% Au can be dissolved in $Ni_{13}In_9$. A similar phase distribution was found in the system Ni-Pt-In, as shown in Fig. 3.7.

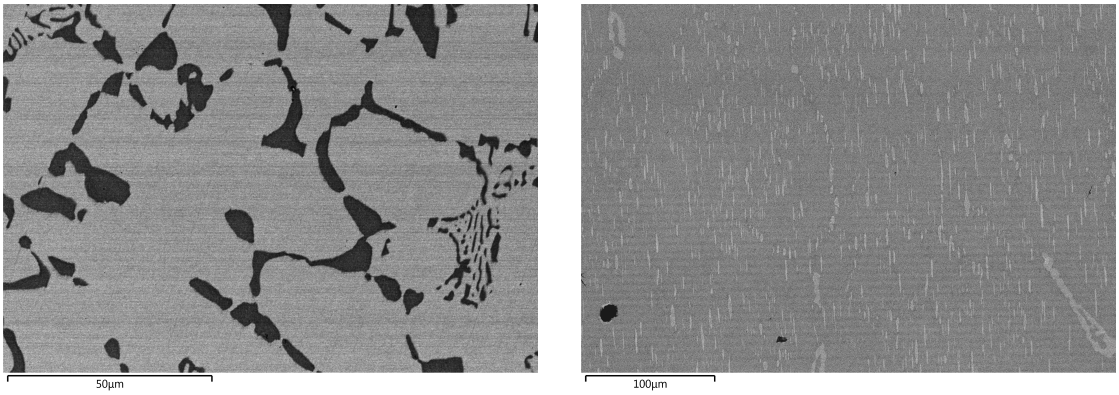

(a) Nominal composition $Ni_{3.5}Pt_{3.5}In_3$ (b) Nominal composition $Ni_{1.5}Pt_{1.5}In_2$

Figure 3.7.: Miscibility gaps in the ternary phase diagram Ni-Pt-In at 773 K, phase gaps remain at lower annealing temperatures like 423 K. TM-rich sample (a): dark In-doped Ni_3Pt and bright $Pt_{2.8}Ni_{2.2}In_3$; sample at about 40 at.-%In (b): dark $Ni_{7.3}Pt_{6.7}In_9$ and bright Ni-doped Pt_2In_3.

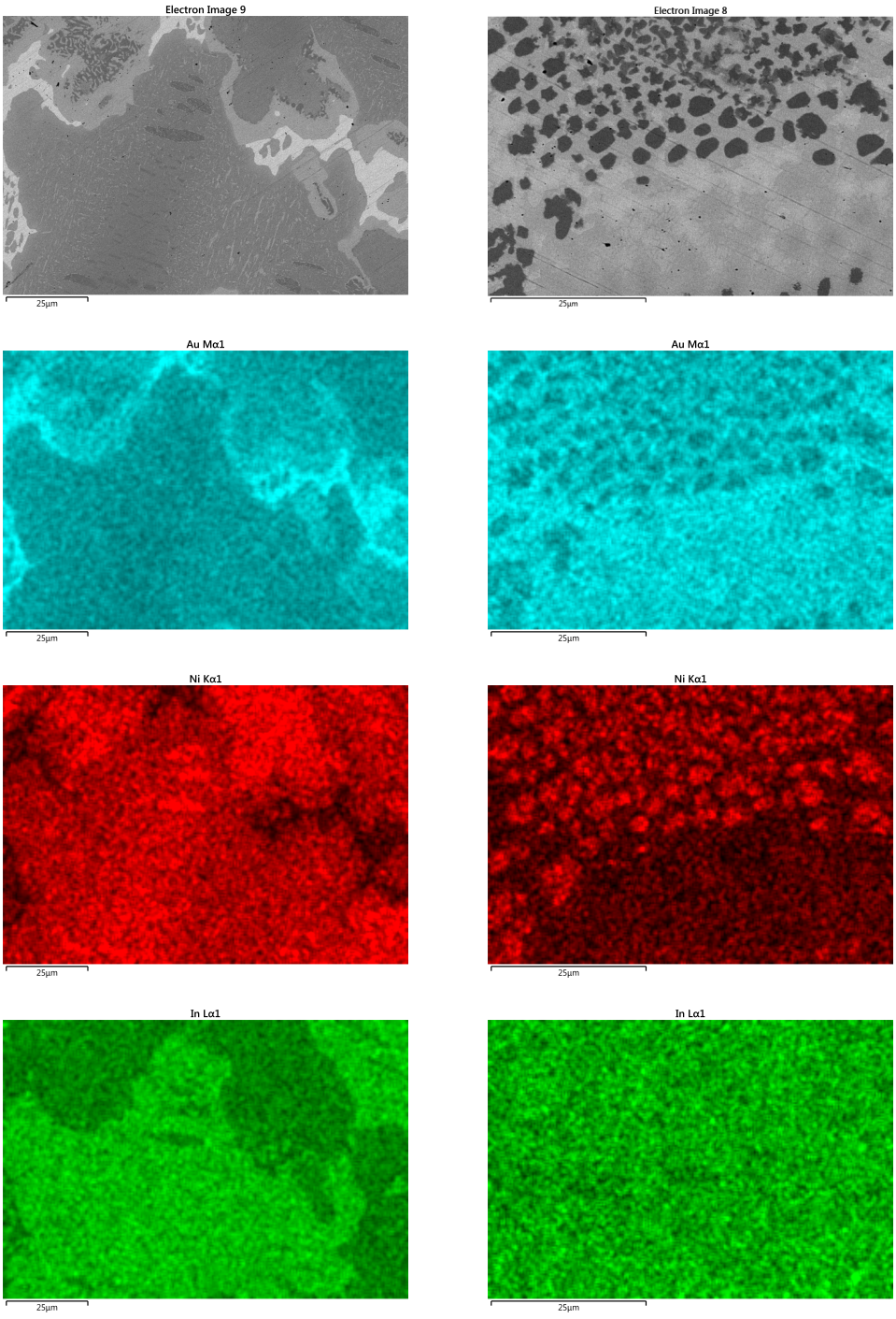

Figure 3.8.: Miscibility gaps in the ternary phase diagram Au-Ni-In: Electron micrographs and accompanying elemental maps from samples with the nominal composition $Au_{3.5}Ni_{3.5}In_3$ (left, 573 K) and AuNiIn (right, 923 K). The crystal structures of the pseudobinary compounds $Au_{1.33}Ni_{1.84}In_2$ and $Au_{2.92}Ni_{0.36}In_2$ were elucidated after annealing at 623 K.

Nevertheless, the presence of pseudo-binary phases does not prohibit the formation of ternary compounds. Interestingly, two transition metals of significantly different size appear to prefer the formation of pseudo-binary compounds whereas transition metals of similar size like Ni and Cu form ternary compounds with Ni_2In type superstructures. Besides the presence of different TM in the interstices of the structure, different elements on the network sites can entail the formation of ternary compounds and a ternary epf in the ternary phase diagram. In Cu-In-Sn and Ni-In-Sn, there are two binary epf but only the TM-In epf consist of more than one compound; the necessary condition for the existence of ternary compounds (Confer Fig. 3.9 and 3.5). The Ni_2In type superstructures of their ternary epfs will be discussed in detail in section 4.2.

Case 4: Two isostructural compounds of a competing structure type

The concept of guided synthesis has been demonstrated for ternary compounds with Ni_2In type (super)structures, although it is not limited to this family of superstructures. As a last case, some impacts of competing structure types on the compound formation shall be discussed which have not been covered in case 1.
A trivial case would be the formation of a new ternary type structure, meaning a ternary compound which crystallizes in a structure that is not related to any known structure type (by group-subgroup relations). For instance, the structure motifs of intergrowth compounds like $Cu_{10}In_7$ [57] are not originating from Ni_2In type structures exclusively. Within this study, however, no entirely new type structure has been found. For cases where only the LT modification of a compound is related to the Ni_2In structure type, the addition of a third element may stabilize the structure of the HT modification. An excellent choice to study this effect was the dimorphic compound Cu_7In_3 [58;59]. On the addition of third elements where this body centered cubic (bcc) type superstructure TM_9P_4 is unknown, such as Ni, Sn or Sb, pseudo-binary Cu_7In_3 compounds were found. (Paper VI) Upon addition of third elements where this cubic structure type is known, such as Au, Ag, or Ga, the HT modification is stabilized, and solid solutions can be found. A rather extreme case of this scenario has been observed in a sample of the nominal composition Au_2AgIn_2 wherein a cubic alloy of the approximate composition $Au_{4.5}Ag_{4.5}In_4$ has been stabilized at 473 K, in addition to the compounds AuIn and $AuIn_2$. The observed miscibility gap in the compositional range of Ni_2In type superstructures is surprisingly not arising from a stabilization of completely different structure motifs. On the contrary, the cubic structures of Au_9In_4 and Ag_9In_4 have similar atomic arrangements to the ones found in the hexagonal structure of Au_3In_2, which are not present in AuIn and $AuIn_2$.

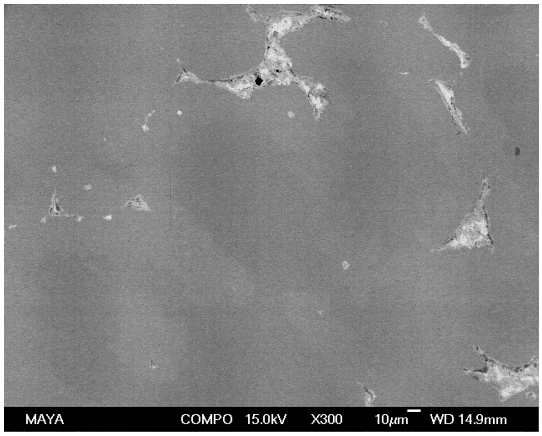

(a) $Cu_7In_{1.8}Sn_3$-$InSn_4$, 476 K

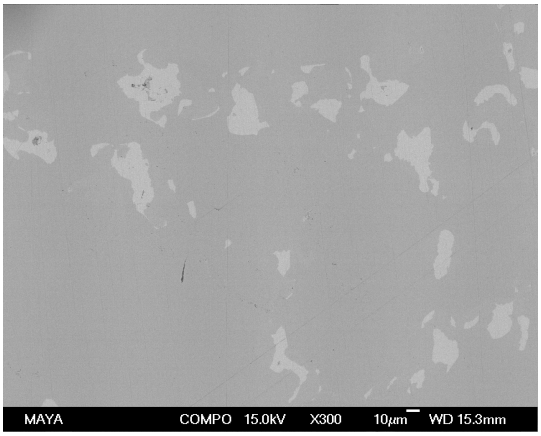

(b) $Cu_7In_{4-x}Sn_x$-In_3Sn, 373 K

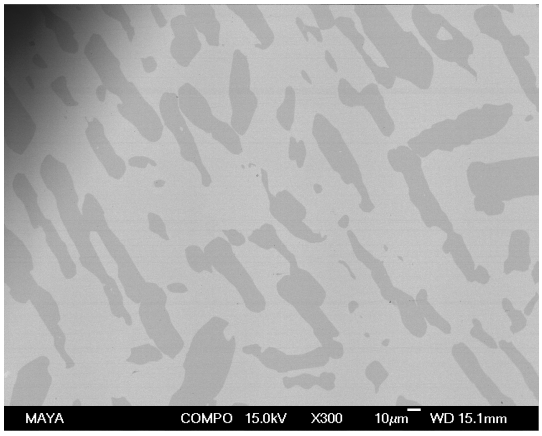

(c) $Cu_7In_{1.8}Sn_3$-$Cu_3In_xSn_{1-x}$, 473 K

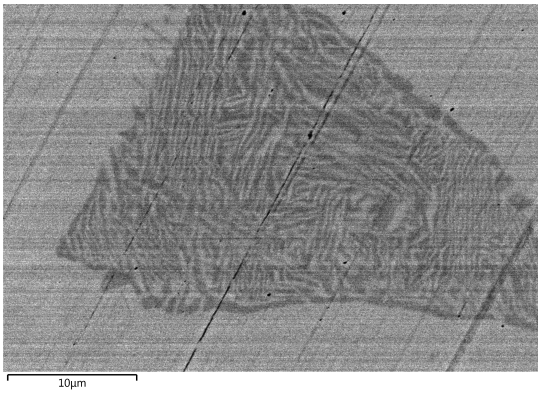

(d) $Cu_7In_{2-x}Sn_x$-$Cu_3In_{0.33}Sn_{0.67}$, 523 K

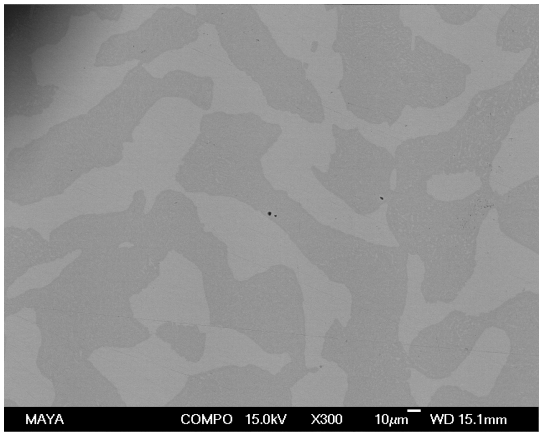

(e) $Cu_7In_{1.8}Sn_3$-$Cu_3In_xSn_{1-x}$, 523 K

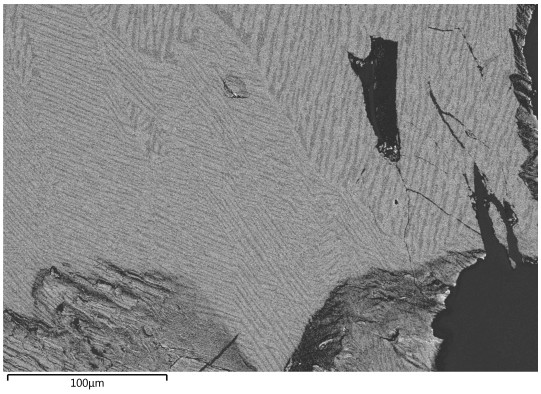

(f) $Cu_{11}In_2Sn$-$Cu_7In_{2-x}Sn_x$, 773 K

Figure 3.9.: Miscibility gaps in the ternary phase diagram Cu-In-Sn. Dark phases are TM-rich whereas bright phases are P-rich.

Further Factors on the Superstructure Ordering

A good knowledge of the structure chemistry of the binary epf proved to be a powerful tool, indeed. For this reason, a number of binary compounds has been re-investigated whenever a discrepancy between literature and experiment was observed, or to create reference diffraction patterns. Within these re-investigations, further factors that govern the formation with this structure type were identified.

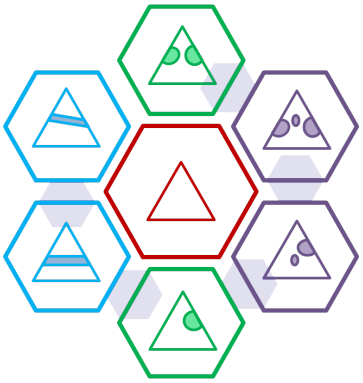

Annealing temperature is a crucial factor for the formation of structure motifs. Interestingly, some HT atomic arrangements are metastable at room temperature for several years, for instance in Cu-In-Sb or Au-In-Sn samples, whereas others transform to the LT modification after several month storage at room temperature. It has been a free-spirited but wise decision to re-measure single crystals after several month and search for new reflections in the diffraction patterns.

Annealing time is an invaluable resource for atomic ordering processes as diffusion is the dominating driving force from a kinetic point of view. An example is the fact that $Cu_{11}In_9$ transforms to $Cu_{10}In_7$ after annealing for at least nine month. (Paper V) Remarkably, the kinetics of phase transformations in the studied systems are basically unknown and expected to be very slow at the temperatures of interest. Hence, one has to assume that any of the observed compounds resembles an equilibrium state in the phase diagram unless this is disproved by further studies with even longer annealing times.

4. The Structure Chemistry of the Compounds

The attentive reader has probably noticed the peculiar introduction of the NiAs structure type in the first part of the thesis. Hence, the underlying structural relations of the structure type to other common structure types will be discussed and replenished in this chapter. Moreover, different kinds of superstructure ordering will be presented by using examples of the new intermetallic compounds from the previous chapter. The final part is an excursion to some cubic structures.

4.1. The Ni_2In Structure Type - Review of its Description

The Ni_2In structure type crystallizes in the hexagonal space group $P6_3/mmc$ (No. 194) wherein the special positions $2a$, $2c$ and $2d$ are occupied. The coordination polyhedron of atoms on site $2c$ is either an Edshammar polyhedron[60] or a trigonal prism due to vacancies on $2d$. These coordination polyhedra are rarely used, however, as it appears to be more convenient to describe the type structure in a host-guest like fashion: Atoms on site $2c$ are building the hexagonal "host" network which consists of layers with trigonal point symmetry that are stacked in an $ABAB$ sequence along [001]. Within this network, interstitial "guest" atoms are located on sites $2a$ and $2d$ which implies that they have a trigonal anti-prismatic (distorted octahedral[1]) or a trigonal bipyramidal coordination, respectively. (Confer Fig. 4.1) This selection of nearest neighbours is ignoring the present interatomic distances as it is inspired by compounds with ionic bonding, meaning that "anionic" host atoms are coordinated by "cationic" guest atoms, and *vice versa*.

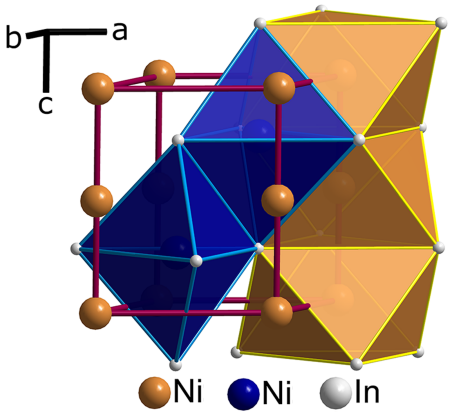

2a	2d	2c
0	1/3	1/3
0	2/3	2/3
0	3/4	1/4

Figure 4.1.: Sites in the Ni_2In structure type

[1] In order to avoid mix-ups with the trigonal bipyramidal interstices, the trigonal anti-prismatic interstices are addressed as octahedral interstices, although this terminology is technically incorrect.

Using this host-guest concept, structures of the Ni_2In type have been discussed either as stuffed, distorted hcp or as ternary AlB_2 hettotype (BeZrSi)[61]. While the first depiction has the benefit of an easy comparison to cubic structure types such as NaCl, the latter's advantage is its relation to other intermetallic compounds, for instance the Laves phases. Nevertheless, it is questionable whether the similarities are sufficient enough to use the term isotypic[2], because the lattice coincidences are not the same, and therefore, the coordination polyhedra of (super)structures of the three different structure types are not as similar as indicated by the identical point symmetries of the occupied lattice sites. Notably, statistical evaluations of reported (pseudo)hexagonal structures indicate that c/a ratios can be used as threshold values to assign crystal structures to structure type families, because there are sharp peaks in the frequency distribution of known (pseudo)hexagonal compounds.[63;64]

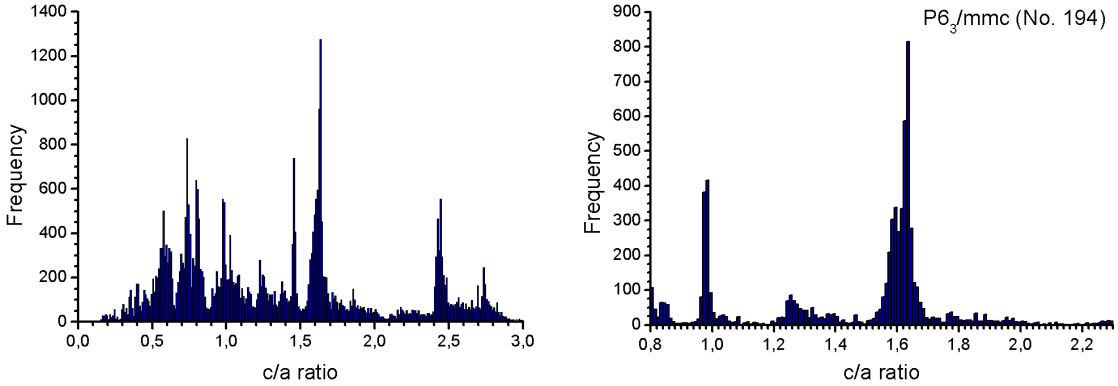

(a) all hexagonal/ trigonal space groups, no further search restrictions

(b) $P6_3/mmc$ (No. 194), Wyckoff sequence *dca*

Figure 4.2.: Frequency distributions of structures with hexagonal and trigonal crystal symmetry for inorganic compounds that are enlisted in Pearson's database[65].

In Fig. 4.2 the frequency distribution of c/a ratios is shown for inorganic compounds, the peak that occurs around $c = a$, the hexagonal isometric case, is not isopointal to the structures discussed above. Surprisingly, there is a clear gap around $c/a = 1.94$, the ideal value for BeZrSi type structures. The largest peak at $\sqrt{8/3} = 1.633$ corresponds hcp related structures, whereas the peak at $\sqrt{3/2} = 1.225$ is the characteristic value for compounds with Ni_2In type structures and metallic bonding.[12] The peak at about $\sqrt{2} = 1.414$ has been set as the upper threshold value for Ni_2In type structures[12] previously, because it is characteristic for compounds with Ni_2In type (super)structures with localized electrons, i.e. ionic bonding. Within this study, these compounds will be

[2]Two structures are isostructural (isotypic) if they "have the same (or closely related) structure, space group, lattice type and lattice coincidences." [62]

treated as part of a different structure family. It means that only (pseudo)hexagonal compounds with basic lattices fulfilling the condition[3] $1.155 \leq c/a \leq 1.333$ are assigned to the family of Ni_2In type (super)structures. Consequently, NiAs type structures whose c/a ratios are within the new thresholds were assigned to the AuSn structure type within this study.
Interestingly, the peaks, that were observed in data mining studies, may carry additional crystallographic information as they can correspond to the so-called integral lattices.[66;67] The value of $\sqrt{8/3} = 1.633$ for the (stuffed) hcp structures implies that these structures are veritable hexagonal relatives of (stuffed) ccp structures like NaCl[4], and not NiAs that has a value of 1.39. Nevertheless, the value of $\sqrt{3/2} = 1.225$ does correspond to a pseudocubic lattice as well, the coloured primitive cubic bcc lattice. These geometric properties remain stable with respect to small deviations and result in similar diffraction patterns and structural motifs for both bcc superstructures and Ni_2In type superstructures (Paper VI). Consequently, the ideal Ni_2In structure can be understood as coloured hexagonal bcc structure.

A coloured hexagonal bcc structure

In Paper VI, the pseudo cubic nature of the structure type has been demonstrated not only from the point of view of c/a ratios but also by using a cluster approach. The 600-cell is the common polytope (4D polyhedron) from which both bcc and Ni_2In type superstructures can be generated by different projections to 3D space. Likewise the 8-cell (tesseract) is the 4D object from which both ccp and hcp may be generated via different projections to 3D space. It has been demonstrated that a rhombohedrally distorted bcc corresponds to the ω-Ti(O) structure type in space group $P6/mmm$ (No. 191) with a c/a ratio of 0.608.[69] A ternary hettotype of this structure is ω-$Ti_3Nb_{0.75}Al_{2.25}$[68] which crystallizes in space group $P\bar{3}m1$ (No.164) with a c/a ratio of 1.217. But as shown in Fig. 4.3, it is also a trigonal hettotype of the Ni_2In aristotype structure with full occupation of the trigonal bipyramidal interstices. Its colouring scheme is however different from the one that is characteristic for intermetallic Ni_2In type structures; i.e. TM atoms in octahedral and trigonal bipyramidal interstices and P network atoms.

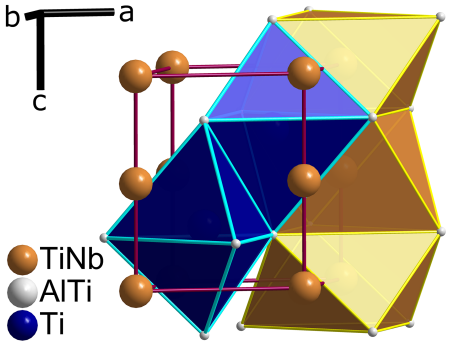

Figure 4.3.: Crystal Structure of ω-$Ti_3Nb_{0.75}Al_{2.25}$[68].

Lattice parameters of Ni_2In type structures with ideal pseudocubic axial ratios c/a can be calculated from the metrics of known chemically related bcc (super)structures. By

[3] These values are based on possible distortions of the Edshammar polyhedron, equal edges lengths are achieved for $c/a = 1.333$ and equal centre-apex distances for $c/a = 1.155$[60].
[4] A hexagonal ccp with an $ABCABC$ stacking sequence has a c/a ratio of $3\sqrt{2/3} = 2.450$. Hence, hcp with an $ABAB$ stacking sequence has to have a value of $3{\cdot}2/3{\cdot}\sqrt{2/3} = 1.633$

comparing the ideal pseudocubic axial ratios with experimentally determined values hidden lattice distortions can be revealed. For instance, the trigonal structure of LT-Au_7In_3 ($P\bar{3}m1$ (No. 164))[70] and the cubic structure of HT-Au_7In_3 (Au_9In_4, $P\bar{4}3m$ (No. 215))[71] are both derivative structures from a hypothetical Au-In alloy with bcc packing ($Im\bar{3}m$ (No. 229) with the lattice parameter $a = 3.28$ Å:

$$a_{\mathrm{AuIn},bcc} = 1/3 \cdot a_{Au_9In_4} = 1/3 \cdot 9.83\ \text{Å} = 3.28\ \text{Å}$$
$$a_{\mathrm{AuIn,rhombohedral}\,bcc} = \sqrt{2} \cdot a_{\mathrm{AuIn},bcc} = \sqrt{2} \cdot 3.28\ \text{Å} = 4.64\ \text{Å}$$
$$c_{\mathrm{AuIn,rhombohedral}\,bcc} = \sqrt{3/8} \cdot a_{\mathrm{AuIn,rhombohedral}\,bcc} = 2.84\ \text{Å}$$
$$a_{Au_7In_3} = 12.22\ \text{Å} \cong a_{\mathrm{AuIn,rhombohedral}\,bcc} \cdot \sqrt{7} = 12.28\ \text{Å}$$
$$c_{Au_7In_3} = 8.51\ \text{Å} \cong 3 \cdot c_{\mathrm{AuIn,rhombohedral}\,bcc} = 8.52\ \text{Å}$$

A hypothetical Ni_2In type structure Au_2In would have the lattice parameters $a = 4.64$ Å and $c = 5.68$ Å with a c/a ratio of $\sqrt{3/2} = 1.225$. The lattice parameters of the incommensurate compound Au_3In_2, a Ni_2In type structure with vacancies on site $2d$, are $a = 4.5619(5)$ Å and $c = 5.6761(8)$ Å. Comparing the c/a ratios, it is obvious that the appearance of the vacancies leads to a shrinking of the dimensions of the AB plane whereas the distance between the trigonal planes remains unchanged. As second example, a similar calculation is performed for a hypothetical compound Au_2Sn starting with the γ brass structure of Au_9Sn_4 ($I\bar{4}3m$ (No. 217))[72]:

$$a_{\mathrm{AuSn},bcc} = 1/3 \cdot a_{Au_9Sn_4} = 1/3 \cdot 9.80\ \text{Å} = 3.27\ \text{Å}$$
$$a_{\mathrm{AuSn,rhombohedral}\,bcc} = a_{Au_2Sn}\sqrt{2} \cdot a_{\mathrm{AuSn},bcc} = \sqrt{2} \cdot 3.27\ \text{Å} = 4.62\ \text{Å}$$
$$c_{\mathrm{AuSn,rhombohedral}\,bcc} = \sqrt{3/8} \cdot a_{\mathrm{AuSn,rhombohedral}\,bcc} = 2.83\ \text{Å}$$
$$c_{Au_2Sn} = 2 \cdot c_{\mathrm{AuSn,rhombohedral}\,bcc} = 5.66\ \text{Å}$$

For comparison, the structure of AuSn[48] has the lattice parameters $a = 4.32$ Å and $c = 5.52$ Å with a c/a ratio of 1.28, a value that is significantly larger than the pseudocubic value of 1.225. It is further interesting that the unit cell volume is shrinking anisotropically, as the interatomic distances in the AB plane decrease more than those perpendicular to the plane. An anisotropic change in the lattice dimensions has also been observed for the pseudo binary phases Au_6Sn_5Sb and Au_3InSn_2. (Paper IV)
But how does the lattice behave on the introduction of vacancies on the network sites, as observed for in the Ni_2In type superstructures of Cu_7In_3 and $Cu_2In_{0.75}Sb_{0.25}$? (Paper VI) We start with bcc type Cu_4In ($Im\bar{3}m$ (No. 229))[59] and its 27 fold superstructure Cu_9In_4 ($P\bar{4}3m$ (No. 215))[59] to create the metrics of HT-Cu_2In[59], whose c/a ratio is very close to pseudocubic value 1.224:

$$a_{Cu_4In} = 2.99\ \text{Å} \cong 1/3 \cdot a_{Cu_9In_4} = 3.03\ \text{Å}$$
$$a_{\mathrm{rhombohedral}\,Cu_9In_4} = \sqrt{2} \cdot a_{Cu_9In_4/3} = 4.29\ \text{Å} = a_{\mathrm{HT-}Cu_2In}$$
$$c_{\mathrm{rhombohedral}\,Cu_9In_4} = \sqrt{3/8} \cdot a_{\mathrm{rhombohedral}\,Cu_9In_4} = 2.62\ \text{Å}$$
$$c_{\mathrm{HT-}Cu_2In} = 5.23\ \text{Å} \cong 2 \cdot c_{\mathrm{rhombohedral}\,Cu_9In_4} = 5.25\ \text{Å}$$

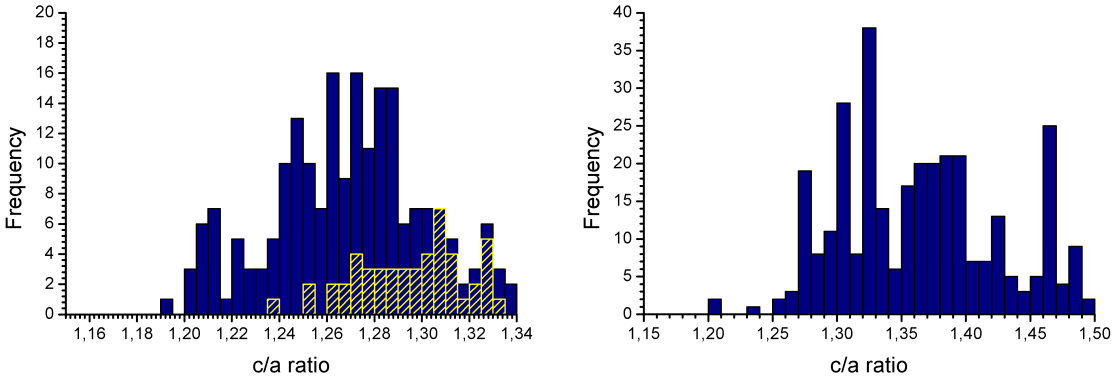

(a) Binary and ternary compounds with Ni_2In type superstructures.

(b) NiAs type structures as enlisted in Pearson's database [65].

Figure 4.4.: Left: Frequency distributions of the c/a ratios of binary and ternary compounds with Ni_2In type superstructures. Compounds with vacancies on the trigonal bipyramidal sites $2d$, such as AuSn type structures, are indicated by the line pattern. References are given in Appendix B. Right: Frequency distributions of the c/a ratios of compounds that are listed as NiAs type structures in Pearson's database [65]. The maximum c/a value for pseudocubic structures of the AuSn structure type is 1.333.

The description of the Ni_2In structure type as coloured hexagonal bcc arrangement implies a more intuitive view on the formation of superstructures, as vacancies appear mainly on the trigonal-bipyramidal sites ($2d$) or the network sites ($2c$). In general, empty trigonal bipyramidal interstices, as in the AuSn type structures, lead to a significant increase of the c/a ratio whereas vacancies on the network sites lead to a decrease of this value. (Fig. 4.4(a)) For instance, the c/a ratio of Cu_7In_3 and Sb-doped Cu_7In_3 are 1.219 and 1.209 whereas it is 1.208 in $Cu_2In_{0.75}Sb_{0.25}$. Vacancies on the octahedral sites are difficult to stabilize, as they disobey the general trend towards close packing [73]; and the subsequent structural distortion is leading to a drastic increase of the c/a ratio. However, localized valence electrons do have an effect on the c/a ratios too, because partial ionic bonding leads to an increase of the c/a ratios that can be imagined as a "hexagonal" distortion away from the pseudocubic case. Unsurprisingly, there is a shallow shift for these compounds from AuSn type structures towards the distorted hcp arrangement of the NiAs type structures (see Fig. 4.4(b)).

Interestingly, small deviations from the colouring scheme do not lead to large deviations from the pseudocubic value, instances are the substitution of some TM atoms with P atoms on octahedral sites in $Ni_{13}In_9$ and $Cu_{11}In_9$ (Paper V). In contrast to that, structures belonging to the Ti_5Ga_4-Mn_5Si_3 structure family or the α-Ti_6Sn_5 and Ni_2Al_3 structure types resemble entirely different colouring schemes of the hexagonal bcc structure. For this reason, they are not members of the family of Ni_2In type superstructures. The driving forces for deviations of their c/a ratios from the ideal pseudocubic value may be different and have not been investigated so far. Supporting Information on this topic id collected in Appendix B.1.

4.2. Superstructure Formation in the Ternary Intermetallic Compounds

Superstructures of the Ni_2In structure family are pseudocubic bcc atom arrangements with a very pronounced colouring scheme. In section 3.2 it was shown how the building blocks that resemble the colouring can be used to guide syntheses of new ternary intermetallic compounds. Nevertheless, their diffraction patterns show very strong pseudohexagonal symmetry of the Ni_2In basic lattice. For instance, orthorhombic distortions are recognizable only from the appearance of weak superstructure reflections that break the hexagonal symmetry in the diffraction patterns, whereas the underlying metric relationships of the hP Bravais lattice are not affected[74]:

$$a_{\mathrm{ortho}} = a_{\mathrm{hex}} \qquad b_{\mathrm{ortho}} = \sqrt{3} \cdot a_{\mathrm{hex}} \qquad c_{\mathrm{ortho}} = c_{\mathrm{hex}} \cong \sqrt{3/2} \cdot a_{\mathrm{hex}}$$

As a result, average structure models based on the strong reflections of the Ni_2In aristotype are accessible both from powder and single crystal diffraction. They become useful in cases where an integration of the weak superstructure reflections fails due to a poor signal to noise ratio or severe peak overlap. Any of those structure models has the lattice coincidences and the space group of the aristotype, $P6_3/mmc$ (No. 194). Notably, the average models describe an artificially disordered atomic arrangement, because any observation of extra reflections indicates site specific ordering that is usually accompanied by a symmetry reduction and larger unit cells, the so-called superstructure formation.
Within the binary compounds TM-P, ordered vacancies on the network ($2c$) or the trigonal bipyramidal interstices ($2d$) are the main reasons for the formation of Ni_2In type superstructures. On addition of a third element, additional ordering schemes are possible.
In the following sections, the influence of composition and temperature on the formation of Ni_2In superstructures will be discussed. The first part is focussed around the question: Which structure motifs are stabilized in the ternary compounds upon mixing two different elements in the network or in the interstices? Besides the Cu-In-Sb compounds and the pseudobinary Au-Sn phases, the crystal structures of novel ternary compounds and solid solutions that are not covered within the manuscripts will be presented. In the second part, the impact of different annealing temperatures on the formation of

superstructures will be discussed in detail for $Cu_{5+\delta}In_2Sb_2$ as well as two new ternary compounds from the ternary epf in Cu-In-Sn. Additionally, selected diffraction images are presented to support the description of observed superstructure reflections visually. In a third part, the superstructure formation in ternary Ni_2In type superstructures is summarized briefly. Details on the structural data of all presented ternary phases and compounds are given in the Appendices B.2 to B.5.

Composition dependent formation of Ni_2In type superstructures

The determination of the composition of any new pseudo-binary or real ternary compound allows for a first prediction on the occupation of the different sites in the aristotype lattice: If the TM content is between 50 and 66 at-%, a full occupation of the octahedral and a partial occupation of the trigonal bipyramidal interstices is expected. Higher TM contents, up to 72 at-%, indicate the presence of vacancies on the network sites. But, this knowledge alone does not allow for model building and structure solution from scratch as the ordering has to be governed either by *size* and/or *site* preference.
The idea behind **size preference** is that, for instance, in ternary compounds with two different TM the larger atoms will prefer the octahedral interstices whereas smaller atoms will prefer trigonal bipyramidal interstices. This hypothesis was tested for ternary phases $Au_{3-x}Ni_xIn_2$, $Pt_{3-x}Ni_xIn_2$ as well as $Au_{3-x}Cu_xIn_2$. Unsurprisingly, this simple geometric concept failed as it neglects other factors like attractive or repulsive interactions of the valence electrons. For this reason, local atomic arrangements are better discussed as a result of site preference.
The idea behind **site preference** is that different atoms prefer specific coordination environments over competing ones with random next neighbour atoms. Instances for this effect are the Ni_2In type superstructures in **Cu-In-Sb**. In the dimorphic compound $Cu_{5+\delta}In_2Sb_2$ (Paper I, III), the pseudohexagonal network is formed by layers with exclusively In atoms or mixed In-Sb layers. Cu atoms occupy all octahedral interstices and less than half of the trigonal bipyramids. Interestingly, extra Cu atoms prefer as few Sb atoms in their coordination sphere as possible. They are located only in In layers wherein their trigonal bipyramidal coordination polyhedra have Sb apexes. (3 In atoms and 2 Sb atoms) The *vice-versa* arrangement which consists of three Sb-atoms in the plane and two In apexes cannot be stabilized. This ordered preference of crystallographic coordination spheres results in an orthorhombic distortion and a doubling of the hexagonal c axis. In the second ternary compound $Cu_2In_{0.75}Sb_{0.25}$ (Paper VI), the coordination sphere around the Cu atoms in trigonal bipyramidal interstices consists of four In atoms and one Sb atom. There is still an orthorhombic distortion of the unit cell, but the number of Sb atoms has to decrease in the network in order to host more Cu atoms in the interstices. Another conclusion from the observed site preferences is that different elements on the network sites will lead to a symmetry reduction from the aristotype symmetry that can by accompanied an enlargement of the unit cell.
Notably, symmetry reductions due to different elements on the network sites do not result in orthorhombic distortions exclusively. An example is the rhombohedral superstructure of $\mathbf{Ni_{1.68}In_{0.33}Sn_{0.67}}$ wherein Ni atoms occupy all octahedral and about 2/3 of the trig-

onal bipyramidal interstices (Confer Fig. 4.5(a)). The network is best understood as an $ABAB$ stacking of Sn layers and mixed In/Sn layers. Within the Sn layers 2/3 of the trigonal bipyramidal interstices are fully occupied with Ni atoms. As shown in Fig. 4.5(c), empty trigonal bipyramidal interstices are constructed by a triangle of three Sn atoms and two In atom apexes whereas occupied interstices have only one In apex. In the second kind of layer (Confer Fig 4.5(d)), the network consists of In atom honeycombs that enclose sole Sn atoms. As a result, roughly 2/3 of the trigonal bipyramidal interstices are occupied randomly and not in an ordered fashion as in the Sn-layers. By this, Ni atoms are coordinated by two In atoms and three Sn atoms, and we can conclude that there is a general tendency towards full coordination of Ni atoms with as few Sn atoms as possible.

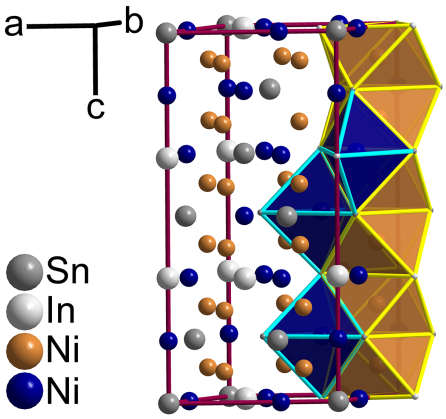

(a) Unit cell of $Ni_{1.68}In_{0.33}Sn_{0.67}$

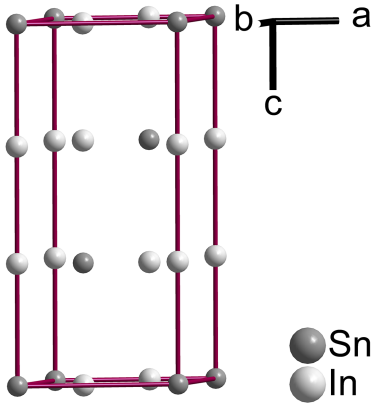

(b) Origin of the rhombohedral distortion: ordered arrangement of Sn atoms.

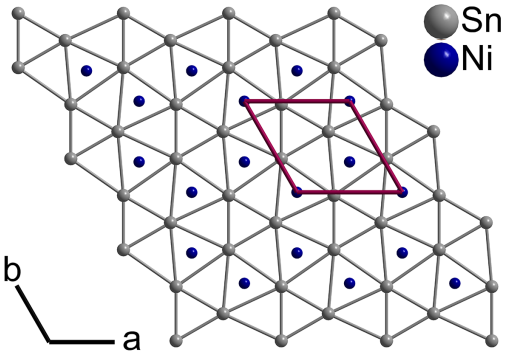

(c) Sn-layers along the (pseudohexagonal) c-axis

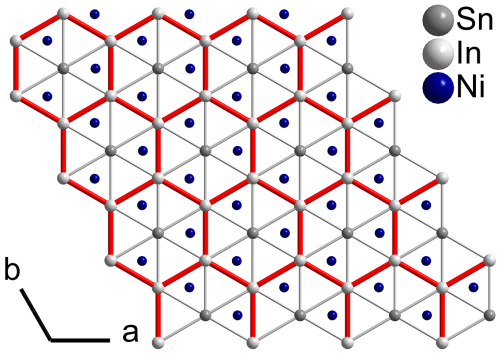

(d) Mixed In/Sn layers: 2/3 of the Ni atoms are occupied randomly.

Figure 4.5.: Crystal Structure of $Ni_{1.68}In_{0.33}Sn_{0.67}$, after annealing at 573 K. Ni atoms in octahedral interstices are depicted in Cu-colour whereas Ni atoms that (partly) occupy trigonal bipyramidal interstices are depicted in blue.

This explains why none of the binary Ni-In compounds with Ni_2In type superstructures forms extended solid solutions on the addition of Sn. But, it does not elucidate the rhombohedral distortion as two different kinds of layers in an *ABAB* stacking sequence should double and not treble the *c* axis of the aristotype structure, as observed in $Cu_5In_2Sb_2$. If we disregard all other atoms and concentrate just on the arrangement of the Sn atoms in the mixed layers, as shown in Fig. 4.5(b), it becomes clear that the rhombohedral symmetry is a result of the atomic order of Sn in the pseudohexagonal network. The crystal structure of $Ni_{1.68}In_{0.33}Sn_{0.67}$ does therefore resemble a new 9 fold superstructure of the Ni_2In structure type.
There is second novel ternary compound in the ternary epf of Ni-In-Sn, i.e. $\mathbf{Ni_5In_2Sn}$. The occurrence of a compound with that particular TM content is interesting, because *Norén and coworkers* found indications of a phase Ni_5In_3 in an electron diffraction study.[56] They assumed that this phase crystallizes isostructural to Ni_5Ge_3[75], but neither they[76] nor experiments within the framework of this project were successful in synthesizing the compound. The crystal structure of Ni_5In_2Sn is however not isostructural to Ni_5Ge_3, and is therefore best described as a new Ni_2In superstructure type.
In contrast to the crystal structure of $Ni_{1.68}In_{0.33}Sn_{0.67}$, the ordering of the In and Sn atoms on different network sites does not lead to an enlargement of the aristotype *c* axis. As depicted in Fig. 4.6(a), it is an orthorhombic distortion which resembles a 3 fold superstructure along the orthohexagonal *a* axis in space group *Cmcm* (No. 63). The mixed In/Sn layers have the same honeycomb motif of In atoms around single Sn atom islands as present in the mixed layers in $Ni_{1.68}In_{0.33}Sn_{0.67}$ (Refer Fig. 4.6(b)).

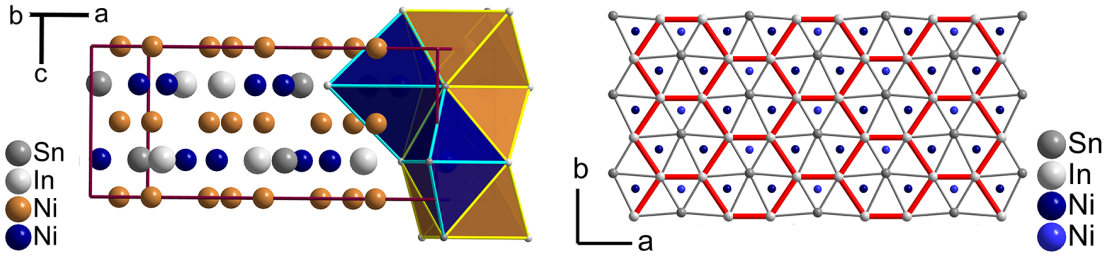

(a) Unit cell of Ni_5In_2Sn

(b) Mixed In/Sn layers: 1/3 of the Ni atoms are occupied.

Figure 4.6.: Crystal Structure of Ni_5In_2Sn, after quenching from 573 K. Ni atoms in octahedral interstices are depicted in Cu-colour whereas Ni atoms that (partly) occupy trigonal bipyramidal interstices are depicted in blue of which dark blue Ni atoms have a site occupancy of 45% and light blue Ni atoms have a site occupancy of 5%.

However, the occupational pattern of the Ni atoms in the trigonal bipyramidal interstices is different, as there are two different kinds of under-occupied coordination polyhedra that have a basic triangular plane built of two In atoms and one Sn atom. Ni atoms with a site occupancy of about 5% have two Sn apexes whereas Ni atoms with a site occupancy of about 45% have two In apexes. As a conclusion, Ni atoms prefer trigonal bipyramidal interstices with as many In vertices as possible in Ni_5In_2Sn while the opposite holds true for $Ni_{1.68}In_{0.33}Sn_{0.67}$. Remarkably, about 2/3 of the trigonal bipyramidal interstices are occupied in both ternary compounds of the Ni-In-Sn ternary epf, but their Ni_2In type superstructures differ in dependence on the composition of the pseudohexagonal network.
In contrast to those findings of real ternary compounds with Ni_2In type superstructures, two different elements on the network sites do not lead to site preference necessarily. For instance, no superstructure ordering was found in $\mathbf{AuIn_{0.33}Sn_{0.67}}$ and $\mathbf{AuSn_{0.83}Sb_{0.17}}$ (Paper IV); both compounds are solid solutions of a third element in the binary compound AuSn. A possible explanation for this observation is that there are no partial vacancies of any kind in these two compounds which can "force" network ordering, for instance, extra TM atoms in trigonal bipyramidal interstices have a preferred P element coordination environment. These energetically stable arrangements. On the other hand, a partial occupation is known for $Au_{3+\delta}In_2$ and it is still unclear why the structural motif from the binary compound $Au_{3+\delta}In_2$ is apparently absent in any ternary system Au-In-P.
Additionally, it is possible to stabilize a HT modification of a binary compound at low temperatures on the addition of a third element. Two very interesting examples of such cases are the incommensurately modulated structures of $\mathbf{Cu_7In_{4-x}Ge_x}$ and $\mathbf{Cu_7In_{4-x}Sn_x}$ (Confer Fig. 4.7 and 4.8). Both are isostructural to the A-phase of Cu_7In_4 which crystallizes in the 3+2 d superspace group $P6_3/m(\alpha,\beta,0)(-\alpha-\beta,\alpha,0)00$ (No. 176.2.80.1). While the binary phase A-Cu_7In_4 is stable between 650 K and at least 773 K[77], the ternary phases show similar diffraction patterns even at 373 K. Notably, there is only one In position in the asymmetric unit of the structural model, and Sn or Ge atoms mix with In atoms on that site randomly. Since B-Cu_7In_4 is also incommensurately modulated[77], the driving force for the aperiodicity in three dimensions is the severe occupational modulation of the Cu atoms in the trigonal bipyramidal interstices. Just like in the incommensurately modulated structure of Cu_3Sn (Paper II), the dominant occupational modulation of one site is accompanied by positional modulations for the other sites in the unit cell, i.e. the Cu atoms in the octahedral interstices and the network atom position. One can imagine this "movement" as relaxation of all interatomic distances with respect to the presence or absence of the extra Cu atoms. The major difference between the A and the B phase is not only the order and the positions of the satellite reflections[77], but the shape of the occupational modulation waves. While harmonic functions are the mathematical model of choice for the A phase, the B phase would be better described by Crenel functions[78;79]. In terms of atomic order in the structures, this means that the two ternary compounds $Cu_7In_{4-x}Ge_x$ and $Cu_7In_{4-x}Sn_x$ are more disordered than the binary compound B-Cu_7In_4 at temperatures below 523 K.

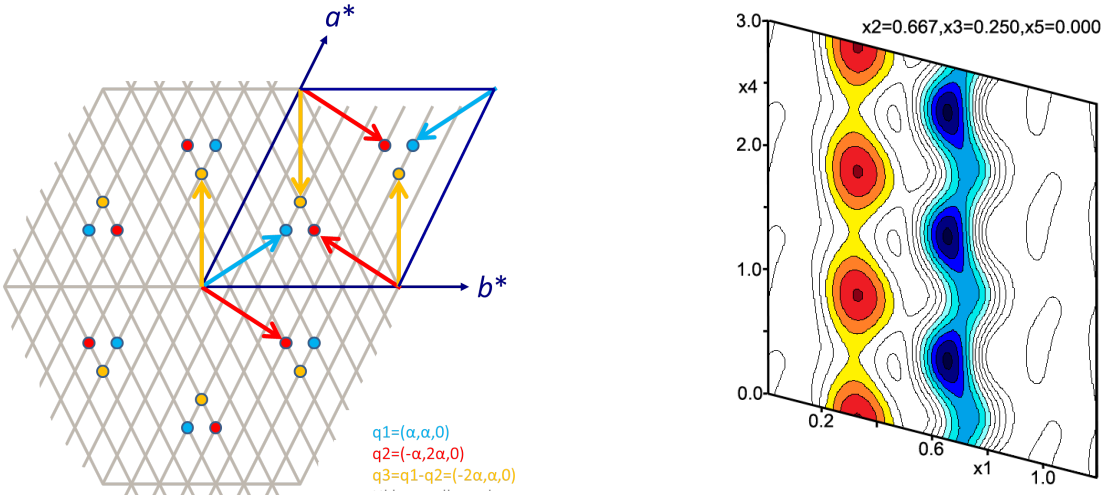

(a) $Cu_7In_{4-x}Sn_x$ construction of observed reflections

(b) $Cu_7In_{4-x}Sn_x$ occupational modulation function

Figure 4.7.: Left: Theoretical construction of the observed superstructure reflections according to modelling in a hexagonal 3+2 d superspace group. Right: Structural implications of the occupational modulation function: Interatomic In(Sn) distances (blue) vary dependent on presence of a Cu atom in the trigonal bipyramidal interstices (yellow-red).

So far, only superstructure formations in compounds of the general formula TM-P1-P2 have been discussed. Ternary compounds of the general formula TM1-TM2-P can form superstructures too. Examples from the literature are $AuCuSn_2$ [80], $AuNiSn_2$ [80] or $CuNiSb_2$ [81] which resemble ordered AuSn type structures with layer formation of the atoms in the octahedral interstices along the hexagonal c axis. But as for the compounds TM-P1-P2, most of the reported ternary compounds are pseudo-binary alloys and not real ternary intermetallic compounds. This has been the case for some of the studied systems TM1-TM2-P too, but an additional problem for understanding the ternary phases is the insufficient knowledge on the correct structures of the surrounding binary compounds.

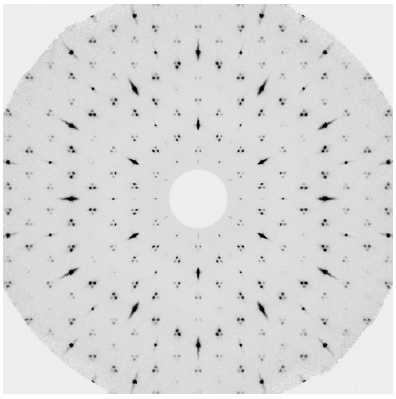

(a) A-Cu_7In_4

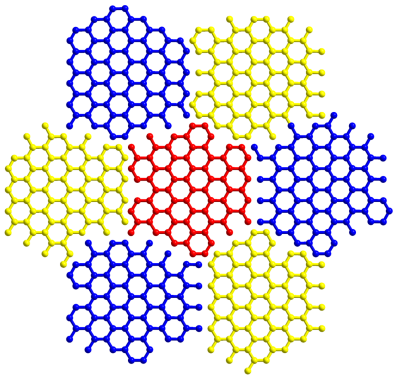

(b) A-Cu_7In_4, 10x10x1 approximant

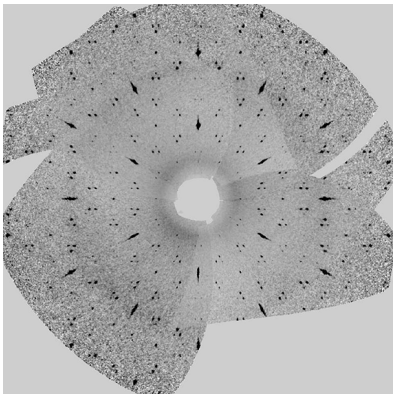

(c) $Cu_7In_{4-x}Sn_x$, 373 K

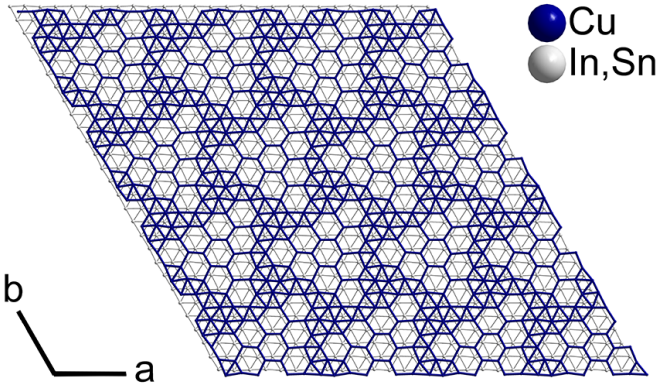

(d) $Cu_7In_{4-x}Sn_x$, 7x7x1 approximant

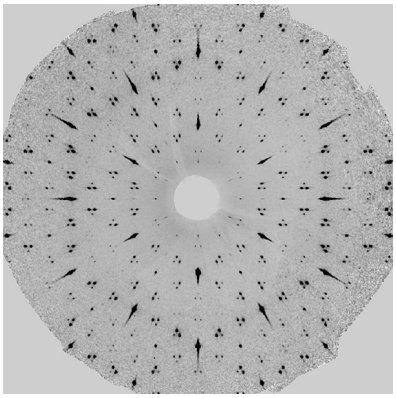

(e) $Cu_7In_{4-x}Ge_x$, 373 K

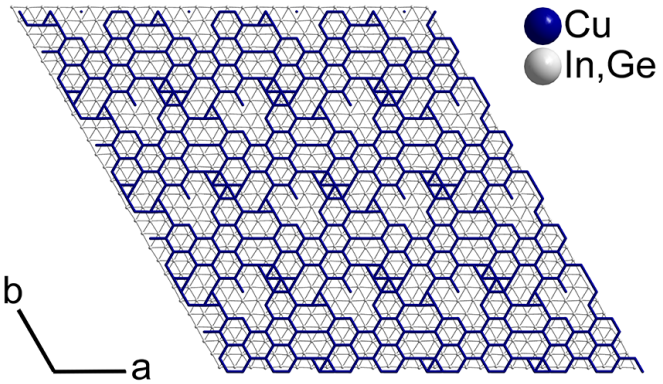

(f) $Cu_7In_{4-x}Ge_x$, 7x7x1 approximant

Figure 4.8.: Left: Reconstructed reciprocal ($hk0$) layers. Right: Trigonal nets in A-Cu_7In_4, $Cu_7In_{4-x}Sn_x$ and $Cu_7In_{4-x}Ge_x$. The images were created by drawing approximant structures at a given cut-off occupancy of 0.5 and t_0=0. Interatomic Cu-Cu distances up to 5Åare shown in blue. The images on A-Cu_7In_4 are depicted by courtesy of Sven Lidin.

The superstructure of **Au_3In_2** has been mentioned on various occasions in the text. As shown in Fig. 4.9, the superstructure formation seems to be dependent on the composition of the sample as well. The satellite reflections indicate that the non-stoichiometric sample is isostructural to A phase Cu_7In_4, but they are too weak and too close for a reliable data integration. Moreover, it is not clear yet whether or not these are two different phases in the same phase field or two different compounds, because the resolution of the X-Ray diffraction experiments suffers from an interesting effect: The exact composition $Au_{3.0}In_{2.0}$ leads to 49 electrons from indium and additional 26 electrons from Au which sum up to 75 electrons. The difference to the neighbouring Au layers where the Au atoms occupy the octahedral interstices of the Ni_2In structure is only four electrons. For a non-stoichiometric composition $Au_{3.14}In_2$, as present in the stoichiometric sample due to AuIn formation as minor phase, the number of electrons in the In layers and the octahedral Au layers is equal with 79 electrons per layer. Therefore, the electron densities suggest a hexagonal bcc arrangement of Au atoms only which does not correspond to the correct crystal structure with a hexagonal c axis that is twice as large. However, the reported crystal structure[82] is giving a rather incomplete insight into the structure motifs because extra superstructure reflections are not modelled.

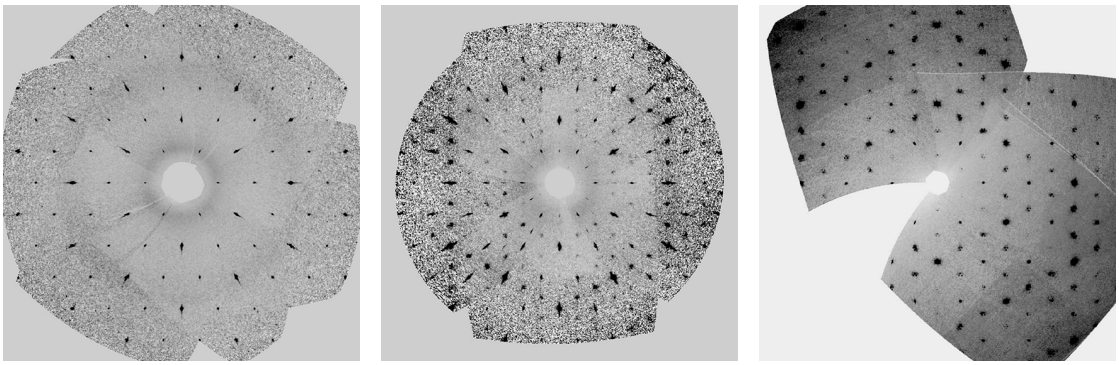

(a) Au_3In_2, in-house data (b) $Au_{3.2}In_2$, in-house data (c) $Au_{3.2}In_2$, I19@Diamond

Figure 4.9.: Reconstructed reciprocal ($hk0$) layers for stoichiometric and non-stoichiometric samples of Au_3In_2, annealing temperature 703 K. For comparison data collected at beamline I19 at the Diamond light source is also shown.

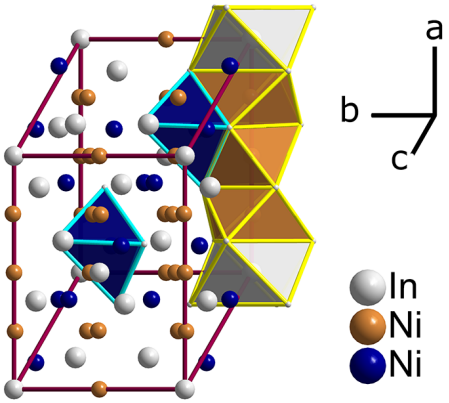

(a) Unit cell of $Ni_{13}In_9$

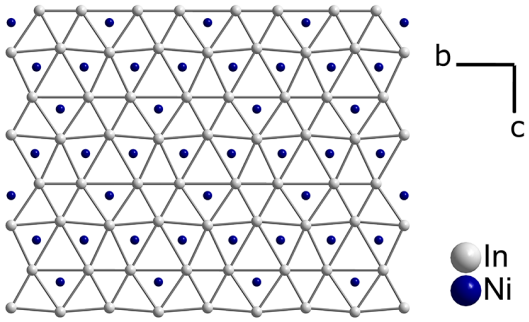

(b) In layer in $Ni_{13}In_9$

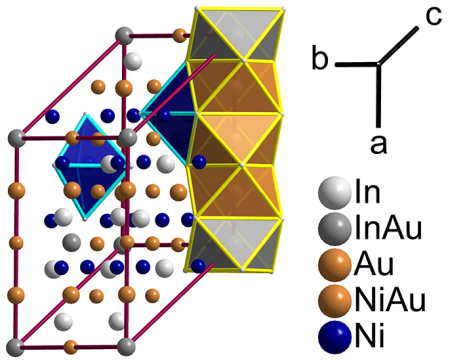

(c) Unit cell of $Au_{3.895}Ni_{9.283}In_{8.812}$

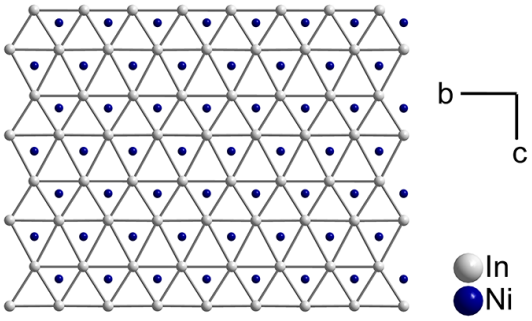

(d) In layer in $Au_{3.895}Ni_{9.283}In_{8.812}$

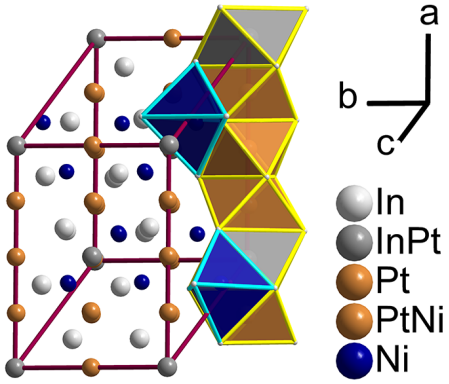

(e) Unit cell of $Ni_{7.642}Pt_{5.498}In_{8.86}$

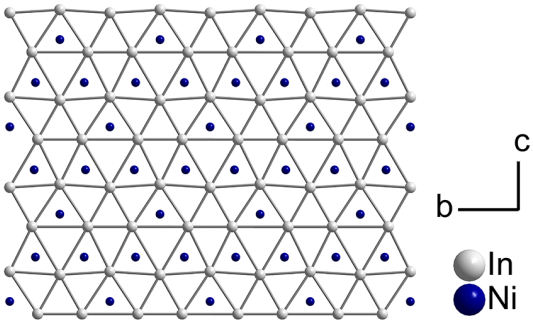

(f) In layer in $Ni_{7.642}Pt_{5.498}In_{8.86}$

Figure 4.10.: Crystal Structures of $Ni_{13}In_9$ and the structurally related pseudobinary phases $Au_{3.895}Ni_{9.283}In_{8.812}$ and $Ni_{7.642}Pt_{5.498}In_{8.86}$; TM atoms in octahedral interstices are depicted in Cu-colour whereas Ni atoms that occupy the trigonal bipyramidal interstices are shown in blue.

Since Au_3In_2 is difficult to understand, the **Au-Cu-In** system clearly needs more work. The average structures do not tell the whole story, because observed diffuse scattering is neglected during the integration. Moreover, the c/a ratios increase on dissolving Au in Cu_7In_4 until they reach a maximum value of approximately 1.27, and then they shrink back to 1.24 - the value for Au_3In_2. This means that a constant solid solubility is not very likely, but also that the hexagonal distortion away from the pseudocubic value of 1.225 is more severe for In atom networks than for Sn atom networks; the Au-Cu-Sn compounds have c/a ratios of 1.237. Although, the different network forming element may not be the reason for this anisotropic behaviour after all, because the TM content is significantly higher in the In-alloys.
Similar effects have been observed in **Au-Ni-In** and **Ni-Pt-In**. The pseudobinary phases $Ni_{13-x}TM_xIn$ may show further superstructure formation upon longer annealing times at lower temperatures since the larger elements Au und Pt do not mix with the smaller Ni atoms on the trigonal bipyramidal interstices. In contrast to binary $Ni_{13}In_9$, they partly replace In atoms from the octahedral site. This means that the ternary compounds have a stronger tendency towards the classical colouring scheme of Ni_2In type superstructures as the binary compound $Ni_{13}In_9$. Hence, their measured compositions are TM-richer than the binary starting compound.
Surprisingly, compounds of the general formula $\mathbf{(Ni,Cu)_{2\pm x}In}$ form entirely new kinds of Ni_2In type superstructures. Different metallic radii of interstitial atoms are not considered to be a driving force for neighbours in the periodic table, such as Ni and Cu. The crystal structures of the ternary compounds are related to the Ni_2In type superstructure of Cu_7In_3, but they are not isostructural. Due to the complexity of the observed structure motifs, the discussion of the structures is omitted and some diffraction images are shown in Fig. 4.11 to illustrate the diversity of the superstructures in the ternary compounds.

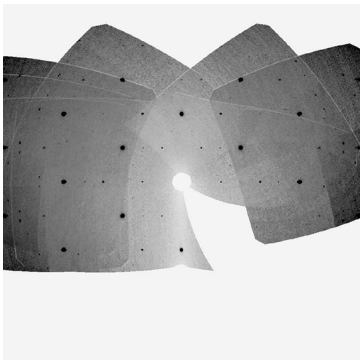

(a) nominal composition Ni_2In, ($hk0$)

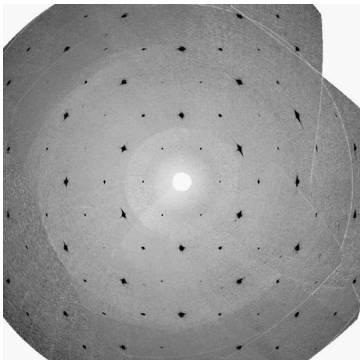

(b) nominal composition $Ni_1Cu_6In_3$, ($hk0$)

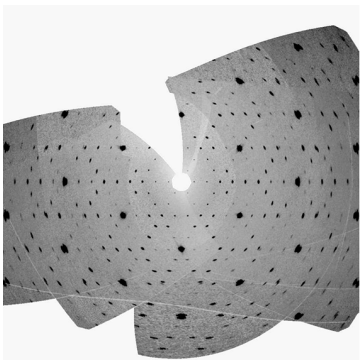

(c) nominal composition $Ni_4Cu_3In_3$, ($hk0$)

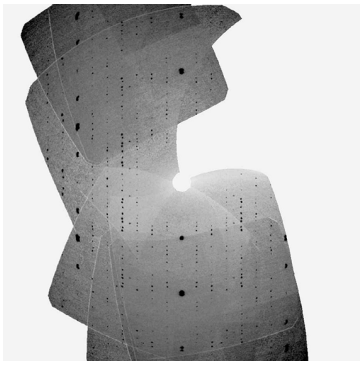

(d) nominal composition Ni_2In, ($1\bar{3}1$)

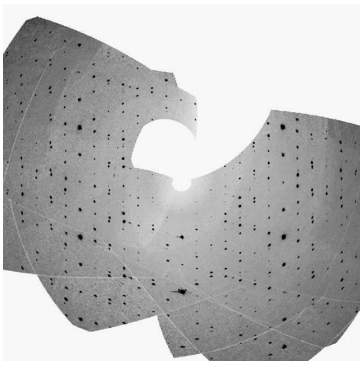

(e) nominal composition $Ni_1Cu_6In_3$, ($1\bar{3}1$)

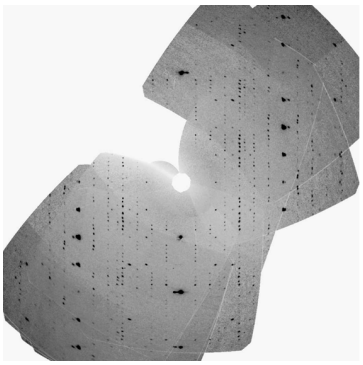

(f) nominal composition $Ni_4Cu_3In_3$, ($1\bar{3}1$)

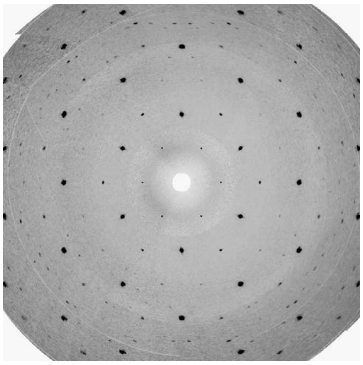

(g) nominal composition $Ni_6Cu_1In_3$, ($hk0$)

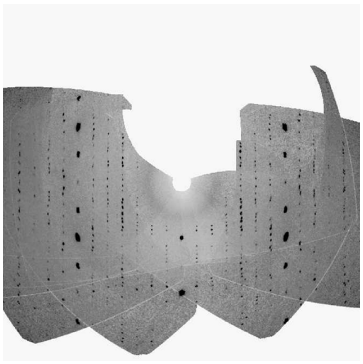

(h) nominal composition $Ni_6Cu_1In_3$, ($1\bar{3}1$)

Figure 4.11.: Selected examples for the occurrence of weak satellite reflections in $Ni_{7-x}Cu_xIn_3$, annealing temperature 573 K. The diffraction patterns were recorded at I19@Diamond whereas observed strong reflections were indexed in the Ni_2In aristotype lattice for the reconstruction of the layers.

Temperature dependent formation of Ni_2In type superstructures

Most of the superstructure formations and transformations within the studied ternary intermetallic compounds are diffusive and not re-constructive. This is a clear advantage for solving and refining their crystal structures, because the superstructures are related via group-subgroup relations to the Ni_2In aristotype. For this reason, idealized atomic positions can be calculated by transforming the aristotype lattice to the supposed hettotype lattice, which may be used as a starting model for subsequent structure solution and refinement.
At high temperatures, the crystal structures are disordered and can be solved in the aristotype lattice in the hexagonal space group $P6_3/mmc$ (No. 194). For phases TM1-TM2-P, a random occupation of the TM atoms and vacancies is expected on the interstitial sites $2a$ and $2c$. For phases TM-P1-P2, the P atoms form the hexagonal network by random occupation of site $2c$. Pronounced site specific atomic ordering requires lower temperatures. For instance, in the case of an incommensurate HT modification, a lock-in of the modulation vector at a metrical commensurate value is expected to occur on annealing at reasonably low temperatures. As depicted in Fig. 4.12(a) to 4.12(c), the sharp Bragg reflections of the HT modification of $Cu_{5+\delta}In_2Sb_2$ smear out to trident like diffuse spots before they reach the final positions of the LT modification. Interestingly, by this they are following the group-subgroup relation between the polymorphs (Paper III).

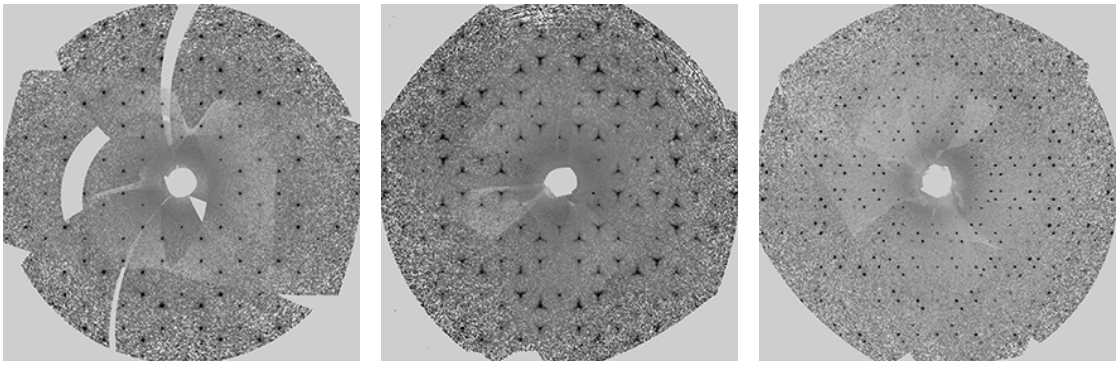

(a) $Cu_{5.5}In_2Sb_2$, 673 K (b) $Cu_{5.5}In_2Sb_2$, 623 K (c) $Cu_{5.5}In_2Sb_2$, 573 K

Figure 4.12.: Reconstructed reciprocal ($hk1$) layers in samples $Cu_{5+\delta}In_2Sb_2$: Structure transformation from the HT to the LT modification that is stable at room temperature.

Resulting ternary superstructures are periodic, but not necessarily in 3D space. Moreover, a lock-in of the modulation at commensurate values at lower temperatures is not necessarily representing a stable atomic arrangement, as the example of the polymorphic compound **$Cu_7In_{1.8}Sn_3$** will illustrate. In contrast to the results of PND studies by *Sommadossi and coworkers* [83;84], the ternary epf is consisting of different ternary compounds and miscibility gaps, refer Fig. 3.9. The crystal structure of $Cu_7In_{1.8}Sn_3$ is neither resembling a pseudo-binary phase of Cu_5Sn_4 [85], including Cu_6Sn_5 [44], nor is it closely related to $Cu_{10}In_7$ [57] or B-phase Cu_7In_4 [77]. As shown in Fig. 4.14 and 4.15, the observed diffraction patterns and, thus, the crystal structure of this compound are significantly changing in dependence on the annealing temperature.
At 673 K, there are no superstructure reflections in addition to the strong reflections of the Ni_2In aristotype. In its crystal structure, Cu atoms occupy all octahedral interstices ($2a$) and randomly about half of the trigonal bipyramidal interstices ($2d$) whereas about 38 at.-% of the Sn atoms in the hexagonal network ($2c$) are substituted by In atoms randomly. Remarkably, the presence of the aristotype structure at 673 K does not imply that there is a solid solution from Cu_7In_4 or HT-Cu_2In to Cu_5Sn_4 wherein the lattice parameters of the aristotype lattice change continuously. The reason is that the 3+2 d superstructure of the ternary phase $Cu_7In_{4-x}Sn_x$ is not isostructural to the aristotype lattice. Moreover, the HT modification of $Cu_7In_{1.8}Sn_3$ is a metastable phase that transforms the LT modification within one year of RT annealing.

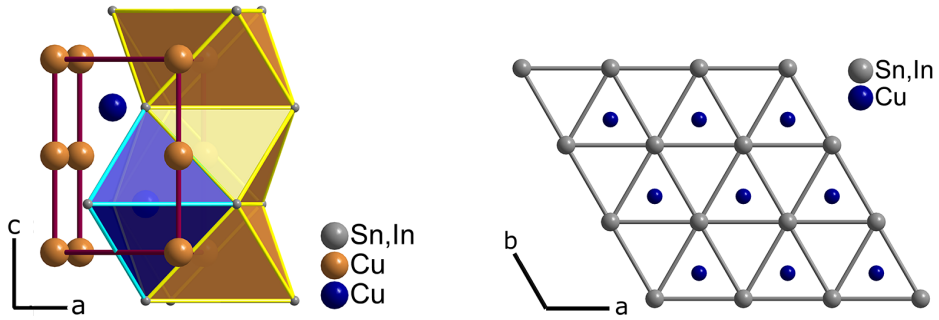

(a) Unit cell (b) Mixed In/Sn layer

Figure 4.13.: Crystal Structure of HT-$Cu_7In_{1.8}Sn_3$ at 673 K; Cu atoms in octahedral interstices are depicted in Cu-colour whereas Cu atoms that occupy about 1/3 of the trigonal bipyramidal interstices are shown in blue.

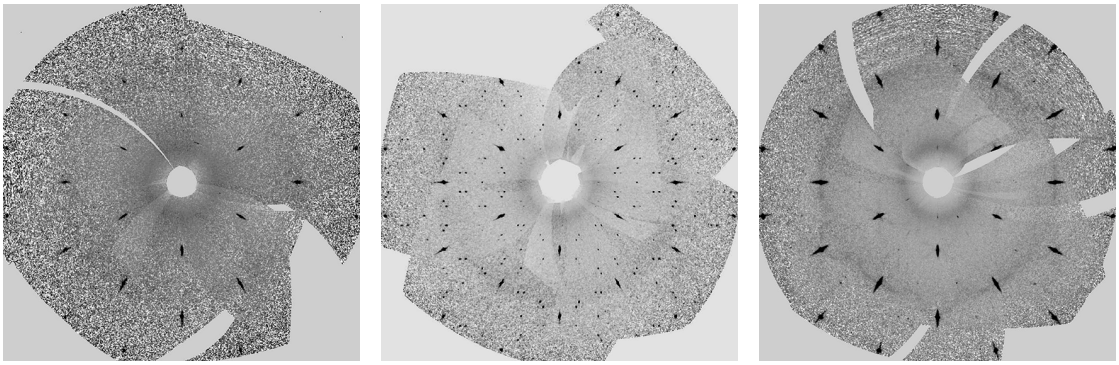

(a) $Cu_7In_{1.8}Sn_3$, ($hk0$) (b) $Cu_7In_{4-x}Sn_x$, ($hk0$) (c) $Cu_7In_{1.8}Sn_3$, ($hk0$)

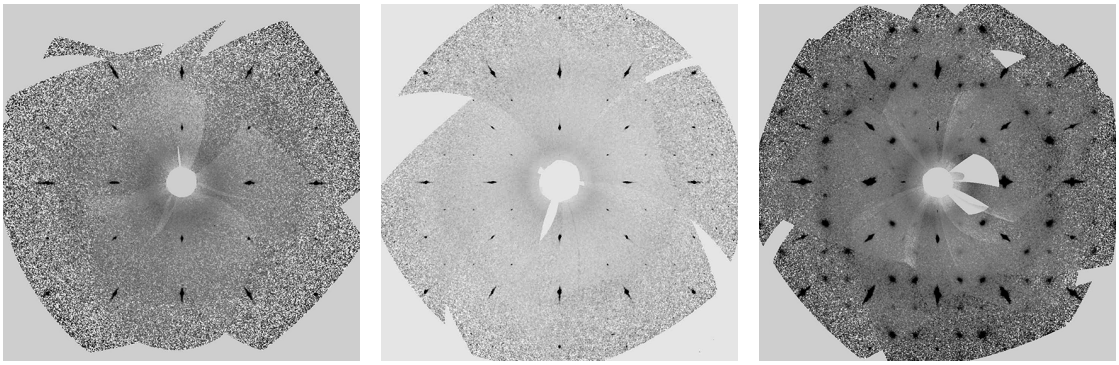

(d) $Cu_7In_{1.8}Sn_3$, (hhl) (e) $Cu_7In_{4-x}Sn_x$, (hhl) (f) $Cu_7In_{1.8}Sn_3$, (hhl)

Figure 4.14.: Reconstructed reciprocal layers: $Cu_7In_{1.8}Sn_3$ (left) and $Cu_7In_{4-x}Sn_x$ (centre) after quenching from 673 K, and $Cu_7In_{1.8}Sn_3$ (right) after quenching from 673 K and storing at RT for more than one year.

Below 673 K, weak superstructures of a 3+1 d orthorhombic superstructure in superspace group $P2_1nb$ (No. 33.1.9.2) forms upon long time-annealing (see Fig. 4.15). Interestingly, In and Sn atoms are ordering on two different crystallographic sites while the Cu atoms do no longer occupy the trigonal bipyramidal interstices randomly, as depicted in Fig. 4.16(a). In similarity to the modulated structures of $Cu_7In_{4-x}Sn_x$ and HT-$Cu_{5+\delta}In_2Sb_2$ (Paper III), the occupational modulation of the extra Cu atoms is responsible for the relaxation of all interatomic distances with respect to presence or absence of these atoms; which means that the occupational modulation of one atom is causing displacive modulations of all other atoms (Confer Fig. 4.16(b) and 4.17(b)). Another similarity is that the ordered repetition of structural motifs (translation) expands the lattice in the hexagonal AB plane, perpendicular to the c axis. But in contrast to the superstructure of $Cu_7In_{4-x}Sn_x$, the ordering of In and Sn on specific network sites leads to an elongation of the (pseudo) 6-fold axis as well.

While the structure is ordered in a small 3+1 d supercell, it can be projected to 3D space as a 10 fold superstructure of the orthorhombic distortion of the HT modification of $Cu_7In_{1.8}Sn_3$. Consequently, there is an underlying group-subgroup relation between the two polymorphs.

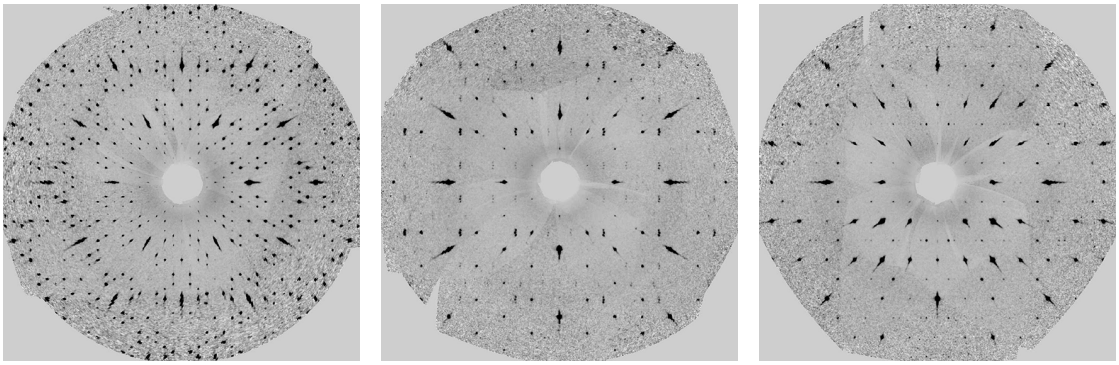

(a) $(0kl)$ (b) $(h0l)$ (c) $(hk0)$

Figure 4.15.: Reconstructed reciprocal layers from $Cu_7In_{1.8}Sn_3$ at 473 K.

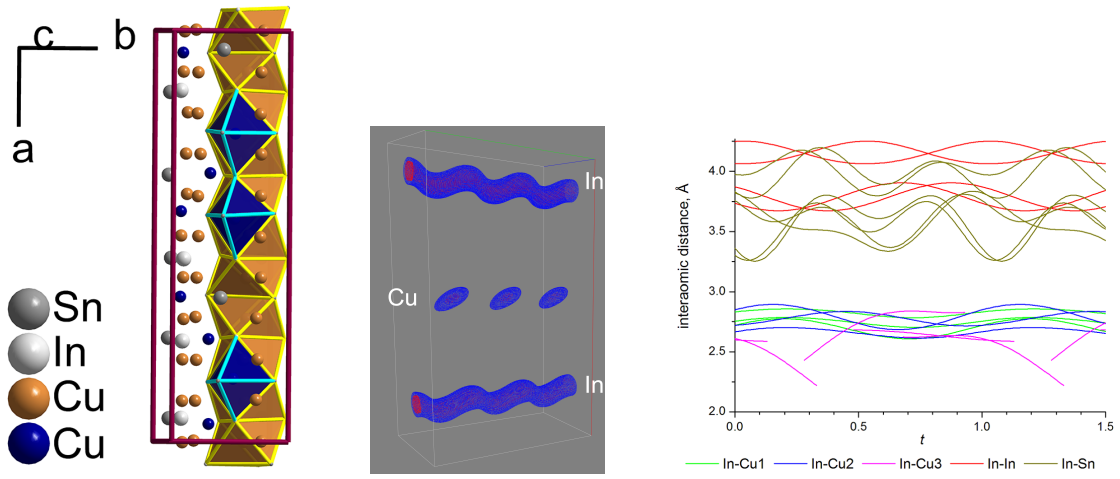

(a) Unit Cell of a 5x1x1 supercell in $P2_111$ (No. 4)

(b) Occupational modulation functions for partially occupied Cu positions

(c) Interatomic distance(t) plot

Figure 4.16.: Crystal Structure of LT-$Cu_7In_{1.3}Sn_{7.8}$ with Cu atoms in octahedral interstices in Cu-colour and Cu atoms in trigonal bipyramidal interstices in blue. Occupied trigonal biyramidal interstices consist of two In apexes and a basic triangle of two Sn and one In atoms.

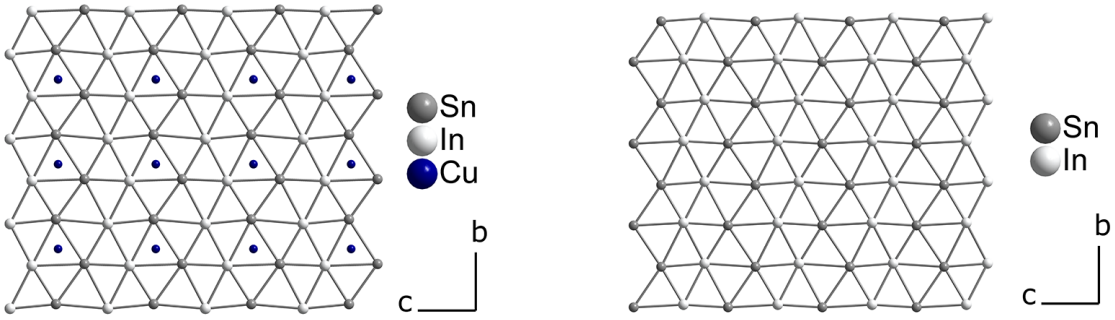

(a) mixed In/Sn layer with interstitial Cu atoms

(b) mixed In/Sn layer without interstitial Cu atoms

Figure 4.17.: Mixed In/Sn layers in the 5x1x1 supercell of LT-$Cu_7In_{1.3}Sn_{7.8}$. The two kinds of layers are stacked in an *ABAB* sequence along the *a* axis that corresponds to the *c* axis in the Ni_2In aristotype structure.

However, this is not the only Cu-Sn-rich ternary compound within the ternary epf of Cu-In-Sn at temperatures that are interesting for the permanent wetting of In-Sn solders to Cu substrates. Below 573 K, a ternary compound with a slightly higher Cu-content than $Cu_7In_{1.8}Sn_3$ and the composition $\mathbf{Cu_7In_{1.55}Sn_{2.45}}$ crystallizes in a very related Ni_2In type superstructure in the orthorhombic space group *Pnma* (No. 62), as depicted in Fig. 4.19(a). Notably, the crystal structure of this ternary compound is not isostructural to the Ni_3Sn_2 structure type, although the diffraction patterns are very alike (Confer Fig. 4.18). At 373 K, the ordering of In and Sn atoms in the orthohexagonal network is leading to In vacancies, a structural motif that has been observed exclusively in structures isostructural to the Cu_7In_3 structure type prior to this thesis. It is however remarkable that this is a LT phase, because the In vacancy structure of $Cu_2In_{0.75}Sb_{0.25}$ was stabilized upon annealing above 573 K only (Paper VI).

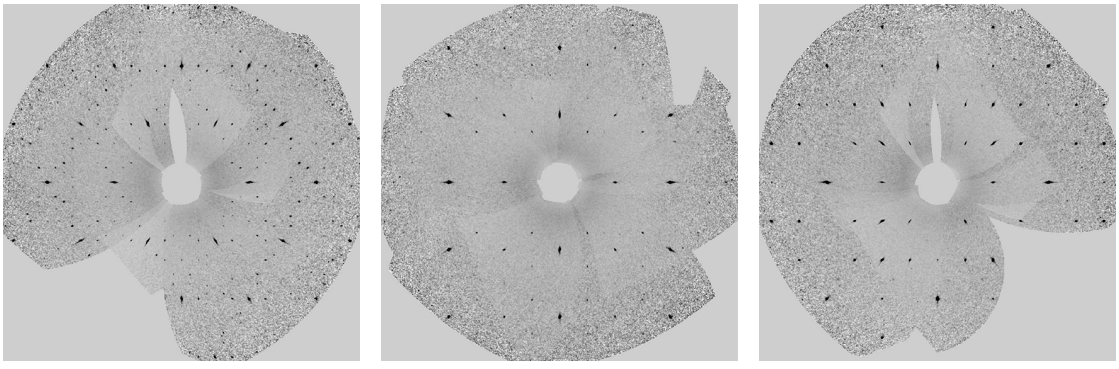

(a) 0*kl* (b) *h*0*l* (c) *hk*0

Figure 4.18.: Reconstructed reciprocal layers from $Cu_7In_{1.55}Sn_{2.45}$ at 373 K.

In similarity to the Cu-In-Sb structure, Cu atoms occupy all octahedral interstices in the network as well as the majority of the trigonal bipyramidal interstices with under-occupation of the specific sites. Hence, there are disordered Cu atoms around the In vacancies that change their position in dependence on the presence or absence of the In vacancy (see Fig. 4.19(b)). And interestingly, as discussed in Paper VI, the presence of network vacancies is leading to less distorted pseudocubic clusters in the crystal structure. In fact, the small c/a ratio of 1.213 is the result and not the cause of the nearly perfect pseudocubic symmetry. The latter has its origin in tetrahedral close packing in 4D and higher dimensional space.

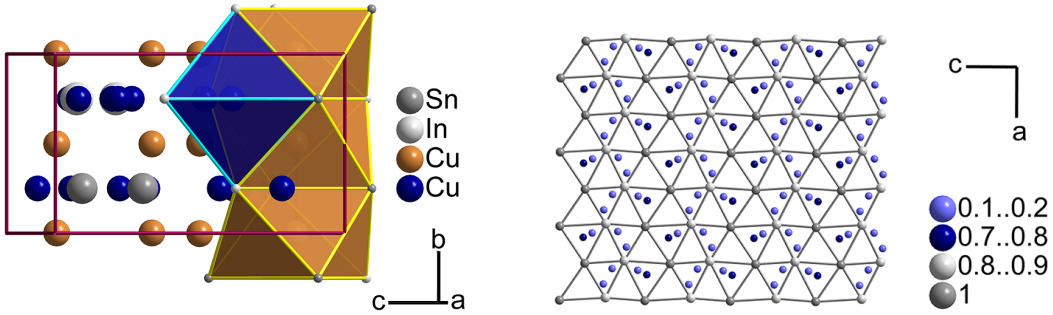

(a) Unit cell (b) Mixed In/Sn layer with In vacancies

Figure 4.19.: Crystal Structure of $Cu_7In_{1.55}Sn_{2.45}$ at 373 K; Cu atoms in octahedral interstices are depicted in Cu-colour whereas Cu atoms that occupy about 2/3 of the trigonal bipyramidal interstices are shown in different shades of blue depending on their occupancy.

A brief summary on the superstructure formation

The number of investigated ternary compounds, especially at temperatures below 673 K, is still too small to make statements of a general character. The actual transition temperatures are difficult to detect using thermal analysis methods, as metastable phases require long-time annealing at a temperature where this phase is stable. Furthermore, the transition temperatures are different for every ternary system, and may be higher or lower than transition temperatures of the binary phases.
The application of annealing temperatures that are significantly lower than the melting points of the ternary compound can but does not have to lead to superstructure formation, because composition is the stronger driving force. An indication for this statement is that the pseudocubic c/a ratios are independent from the modification of a Ni_2In type superstructure, but they are very sensitive to small compositional changes and therefore changes in the chemical bonding. Ternary compounds like $Cu_2In_{0.75}Sb_{0.25}$ and $Cu_7In_{1.55}Sn_{2.45}$ proof that the number of Ni_2In type superstructures with vacancies on the network sites is larger than expected. Moreover, they give an insight on how Ni_2In type superstructures order in general: Network atoms from the P block elements order in a site specific fashion first whereas the TM elements prefer to occupy the interstices more randomly. One ordering principle that all of the presented ternary Ni_2In type superstructures have in common is that trigonal bipyramidal interstices start to fill only when all octahedral interstices are fully occupied. A simple general composition based prediction of the site occupation in ternary compounds, is however still impossible, because we do not understand when, where and why vacancies are formed in the Ni_2In superstructures. As a result, it remains unclear why in some superstructures an orthorhombic distortion of the aristotype symmetry is preferred over trigonal or monoclinic distortions while in others the *vice versa* situation can be found. Until this knowledge gap is closed, every new compound has to be investigated experimentally.

4.3. Hexagonal Structure Motifs in Coloured Cubic bcc Superstructures

The pseudocubic nature of the Ni_2In type superstructures as part of the family of hexagonal coloured bcc structures has been debated in terms of their integral lattice properties. The consequent follow-up research question has to be: Are there any pseudohexagonal structural motifs in superstructures that can be derived from the cubic bcc aristotype?

The answer is yes, and it shall be discussed by starting with the description of a new 8x8x8 superstructure type of bcc, the crystal structure of $Cu_{11}In_2Sn$. The composition of the ternary compound was found in a Cu-In-Sn phase diagram study by *Köster and coworkers* [87], although its crystal structure was not determined. It crystallizes in the cubic space group $Ia\bar{3}d$ (No. 230), wherein all three different elements occupy lattice sites of their own. In similarity to the crystal structures of the neighbouring cubic structures HT-Cu_7In_3 [59] and Cu_4Sn [71], it contains the cell-centred cluster, which is the cell-centred 3D projection of the 4D 600-cell. [88] But, in terms of its temperature stability range, the neighbouring phase on the Cu-In side of the ternary phase diagram is indeed the Ni_2In type superstructure of Sn-doped Cu_7In_4.

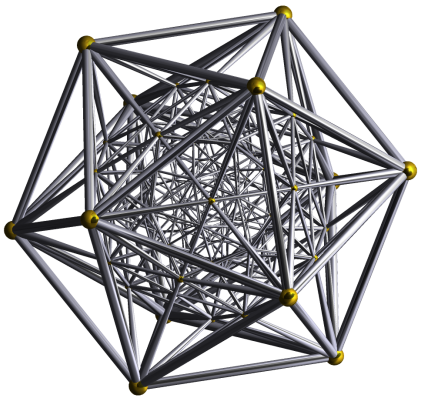

Figure 4.20.: Schlegel diagram, vertex-centered, of the $\{3, 3, 5\}$ polytope (600-cell) [86].

As discussed in Paper VI and depicted in Fig. 4.22, the characteristic structure motif of Cu_7In_3 is its trigonal net that contains an In vacancy that is surrounded by three Cu atoms with short Cu-Cu interatomic distances, a feature that reduces the overall crystal symmetry from hexagonal to triclinic. Notably, this motif and the surrounding atoms correspond to the ideal polygon-centred 3D projection of the 600-cell wherein the centre is empty.[5] For this reason, one needs to look for trigonal nets in the cubic structures in order to find pseudohexagonal structure motifs.

[5] If the centre is occupied by a network atom, as in the ideal Ni_2In structure type, the cluster is distorted but not truncated. Upon emptying the trigonal bipyramidal interstices in a fully occupied (pseudo)hexagonal network, the network atom in the centre of the distorted polygon-centred cluster remains, whereas it is increasingly truncated. Thus, the c/a ratios increase and therefore, AuSn type structures have significantly higher c/a ratios than Ni_2In type superstructures with vacancies on the network sites.

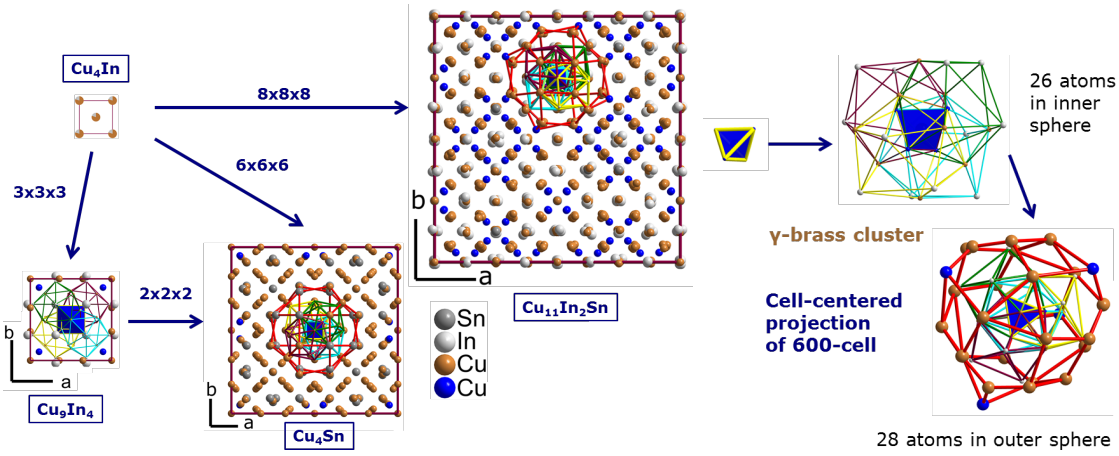

(a) Relation of the 8x8x8 superstructure of $Cu_{11}In_2Sn$ to bcc type Cu_4In [59]

(b) Construction of the cell-centered cluster in $Cu_{11}In_2Sn$

Figure 4.21.: Crystal Structure of $Cu_{11}In_2Sn$ and its relation to other bcc superstructures.

What makes every cubic crystal structure describable in any cubic space group are the three-fold axes along the body diagonals of the cubic unit cell. Hence, one needs to check layers whose normals are the ⟨111⟩ directions in the cubic unit cells. If we do so in $Cu_{11}In_2Sn$, the Cu_7In_3 arrangement of the network atoms is visible at first glance. On including the closest Cu atoms that are located slightly above and below this layer, we find the same arrangement as in the Ni_2In type superstructure on additional drawing of the closest octahedral Cu atoms. This is a yet another proof that Ni_2In type structures are hexagonal coloured bcc structures.
Following this argumentation, the smaller coloured cubic bcc superstructure of HT-Cu_7In_3 should contain the same pseudohexagonal structure motif, and it does as shown in Fig. 4.22(g). It means that the characteristic Cu_7In_3 network vacancy ordering is present in one of the two kinds of layers in Cu_9In_4 at high temperatures already. Nevertheless, it is the one that is preserved at low temperatures, whereas the second layer motif corresponds to the typical Ni_2In layer as present in the Cu-In C-phase which is also referred to as RT-Cu_2In [77;79] (see Fig. 4.22(h)).
As a inclusion, cubic bcc superstructures and (pseudo)hexagonal Ni_2In type superstructures have incompatible symmetries in 3D space. But, especially the pseudo five-fold axes that are present in both structure type families are originating from different projections of 4D symmetry operations to 3D space. It means that the cubic bcc structure and the hexagonal Ni_2In structure have a common aristotype in higher-dimensional space, and that the observed common motifs are just 3D projections of the same structural motifs in the common 4D polytope, the 600-cell. This polytope consists of 600 tetrahedral cells, and is therefore also denoted as tetraplex or polytetrahedron (Confer Fig. 4.20), but more importantly, it relates both structure types to tetrahedrally closed packed structures.

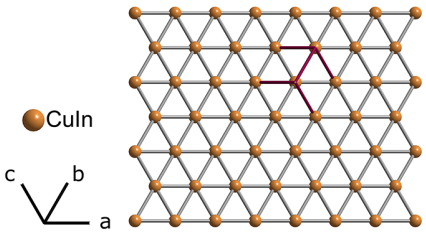

(a) Cu_4In along ⟨111⟩

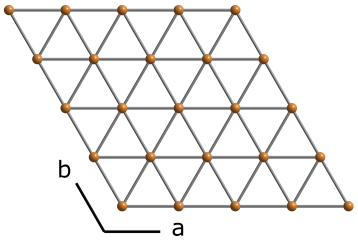

(b) Octahedral interstices in Cu_2In [59]

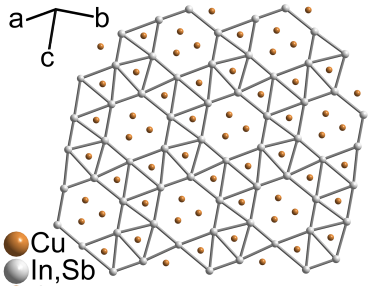

(c) $Cu_7In_{2.5}Sb_{0.5}$ (Paper VI)

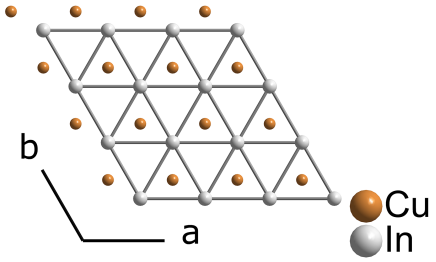

(d) Trigonal biyramidal interstices Cu_2In [59]

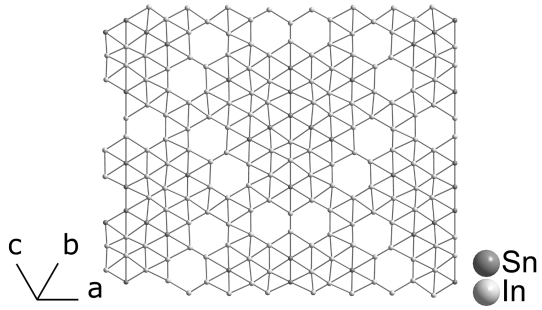

(e) Trigonal net of In and Sn atoms in $Cu_{11}In_2Sn$ along ⟨111⟩

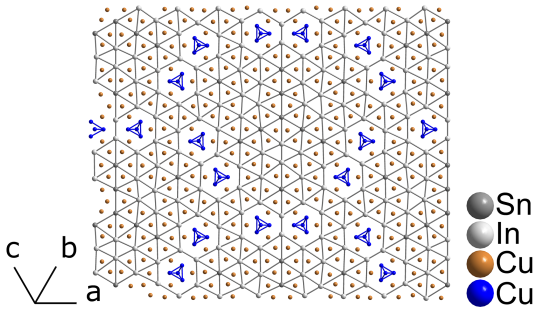

(f) Trigonal net and closest Cu atoms in $Cu_{11}In_2Sn$ along ⟨111⟩

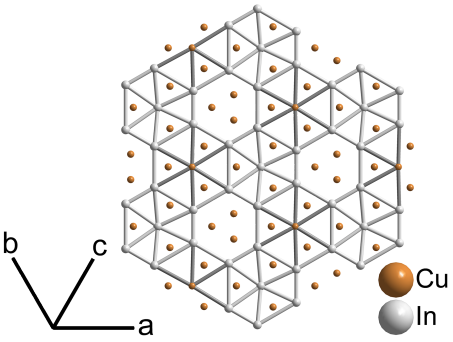

(g) Cu_7In_3 structure motif in Cu_9In_4 along ⟨111⟩

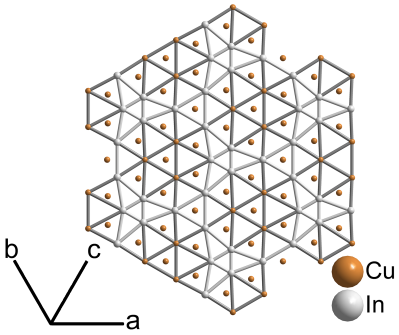

(h) Ni_2In structure motif in Cu_9In_4 along ⟨111⟩

Figure 4.22.: Trigonal nets in $Cu_{11}In_2Sn$ and its relation to the Ni_2In structure type and other bcc superstructures

5. Conclusions

The presented thesis has been focussed on the synthesis and chemical as well as structural characterization of intermetallic compounds that are relevant for the challenges in the field of lead-free electronic devices. It is the first extensive study on ternary intermetallic compounds whose crystal structures are Ni_2In type superstructures, even though, only a selection of the studied ternary systems is discussed in detail. New intermetallic compounds and alloys were synthesized by applying a building block principle wherein elements from the p-block build a (pseudo)hexagonal network whose interstices can be filled with transition metal elements. It was found that the formation of the ternary compounds as well as their crystal structures is not only dependent on the composition but also on the annealing temperature.
In order to reveal trends in the superstructure formation, it was inevitable to review the common understanding of the Ni_2In structure type. It is neither a stuffed NiAs structure nor is its network a highly distorted hexagonal close packing. The preference of pseudocubic axial ratios and the presence of pseudocubic clusters in every Ni_2In type superstructure imply that it is a structure type of its own. The presented description as a coloured hexagonal bcc structure as well as the new range of the axial ratios c/a from 1.155 to 1.333 are just consequences of these findings. On one hand, the revised c/a range is more restrictive than the one given by *Lidin.*[12] On the other hand, it is this restriction in particular that allows the description of Ni_2In type superstructures as members of the larger family of (pseudo)cubic structures. And as a result, characteristic structure motifs from the Ni_2In type superstructures can be revealed in bcc superstructures such as $Cu_{11}In_2Sn$ or Cu_9In_4.
This re-definition of the structure type may seem as an unnecessary mind game at first glance, but there are practical implications of this theoretical concept. The Hume Rothery electron concentration rule is a common tool to predict and describe bcc superstructures.[89] Recently, this rule has been expanded from metallic compounds to systems with covalent or ionic bonding.[90] By testing and applying this rule to the family of coloured (pseudo)cubic bcc structures one may reveal electronic stabilization principles that influence the stability of certain structure motifs, and thus, the formation of the observed superstructures. The Hume Rothery rule is however not the only possibility to use the concepts that are presented within this thesis.

The guided synthesis approach gives an idea on how metals react with each other to alloys or intermetallic compounds, and which crystal structures can be formed. This is the basis to understand mechanical, thermal or electronic properties that have been predicted or determined experimentally. But more importantly, it has been shown that the crystal structures of intermetallic compounds in lead-free electronics should be studied at temperatures that are close to the working temperatures of the device, and that the time-scale of the formation of thermodynamically stable superstructures is rather in the range of months than days.

6. Populärvetenskaplig sammanfattning

Kunskap om intermetalliska föreningar och legeringar är avgörande för tekniksprång. Den senaste av dessa, den så kallade digitala revolutionen, började perioden för informationsåldern som kännetecknas av snabb informationsöverföring. Den ständiga utvecklingen av snabbare och mindre elektroniska apparater kommer med nackdelen av ökade mängder avfall, vilket innebär produkter som används för att genom avancerad teknik. Föga förvånande, inte alla delar av en elektronisk anordning är återvinningsbara, och vissa av de intermetalliska föreningarna och legeringar är i själva verket skadlig för miljön. Av denna anledning förbud och restriktioner för farligt material i elektroniska apparater har satts i lagstiftningen i vissa länder under de senaste tio åren, även i Europeiska unionen.
Den direkta följden av dessa regler är att ersätta de drabbade metaller nya tvärvetenskapliga forskningsfält med andra skapas som traditionella material som bly i lödtenn är inte tillåtna längre. Den här presenterade avhandling riktar sig inte att finna nya löda eller halvledarmaterial. Tanken bakom är att hitta och karakterisera intermetalliska föreningar som bildas när metall-metallkontakter är närvarande i elektroniska enheter. Förutom kemiska karakteriseringstekniker användes kristallografiska metoder såsom röntgendiffraktion för att bestämma kristallstrukturer hos de nya föreningarna. Detta är av särskild betydelse för tekniska tillämpningar som egenskaperna hos varje given intermetallisk förening varken kan förstås eller förutspås utan kunskap om dess kristallstruktur.

7. Acknowledgements

This PhD project has been challenging in many aspects, but I have had the invaluable luxury of the freedom to choose research projects myself. To this effect it really is my PhD project. And I want to thank Sven Lidin for being an open-minded PhD supervisor who has reliance on his students.
However, a project like this does not work without help: Gunnel Karlsson has been a patient teacher on the SEM, whereas Hossein Sina and Kumar Babu Surreddi always found an open measurement slot on the TG-DSC machine. Staffan Hansen, who has upgraded my view of crystal structures. I also want to thank Masoomeh Ghasemi, Volodymir Bushlya and Fei Wang for discussions on how to learn more about thermodynamic, mechanical and electronic properties of the compounds. It was a pleasure to work with many different students of whom Alexis Ditta and Kalle Gustavsson were brave enough to stay for several weeks.
Outside of Lund, Susana Ramos de Debiaggi and her group as well as Eduardo Cuervo-Reyes were very helpful in understanding structures from an energetic point of view, whereas Martin Valldor and Gerhard Kolland measured physical properties.
In the past five years, I have been travelling a lot. This would have been impossible without the administrative help of Bodil Eliasson, Truss Friid and Maria Levin. Amongst these trips, I had an enjoyable stay in Ray Withers group at the ANU in Canberra. And I am indebted to Lasse Norén for his suggestions on the Ni-In system.
Starting to do Neutron diffraction experiments, would not have been possible without Cedric Dicko and Paul Henry, and I am very glad that Paul joined for the first beamtime at ILL. Throughout these field-trips, the beamline scientists have been very helpful to obtain results: Marie-Hélene Lemée-Cailleau and Clemens Ritter (D2B@ILL), Markus Hölzel (Sprodi@FRM-II), Vladimir Pomjakushin (HRPT@SINQ-PSI), Ashfia Huq and Pamela Whitfield (POWGEN@SNS-ORNL). The synchrotron experiments were performed with help of Harriet Nowell (I19@Diamond Light Source) and Pierre Fertey (CRISTAL@Soleil) as well as Hanna Karlsson and Erik Sjöberg, who joined the experiments in France. The large facilty projects were supported by the European Union NMI-3 network action as well as the Royal Physiographical Society in Lund.
Learning Swedish was sometimes a challenge of its own. A fortiori, I do appreciate that Isa and my other Swedish colleagues did their best to help me when I was sort of lost in translation. I also want thank Anita Diehl who has been a great Swedish teacher.
My family as well as Sebastian and his family and my friends have supported this thesis with lots of understanding and empathy. You are amazing!

Bibliography

[1] H.-G. Bachmann, *Chemie in unserer Zeit* **1983**, *17*, 120–128.

[2] K. Volke, *Chemie in unserer Zeit* **2006**, *40*, 20–31.

[3] *Official Journal of the European Union* **2003**, *L37*, 19–23.

[4] *Official Journal of the European Union* **2003**, *L37*, 24–38.

[5] *Official Journal of the European Union* **2006**, *L266*, 1–14.

[6] Kemikalieinspektionen, *Årsredovisning 2013*, Modintryckoffset, **2014**, p. 20.

[7] `https://www.ifixit.com/Teardown/iPhone+5s+Teardown/17383`.

[8] J. Lau, *CSR Tech Monthly* **2014**, 32–36.

[9] A. Kroupa, D. Andersson, N. Hoo, J. Pearce, A. Watson, A. Dinsdale, S. Mucklejohn, *Journal of Materials Engineering and Performance* **2012**, *21*, 629–637.

[10] J. K. Kivilahti, *JOM* **2002**, *54*, 52–57.

[11] Z. Fang, X. Mao, J. Yang, F. Yang, *Journal of Micromechanics and Microengineering* **2013**, *23*, 095008.

[12] S. Lidin, *Acta Crystallographica Section B* **1998**, *54*, 97–108.

[13] R. Vincent, R. L. Withers, *Philosophical Magazine Letters* **1987**, *56*, 57–62.

[14] M. Ellner, *Journal of the Less Common Metals* **1976**, *48*, 21 – 52.

[15] H. Ipser, K. Richter, *Journal of Electronic Materials* **2003**, *32*, 1136–1140.

[16] M. Boström, S. Hovmöller, *Journal of Alloys and Compounds* **2001**, *314*, 154–159.

[17] Naturrvårdsverket, *Mercury management in Sweden*, **2014**.

[18] *WinXPow, Powder Diffraction Software, Version 3.1; Stoe & Cie: Darmstadt, Germany*, **2011**.

[19] V. Petříček, M. Dušek, L. Palatinus, *Zeitschrift für Kristallographie* **2014**, *229*, 345–352.

[20] H. Nowell, S. A. Barnett, K. E. Christensen, S. J. Teat, D. R. Allan, *Journal of Synchrotron Radiation* **2012**, *19*, 435–441.

[21] M. Clarke, R. Elbourne, *Electrochimica Acta* **1971**, *16*, 1949 – 1954.

[22] *CrysAlisPro Software system, Version 1.171.36.32; Agilent Technologies UK Ltd., Oxford, UK*, **2012**.

[23] G. Oszlányi, A. Süto, *Acta Crystallographica Section A* **2004**, *60*, 134–141.

[24] G. Oszlányi, A. Süto, *Acta Crystallographica Section A* **2005**, *61*, 147–152.

[25] G. Oszlányi, A. Süto, *Acta Crystallographica Section A* **2008**, *64*, 123–134.

[26] L. Palatinus, G. Chapuis, *Journal of Applied Crystallography* **2007**, *40*, 786–790.

[27] L. Palatinus, *Acta Crystallographica Section B* **2013**, *69*, 1–16.

[28] R. Pynn, *Los Alamos Science* **1990**, *19*, 1–31.

[29] V. F. Sears, *Neutron News* **1992**, *3*, 26–37.

[30] E. Suard, A. Hewat, *Neutron News* **2001**, *12*, 30–33.

[31] P. Fischer, G. Frey, M. Koch, M. Könnecke, V. Pomjakushin, J. Schefer, R. Thut, N. Schlumpf, R. Bürge, U. Greuter, S. Bondt, E. Berruyer, *Physica B: Condensed Matter* **2000**, *276278*, 146 – 147.

[32] M. Hoelzel, A. Senyshyn, N. Juenke, H. Boysen, W. Schmahl, H. Fuess, *Nuclear Instruments and Methods in Physics Research Section A* **2012**, *667*, 32 – 37.

[33] A. Huq, J. P. Hodges, L. Heroux, O. Gourdon, *Zeitschrift für Kristallographie* **2011**, *226*, 127–135.

[34] M. Bowden, M. Ryan, *Journal of Applied Crystallography* **2010**, *43*, 693–698.

[35] *AZtec, Version 2.0; Oxford Instruments Nanotechnology, Tools Ltd.: Oxford, UK*, **2010–2012**.

[36] *NETZSCH Proteus - Thermal Analysis - Version 5.1.0 (02.02.2010), Netzsch Gertebau GmbH, Selb, Germany*.

[37] W. F. Hemminger, H. K. Cammenga, *Methoden der Thermischen Analyse*, Springer, Berlin, Heidelberg, **1989**.

[38] V. Tomashik, R. Schmid-Fetzer, L. Tretyachenko, J. D. Keyzer in *Non-Ferrous Metal Systems. Part 3*, *Vol. 11C3* (Eds.: G. Effenberg, S. Ilyenko), Springer Berlin Heidelberg, **2007**, pp. 96–112.

[39] N. Solak in *Non-Ferrous Metal Systems. Part 3*, *Vol. 11C3* (Eds.: G. Effenberg, S. Ilyenko), Springer Berlin Heidelberg, **2007**, pp. 86–95.

[40] S.-W. Chen, P.-Y. Chen, C.-N. Chiu, Y.-C. Huang, C.-H. Wang, *Metallurgical and Materials Transactions A* **2008**, *39*, 3191–3198.

[41] R. Kubiak, K. Schubert, *Zeitschrift für Metallkunde* **1980**, *71*, 635–637.

[42] S. Furuseth, K. Selte, A. Kjekshus, *Acta Chemica Scandinavica* **1965**, *19*, 735–741.

[43] S. Lidin, S. Y. Piao, *Zeitschrift für Anorganische und Allgemeine Chemie* **2009**, *635*, 611–613.

[44] A. K. Larsson, L. Stenberg, S. Lidin, *Acta Crystallographica Section B* **1994**, *50*, 636–643.

[45] A.-K. Larsson, L. Stenberg, S. Lidin, *Acta Chemica Scandinavica* **1995**, *49*, 800 – 802.

[46] L. Vegard, *Zeitschrift für Physik* **1921**, *5*, 17–26.

[47] S. Bhan, K. Schubert, *Journal of the Less Common Metals* **1969**, *17*, 73 – 90.

[48] J. P. Jan, W. B. Pearson, A. Kjekshus, *Canadian Journal of Physics* **1963**, *41*, 2252–2266.

[49] W. F. De Jong, W. V. Willems, *Physica (The Hague)* **1927**, *7*, 74–79.

[50] B. Grison, P. A. Beck, *Acta Crystallographica* **1962**, *15*, 807–808.

[51] E. I. Gladyshevskii, E. E. Cherkashin, *Visn. Lviv. Derzh. Univ. (Ser. Khim.)* **1955**, 4–51.

[52] R. Mishra, A. Kroupa, P. Terzieff, H. Ipser, *Thermochimica Acta* **2012**, *536*, 6873.

[53] A. Kroupa, R. Mishra, D. Rajamohan, H. Flandorfer, A. Watson, H. Ipser, *Calphad* **2014**, *45*, 151 – 166.

[54] C. Schmetterer, A. Zemanova, H. Flandorfer, A. Kroupa, H. Ipser, *Intermetallics* **2013**, *35*, 90 – 97.

[55] C. Schmetterer, H. Flandorfer, C. Luef, A. Kodentsov, H. Ipser, *Journal of Electronic Materials* **2009**, *38*, 10–24.

[56] L. Norén, R. L. Withers, Y. Tabira, *Journal of Alloys and Compounds* **2000**, *309*, 179 – 187.

[57] S. Piao, S. Lidin, *Zeitschrift für Anorganische und Allgemeine Chemie* **2008**, *634*, 2589–2593.

[58] S. Lidin, L. Stenberg, M. Elding-Pontén, *Journal of Alloys Compounds* **1997**, *255*, 221–226.

[59] G. Che, M. Ellner, *Powder Diffraction* **1992**, *7*, 107–108.

[60] S. Lidin, T. Popp, M. Somer, H. G. von Schnering, *Angewandte Chemie* **1992**, *104*, 936–939.

[61] R. D. Hoffmann, R. Pöttgen, *Zeitschrift für Kristallographie* **2001**, *216*, 127–145.

[62] T. Hahn, H. Klapper in *International Tables for Crystallography Volume D: Physical properties of crystals, Vol. D* (Ed.: A. Authier), Springer Netherlands, **2003**, pp. 393–448.

[63] R. de Gelder, A. Janner, *Acta Crystallographica Section B* **2005**, *61*, 287–295.

[64] B. Constant, P. J. Shlichta, *Acta Crystallographica Section A* **2003**, *59*, 281–282.

[65] P. Villars, K. Cenzual, *Pearson's Crystal Data - Crystal Structure Database for Inorganic Compounds (on CD-ROM)*, **2012/2013**.

[66] A. Janner, *Acta Crystallographica Section A* **2004**, *60*, 198–200.

[67] A. Janner, *Acta Crystallographica Section A* **2004**, *60*, 611–620.

[68] C. B. Shoemaker, D. P. Shoemaker, L. A. Bendersky, *Acta Crystallographica Section C* **1990**, *46*, 374–377.

[69] S. Andersson, *Acta Chemica Scandinavica* **1959**, *13*, 415–419.

[70] M. Puselj, K. Schubert, *Journal of the Less Common Metals* **1975**, *41*, 33 – 44.

[71] J. K. Brandon, R. Y. Brizard, W. B. Pearson, D. J. N. Tozer, *Acta Crystallographica Section B* **1977**, *33*, 527–537.

[72] B. Giessen, *Zeitschrift für Metallkunde* **1968**, *59*, 805–809.

[73] R. Nesper, *Angewandte Chemie* **1991**, *103*, 805–834.

[74] H. Grimmer, *Acta Crystallographica Section A* **2015**, *71*, 143–149.

[75] A.-K. Larsson, R. Withers, *Journal of Alloys and Compounds* **1998**, *264*, 125 – 132.

[76] L. Norén, *private communication*, **2012**.

[77] M. Elding-Pontén, L. Stenberg, S. Lidin, *Journal of Alloys and Compounds* **1997**, *261*, 162–171.

[78] V. Petricek, A. Van Der Lee, M. Evain, *Acta Crystallographica Section A* **1995**, *51*, 529–535.

[79] S. Lidin, *private communication*, **2015**.

[80] S. Lange, T. Nilges, R.-D. Hoffmann, R. Pöttgen, *Zeitschrift für Anorganische und Allgemeine Chemie* **2006**, *632*, 1163–1166.

[81] Y. K. Kabalov, E. Sokolova, *Materials Science Forum* **1998**, *278/281*, 785–790.

[82] K. Schubert, H. Breimer, R. Gohle, *Zeitschrift für Metallkunde* **1959**, *50*, 146–153.

[83] G. Aurelio, S. A. Sommadossi, G. J. Cuello, *Journal of Applied Physics* **2012**, *112*, 053520.

[84] G. Aurelio, S. A. Sommadossi, G. J. Cuello, *Journal of Electronic Materials* **2012**, *41*, 3223–3231.

[85] A.-K. Larsson, L. Stenberg, S. Lidin, *Zeitschrift für Kristallographie* **1995**, *210*, 832–837.

[86] R. Webb, *This image was created with the Stella software.*, `http://www.software3d.com/Stella.php`.

[87] W. Köster, T. Gödecke, D. Heine, *Zeitschrift für Metallkunde* **1972**, *63*, 802–807.

[88] S. Lee, R. Henderson, C. Kaminsky, Z. Nelson, J. Nguyen, N. F. Settje, J. T. Schmidt, J. Feng, *Chemistry A European Journal* **2013**, *19*, 10244–10270.

[89] V. F. Degtyareva, N. S. Afonikova, *Journal of Physics and Chemistry of Solids* **2013**, *74*, 18 – 24.

[90] U. Mizutani, H. Sato, M. Inukai, Y. Nishino, E. S. Zijlstra, *Inorganic Chemistry* **2015**, *54*, 930–946.

[91] J. W. Kaiser, M. G. Haase, W. Jeitschko, *Zeitschrift für Anorganische und Allgemeine Chemie* **2001**, *627*, 2369–2376.

[92] H. T. Stokes, B. J. Campbella, S. van Smaalen, *Acta Crystallographica Section A* **2011**, *67*, 45–55.

[93] S. van Smaalen, B. J. Campbell, H. T. Stokes, *Acta Crystallographica Section A* **2013**, *69*, 75–90.

[94] A. Palenzona, *Journal of the Less Common Metals* **1968**, *16*, 379 – 384.

[95] R. L. Kift, T. Prior, *Journal of Alloys and Compounds* **2010**, *505*, 428–433.

[96] H. Fjellvåg, A. Kjekshus, *Acta Chemica Scandinavica* **1986**, *A40*, 23–30.

[97] A. Kjekshus, A. P. Walseth, *Acta Chemica Scandinavica* **1969**, *20*, 2621–2630.

[98] M. El-Boragy, R. Szepan, K. Schubert, *Journal of the Less Common Metals* **1972**, *29*, 133 – 140.

[99] L. D. Gulay, B. Harbrecht, *Journal of Alloys and Compounds* **2004**, *367*, 103 – 108.

[100] O. B. Karlsen, A. Kjekshus, E. Røst, *Acta Chemica Scandinavica* **1992**, *46*, 147–156.

[101] A. Saccone, S. Delfino, G. Cacciamani, R. Ferro, *Journal of the Less Common Metals* **1988**, *136*, 249 – 259.

[102] B. Malaman, J. Steinmetz, B. Roques, *Journal of the Less Common Metals* **1980**, *75*, 155 – 176.

[103] H. Kudielka, *Zeitschrift für Kristallographie* **1977**, *145*, 177–189.

[104] H. Giefers, M. Nicol, *Journal of Alloys and Compounds* **2006**, *422*, 132 – 144.

[105] S. Delfino, A. Saccone, R. Ferro, *Zeitschrift für Metallkunde* **1983**, *74*, 674–679.

[106] D. Anh, G. Nakamoto, T. Tsuji, M. Kurisu, Y. Andoh, T. Tsutaoka, N. Achiwa, S. Kawano, *Physica B: Condensed Matter* **2006**, *381*, 132 – 138.

[107] S. Bhan, K.Schubert, *Zeitschrift für Metallkunde* **1960**, *51*, 327*339.

[108] A. Palenzona, P. Manfrinetti, A. Palenzona, *Journal of Alloys and Compounds* **1998**, *267*, 154–157.

[109] M. Ellner, *Journal of Applied Crystallography* **1980**, *13*, 99–100.

[110] M. Elding-Pontén, L. Stenberg, A.-K. Larsson, S. Lidin, K. Ståhl, *Journal of Solid State Chemistry* **1997**, *129*, 231 – 241.

[111] M. Elding-Pontén, L. Stenberg, S. Lidin, G. Madariaga, J.-M. Pérez-Mato, *Acta Crystallographica Section B* **1997**, *53*, 364–372.

[112] L. Myzenkova, V. V. Baron, E. M. Savitskii, *Russian Metallurgy* **1966**, *2*, 89–91.

[113] S. Delfino, A. Saccone, G. Borzone, R. Ferro, *Journal of the Less Common Metals* **1978**, *59*, 69 – 78.

[114] M. Ruck, *Zeitschrift für Anorganische und Allgemeine Chemie* **1999**, *625*, 2050–2054.

[115] S. Lidin, V. Petricek, L. Stenberg, S. Furuseth, H. Fjellvåg, A.-K. Larsson, *Solid State Sciences* **2000**, *2*, 353 – 363.

[116] G. Hägg, G. Funke, *Z. Phys. Chem. (Abt. B)* **1929**, *6*, 272–283.

[117] M. Ellner, S. Bhan, K. Schubert, *Journal of the Less Common Metals* **1969**, *19*, 245 – 252.

[118] E. Hellner, *Zeitschrift für Metallkunde* **1950**, 480–484.

[119] M. Ellner, T. Gödecke, K. Schubert, *Journal of the Less Common Metals* **1971**, *24*, 23 – 40.

[120] P. Brand, *Zeitschrift für Anorganische und Allgemeine Chemie* **1967**, *353*, 270–280.

[121] L. Norén, R. Withers, S. Schmid, F. Brink, V. Ting, *Journal of Solid State Chemistry* **2006**, *179*, 404–412.

[122] K. Toman, *Acta Crystallographica* **1952**, *5*, 329–331.

[123] K. Cenzual, L. M. Gelato, M. Penzo, E. Parthé, *Acta Crystallographica Section B* **1991**, *47*, 433–439.

[124] A. Leineweber, O. Oeckler, U. Zachwieja, *Journal of Solid State Chemistry* **2004**, *177*, 936–945.

[125] H. Mayer, M. Ellner, K. Schubert, *Journal of the Less Common Metals* **1980**, *71*, P29 – P38.

[126] M. Ellner, T. Gödecke, K. Schubery, *Zeitschrift für Metallkunde* **1973**, *6564*, 566–568.

[127] N. Sarah, K. Alasafi, K. Schubert, *Zeitschrift für Metallkunde* **1981**, *72*, 517–520.

[128] P. Panday, K. Schubert, *Journal of the Less Common Metals* **1969**, *18*, 175 – 202.

[129] N. N. Zhuravlev, G. S. Zhdanov, Y. M. Smirnova, *Physics of Metals and Metallography* **1962**, *13*, 4–51.

[130] S. Heinrich, K. Schubert, *Journal of the Less Common Metals* **1978**, *57*, P1 – P7.

[131] K. C. Jain, S. Bhan, *Transactions of the Indian Institute of Metals* **1972**, *25*, 100–102.

[132] R. Graham, G. C. S. Waghorn, P. T. Davies, *Acta Crystallographica* **1954**, *7*, 634–635.

[133] I. Harris, M. Norman, A. Bryant, *Journal of the Less Common Metals* **1968**, *16*, 427 – 440.

[134] H. Nowotny, K. Schubert, U. Dettinger, *Zeitschrift für Metallkunde* **1946**, *37*, 137–145.

[135] M. El-Boragy, K. C. Jain, H. W. Mayer, K. Schubert, *Zeitschrift für Metallkunde* **1972**, *63*, 751–753.

[136] L. Schellenberg, J. Jorda, J. Muller, *Journal of the Less Common Metals* **1985**, *109*, 261 – 274.

[137] K. Schubert, *Zeitschrift für Naturforschung A* **1947**, *2*, 120–.

[138] J. C. Schuster, J. Bauer, *Journal of the Less Common Metals* **1985**, *109*, 345–350.

[139] A. Palenzona, P. Manfrinetti, R. Palenzona, *Journal of Alloys and Compounds* **1996**, *243*, 182 – 185.

[140] S. Delfino, A. Saccone, G. Borzone, R. Ferro, *Zeitschrift für Anorganische und Allgemeine Chemie* **1983**, *503*, 184–192.

[141] M. Pötzschke, K. Schubert, *Zeitschrift für Metallkunde* **1962**, *53*, 474–488.

[142] H. G. Meissner, K. Schubert, *Zeitschrift für Metallkunde* **1965**, *56*, 523–530.

[143] E. A. Franceschi, *Journal of the Less Common Metal* **1974**, *37*, 157–160.

[144] G. Zanicchi, D. Mazzone, M. L. Fornasini, P. Riani, R. Marazza, R. Ferro, *Intermetallics* **1999**, *7*, 957 – 966.

[145] C. G. Wilson, D. Sams, *Acta Crystallographica* **1961**, *14*, 71–72.

[146] A. Neumann, A. Kjekshus, C. Rømming, E. Røst, *Journal of Alloys and Compounds* **1996**, *240*, 42 – 50.

[147] A. N. Torgersen, L. Offernes, A. Kjekshus, A. Olsen, *Journal of Alloys and Compounds* **2001**, *314*, 92 – 95.

[148] J. L. Jorda, J. Muller, H. F. Braun, C. P. Susz, *Journal of the Less Common Metals* **1987**, *134*, 99–107.

[149] K. Yamaguchi, H. Watanabe, H. Yamamoto, Y. Yamaguchi, *Journal of the Physical Society of Japan* **1971**, *31*, 1042–1052.

[150] A. Szytula, A. T. Pedziwiatr, Z. Tomkowicz, W. Bazela, *Journal of Magnetism and Magnetic Materials* **1981**, *25*, 176–186.

[151] K. H. J. Buschow, P. G. V. Engen, *Physica Status Solidi A* **1983**, *76*, 615–620.

[152] K. Kanematsu, K. Yasukochi, T. Ohoyama, *Journal of the Physical Society of Japan* **1962**, *17*, 932–936.

[153] M. Ellner, *Zeitschrift für Metallkunde* **1976**, *67*, 246–249.

[154] E. Hellner, G. Heger, D. J. E. Mullen, W. Treutmann, *Materials Research Bulletin* **1975**, *10*, 91–94.

[155] G. I. Makovetskii, G. M. Shakhlevich, *Vestsi Akademii Navuk BSSR Seryya Fizika-Matematychnykh Navuk* **1980**, 5–77.

[156] N. I. Varich, A. N. Varich, I. A. Kravtsov, *Dopovidi Akademii Nauk Ukrains'koi RSR Seriya A* **1973**, 84.

[157] V. Y. Markiv, N. N. Belyavina, *Russian Metallurgy* **1986**, *6*, 204–207.

[158] R. Raman, R. Gupta, M. Sujir, B. S., *Journal of Scientific Research of the Banaras Hindu University* **1964**, *14*, 95–99.

[159] E. M. Sokolovskaya, O. I. Chechernikova, E. I. Gladyshevskii, O. I. Bodak, *Russian Metallurgy* **1973**, *6*, 114–118.

[160] C. Yu, J. Liu, H. Lu, P. Li, J. Chen, *Intermetallics* **2007**, *15*, 1471–1478.

[161] F. Mazzoleni, *Metallurgia Italiana* **1953**, *45*, 366–369.

[162] K. Kanematsu, K. Yasukochi, T.Ohoyama, *Journal of the Physical Society of Japan* **1963**, *18*, 1429–1436.

[163] T. N. Gal'perina, L. P. Zelenin, T. A. Fedorova, F. A. Sidorenko, P. V. Gel'd, *Physics of Metals and Metallography* **1977**, *43*, 3–183.

[164] H. M. V. Noort, D. B. D. Mooij, K. H. J. Buschow, *Physica Status Solidi A* **1984**, *86*, 655–662.

[165] A. Kaprzyk, S. Niziol, *Journal of Magnetism and Magnetic Materials* **1990**, *87*, 267–275.

[166] V. Johnson, *Inorganic Chemistry* **1975**, *14*, 1117–1120.

[167] J. J. Bara, B. V. Gajic, A. T. Pedziwiatr, A. Szytula, *Journal of Magnetism and Magnetic Materials* **1981**, *23*, 149–155.

[168] M. K. Bhargava, K. Schubert, *Zeitschrift für Metallkunde* **1975**, *66*, 542–545.

[169] M. Kareva, E. Kabanova, K. Kalmykov, G. Zhmurko, V. Kuznetsov, *Journal of Phase Equilibria and Diffusion* **2014**, *35*, 413–420.

[170] K. L. Shelton, P. A. Merewether, B. J. Skinner, *Canadian Mineralogist* **1981**, *19*, 599–605.

[171] Y. Noda, M. Shimada, M. Koizumi, *Inorganic Chemistry* **1984**, *23*, 628–630.

[172] X. Yan, A. Grytsiv, P. Rogl, H. Schmidt, G. Giester, A. Saccone, X.-Q. Chen, *Intermetallics* **2009**, *17*, 336 – 342.

[173] Y. V. Verbovytsky, K. Latka, *Journal of Alloys and Compounds* **2007**, *431*, 130–135.

[174] V. A. Saltykov, K. A. Meleshevich, A. V. Samelyuk, O. M. Verbytska, M. V. Bulanova, *Journal of Alloys and Compounds* **2008**, *459*, 348–353.

[175] M. Konyk, L. Romaka, P. Demchenko, V. Romaka, Y. Stadnyk, A. Horyn, *Journal of Alloys and Compounds* **2014**, *589*, 200 – 206.

[176] C. B. H. Evers, C. G. Richter, J. Hartjes, W. Jeitschko, *J. Alloys Compd.* **1997**, *252*, 93–97.

[177] J. Bouwma, C. F. V. Bruggen, C. Haas, *Journal of Solid State Chemistry* **1973**, *7*, 255–261.

[178] Y. F. Lomnytska, O. P. Pavliv, *Inorganic Materials* **2007**, *43*, 608–613.

[179] L. Romaka, A. Tkachuk, Y. Stadnyk, V. Romaka, *Journal of Alloys and Compounds* **2009**, *470*, 233 – 236.

[180] I. Lindeberg, Y. Andersson, *Journal of the Less Common Metals* **1991**, *175*, 155 – 162.

[181] M. Ellner, M. El-Boragy, *Journal of Applied Crystallography* **1986**, *19*, 80–85.

[182] F. Wald, S. J. Michalik, *Journal of the Less Common Metals* **1971**, *24*, 277–289.

[183] C. Greaves, E. Devlin, N. Smith, I. Harris, B. Cockayne, W. MacEwan, *Journal of the Less Common Metals* **1990**, *157*, 315 – 325.

[184] W. Jeitschko, *Acta Crystallographica Section B* **1975**, *31*, 1187–1190.

[185] O. Moze, C. Greaves, F. Bouree-Vigneron, B. Cockayne, W. R. MacEwan, N. A. Smith, I. R. Harris, *Journal of Physics: Condensed Matter* **1994**, *6*, 10435–10444.

[186] N. Smith, P. Hill, E. Devlin, H. Forsyth, I. Harris, B. Cockayne, W. MacEwan, *Journal of Alloys and Compounds* **1992**, *179*, 111 – 124.

[187] A. M. Mills, A. Mar, *Journal of Alloys and Compounds* **2000**, *298*, 82 – 92.

[188] E. A. Vasil'ev, V. A. Virchenko, *Physica Status Solidi A* **1982**, *70*, K141–K143.

[189] V. Pavlyuk, O. I. Bodak, A. Stowinska, D. Kevorkov, G. Dmytriv, *Polish Journal of Chemistry* **1997**, *71*, 11–15.

[190] E. Vasiliev, A. Gelyasin, *Physica Status Solidi A* **1978**, *47*, K55–K57.

[191] S. Députier, R. Guérin, Y. Ballini, A. Guivarc'h, *Journal of Alloys and Compounds* **1995**, *217*, 13–21.

[192] C.-H. Jan, Y. Chang, *Journal of Materials Research* **1991**, *6*, 2660–2665.

[193] K. W. Richter, *Journal of Alloys and Compounds* **2002**, *338*, 43 – 50.

[194] R. Guérin, A. Guivarch, *Journal of Applied Physics* **1989**, *66*, 2122–2128.

[195] T. Sands, V. G. Keramidas, J. Washburn, R. Gronsky, *Applied Physics Letters* **1986**, *48*, 402–404.

[196] G. Nover, K. Schubert, *Zeitschrift für Metallkunde* **1981**, *72*, 26–29.

[197] M. L. Clanche, S. Députier, J. Jégaden, R. Guérin, Y. Ballini, A. Guivarc'h, *Journal of Alloys and Compounds* **1994**, *206*, 21 – 29.

[198] M. El-Boragy, T. Rajasekharan, K. Schubert, *Zeitschrift für Metallkunde* **1982**, *73*, 193–197.

[199] I. Jandl, T. L. Reichmann, K. W. Richter, *Intermetallics* **2013**, *32*, 200 – 208.

[200] P. Brand, J. Briest, *Zeitschrift für Anorganische und Allgemeine Chemie* **1965**, *337*, 209–213.

[201] A. Grytsiv, P. Rogl, S. Berger, C. Paul, H. Michor, E. Bauer, G. Hilscher, C. Godart, P. Knoll, M. Musso, W. Lottermoser, A. Saccone, R. Ferro, T. Roisnel, H. Noel, *Journal of Physics: Condensed Matter* **2002**, *14*, 7071.

[202] H. Flandorfer, K. Richter, G. Giester, H. Ipser, *Journal of Solid State Chemistry* **2002**, *164*, 110 – 118.

[203] C. Luef, H. Flandorfer, A. Paul, A. Kodentsov, H. Ipser, *Intermetallics* **2005**, *13*, 1207 – 1213.

[204] L. A. Tret'yachenko, N. V. Antonova, P. S. Martsenyuk, T. Y. Velicanova, *Journal of Phase Equilibria* **1999**, *20*, 581–592.

[205] I. V. Chumak, V. V. Pavlyuk, G. S. Dmytriv, J. S. Damm, *Journal of Alloys and Compounds* **2000**, *307*, 223–225.

[206] M. Ghasemi, S. Lidin, J. Johansson, F. Wang, *Intermetallics* **2014**, *46*, 40 – 44.

A. Experimental Details

Table A.1.: Starting materials for syntheses, purity and supplier

starting material	supplier	form	purity
Ag	Chempur	granules	99.9%
Au	Alfa Aesar	shot	99,999%
Bi	ABCR	shot	99.999%
Cu	ABCR	pieces	99.99%
Ga	ABCR	pellets	99.99%
Ge	ABCR	pieces	99.999%
In	Alfa Aesar	ingots	99.9999%
Ni	Alfa Aesar	wire	99.98%
Pd	American Elements	pieces	99%
Pt	ABCR	plates	99.9%
Sb	Chempur	shots	99.999%
Sn	Chempur	ingots	99.99%

Table A.2.: Heat treatment details of samples that are not covered within the manuscripts, average annealing times are given in days.

nominal composition	Synthesis T(K), t(d)	Annealing T(K), t(d)
Ag-In-Sn	1323, 3	423, 274-380
Ag-In-Sn	1323, 3	373, 2390
Ag-In-Sb	1323, 3	423, 274-380
Ag-Sn-Sb	1323, 3	473, 274
Au_2AgIn_2	1323, 3	723, 53
Au_2AgIn_2	1323, 3	473, 128
$Au_{9-x}Cu_xIn_4$	1323, 3	673, 40
$Au_{1+x}Cu_{2-x}In_2$	1323, 3	673, 61
$Au_{1+x}Cu_{2-x}In_2$	1323, 3	523, 203
$Au_{3.2-3.0}In_2$	1323, 3	698, 60-400
Au-In-Sb	1323, 3	703, 53
Au-In-Sb	1323, 3	473, 600
Au-Ni-In	1323, 3	573, 7-14
Au-Ni-In	1323, 3	923, 7
Cu-In	1173, 3	573, 48
Cu-In-Ga	1173, 3	573, 152
Cu-In-Ge	1173, 3	673, 60
Cu-In-Ge	1173, 3	523, 40
Cu-In-Sb	1173, 3	523, 420
Cu-In-Sn	1173, 3	373, 94-271
Cu-In-Sn	1173, 3	473, 124-641
Cu-In-Sn	1173, 3	523, 167
Cu-In-Sn	1173, 3	573, 62-83
Cu-In-Sn	1173, 3	673, 34-94
Cu-In-Sn	1173, 3	773, 20-94
Cu-Sn-Sb	1173, 7	673, 93
Cu-Pt-In	1173, 8	573, 237
Ni-In	1323, 3	373, 548
Ni-In	1323, 3	473, 241
Ni-In	1323, 3	573, 120
Ni-In	1323, 3	673, 61
Ni-In	1323, 3	823, 72
Ni-In	1323, 3	923, 19
$Ni_{7-x}Cu_xIn_3$	1323, 3	573, 265
Ni_7In_2Ga	1373, 4	573, 152
Ni-In-Sn	1323, 3	573, 55-183
Ni-In-Sn	1323, 3	673, 90
$Ni_{1+x}Pt_{2-x}In_2$ $(0 \leq x \leq 1)$	1323, 3	773, 149
$Ni_{3.5}Pt_{3.5}In_3$	1323, 3	773, 74
$Ni_{3.5}Pt_{3.5}In_3$	1323, 3	423, 315

B. Crystallographic Background Information

B.1. Supporting Information on Coloured bcc Structures

A few group-subgroup relations have been mentioned in section 4.1. The Figures in this appendix are supporting information for the presented hypothesis.

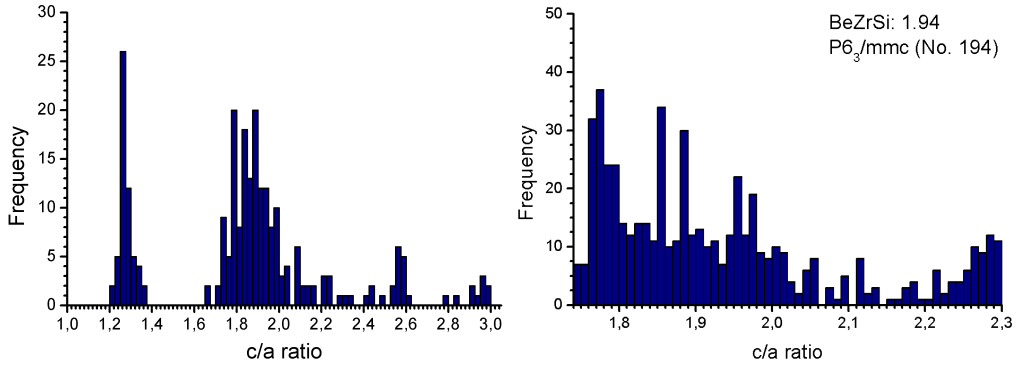

(a) Entries for BeZrSi in Pearson's database[65] (b) space group $P6_3/mmc$ (No. 194): c/a ratios around the ideal value for BeZrSi

Figure B.1.: Frequency distributions for BeZrSi type structures. It is obvious that many of the BeZrSi entries in Pearson's database[65] crystallize in different isopointal structure types.

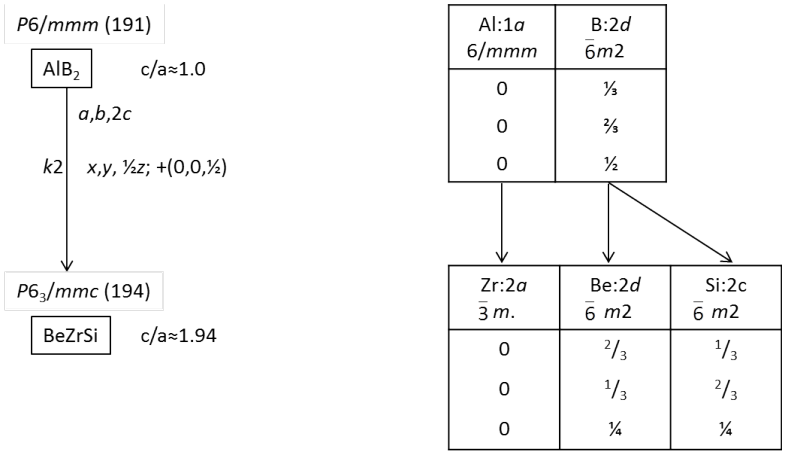

Figure B.2.: Group-subgroup relations for AlB_2 and BeZrSi. The latter is isopointal but not isostructural to the Ni_2In structure type.

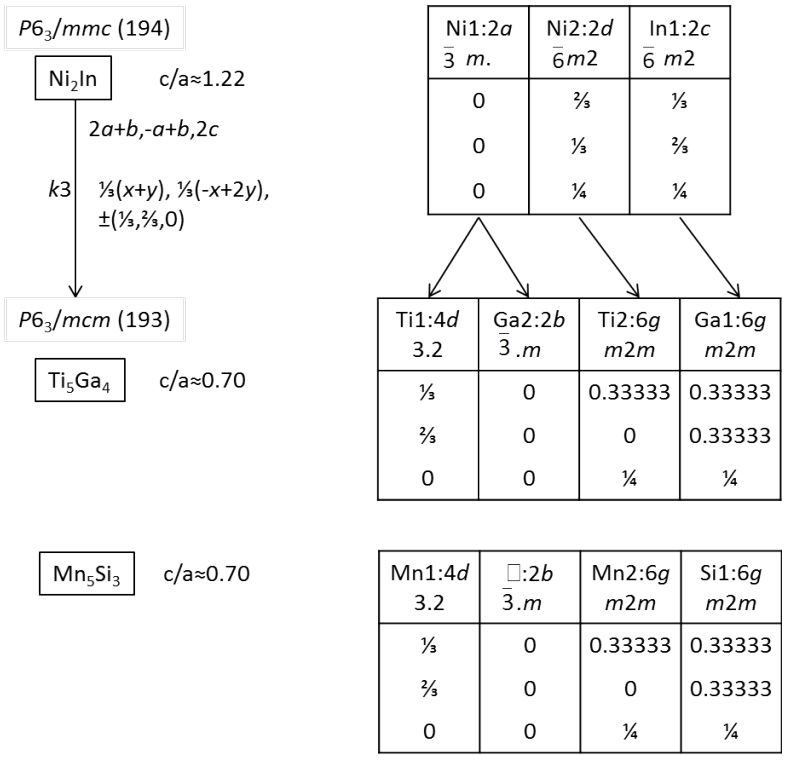

Figure B.3.: Group-subgroup relations for the symmetry reduction from the Ni_2In structure type to Ti_5Ga_5 or Mn_5Si_3. The colouring scheme is clearly different in terms of structure building blocks. The c/a ratios indicate that the Ti_5Ga_5-Mn_5Si_3 structure type family is not a hettotype of the AlB_2 aristotype.

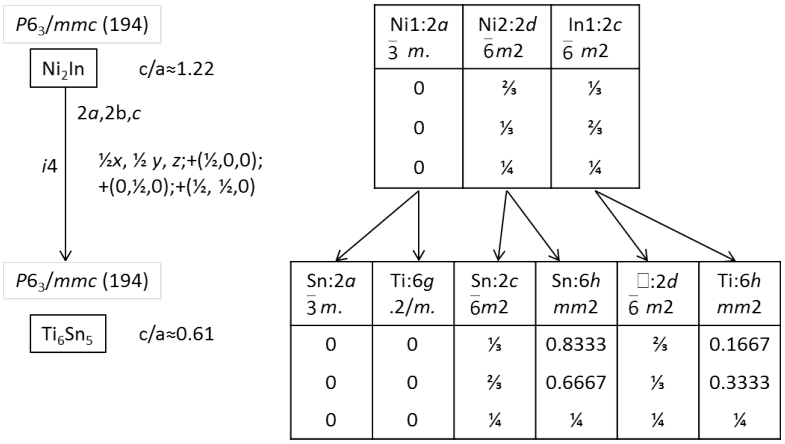

Figure B.4.: Group-subgroup relations for the symmetry reduction from the Ni_2In structure type to α-Ti_6Sn_5. The colouring scheme is different in terms of structure building blocks: TM and P atoms occupy the octahedral interstices in an ordered fashion whereas the network consists of TM atoms and vacancies. Trigonal bipyramidal interstices are occupied by P elements.

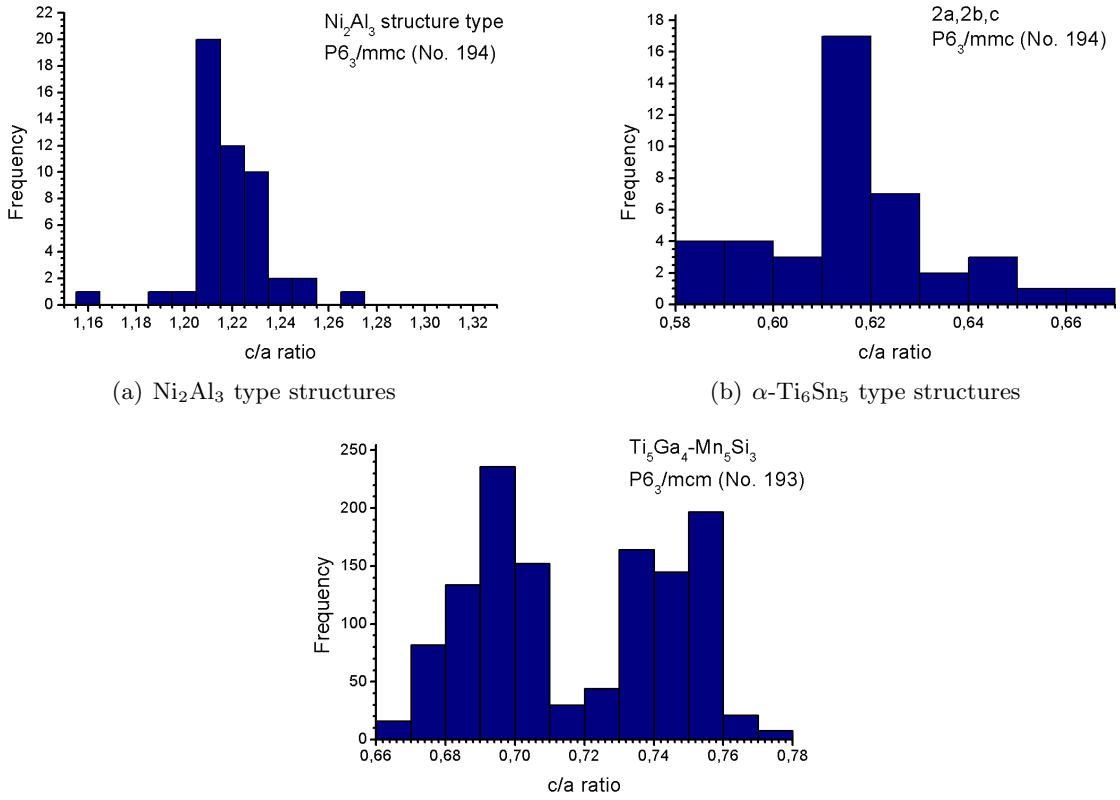

(a) Ni_2Al_3 type structures

(b) α-Ti_6Sn_5 type structures

(c) Ti_5Ga_5-Mn_5Si_3 structure type family

Figure B.5.: Frequency distributions for coloured hexagonal bcc structures with different colouring schemes as realized in the Ni_2In structure type.[65] Superstructures of these hexagonal aristotype structures were not considered for the plots.

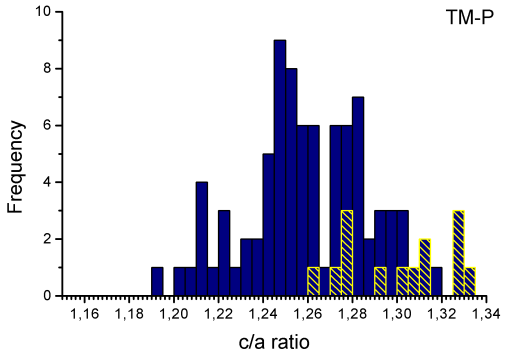

(a) binary compounds TM-P with Ni_2In type superstructures

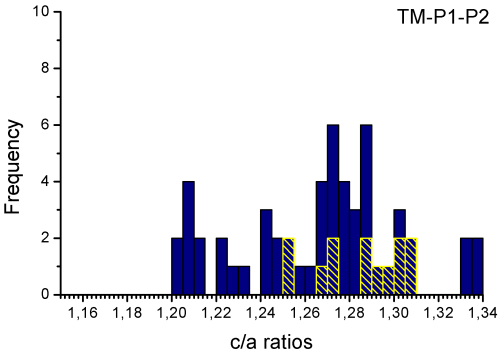

(b) ternary compounds TM-P1-P2 with Ni_2In type superstructures

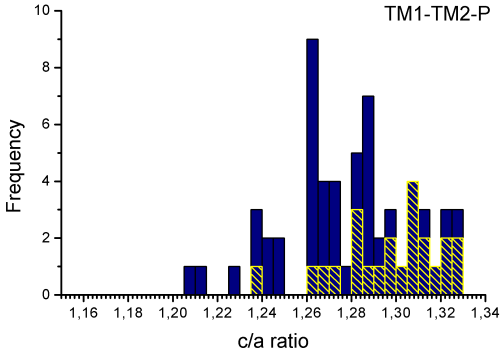

(c) ternary compounds TM1-TM2-P with Ni_2In type superstructures

Figure B.6.: Frequency distributions of binary and ternary compounds with Ni_2In type superstructures. Compounds with vacancies on the trigonal bipyramidal sites $2d$, such as AuSn type structures, are indicated by the line pattern. The references are given in the following appendices.

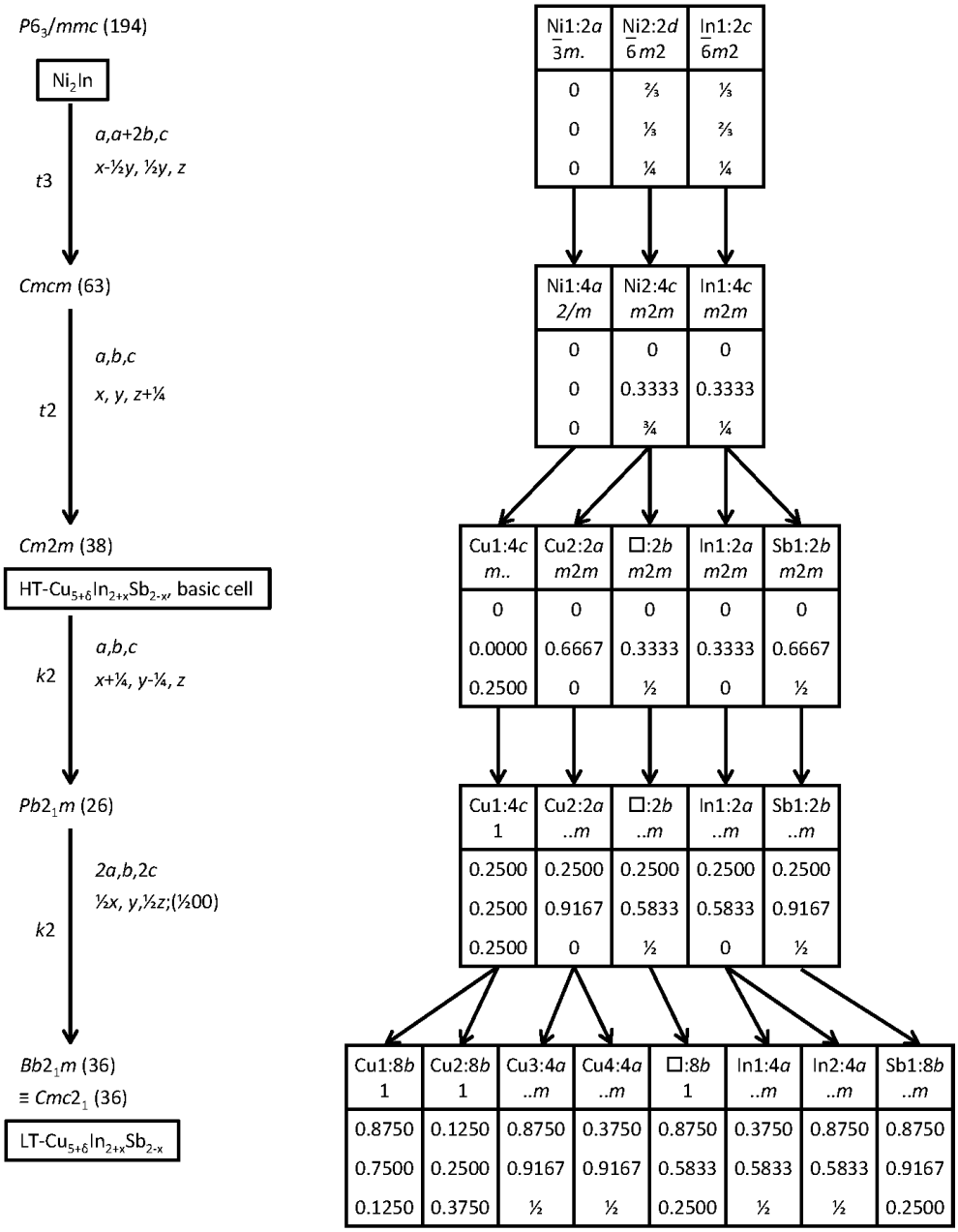

Figure B.7.: Group-Subgroup relations between the Ni_2In aristotype, space group $P6_3/mmc$, and the HT and LT modification of $Cu_{5+\delta}In_2Sb_2$. This symmetry reduction is an equivalent choice to the reduction via space group *Pbcm* (No. 57) that was presented in Paper I.

B.2. Binary Compounds TM-P

Table B.1.: Literature Overview for binary compounds with Ni_2In type superstructures. In contrast to the list given by *Lidin* [12], Ti_5Ga_4, β-Co_2Si and β-Ti_6Sn_5 type structures were excluded as they belong to other structure families [91]. Furthermore, high pressure modifications are not included as well as $Cu_{10}In_7$. Superspace groups and their numbers are given in accordance with the lists by *van Smaalen and Stokes* [92;93]. Axial ratios c/a are given for the underlying Ni_2In aristotype lattice.

Compound	structure type, space group	lattice parameters, Å	c/a	reference
Au_3In_2	Ni_2Al_3, $P\bar{3}m1$ (164)	$a = 4.537$ $c = 5.659$	1.247	[82]
Au_7In_4	A-Cu_7In_4, $P6_3/m(\alpha,\beta,0)(-\alpha-\beta,\alpha,0)00$ (176.2.80.1)	$a = 4.5619(5)$ c =5.6761(8) $\alpha = 0.352$ $\beta = 0.295$	1.244	this study
AuSn	AuSn, $P6_3/mmc$ (194)	$a = 4.3218$ $c = 5.5230$	1.278	[48]
Ce_2In	Ni_2In, $P6_3/mmc$ (194)	a = 5.562 $c = 6.911$	1.243	[94]
$Co_{1.70}Ge$	Ni_2In, $P6_3/mmc$ (194)	$a = 3.914$ $c = 5.004$	1.278	[14]
CoSb	AuSn, $P6_3/mmc$ (194)	a = 3.8906(1) $c = 5.1875(2)$	1.333	[95]
HT-Co_3Sn_2	Ni_2In, $P6_3/mmc$ (194)	$a = 4.097$ $c = 5.216$	1.273	[96]
RT-Co_3Sn_2	Ni_3Sn_2, $Pnma$ (62)	$a = 7.085(1)$ $b = 5.216(1)$ $c = 8.194(1)$	1.273	[96]
CrSb	AuSn, $P6_3/mmc$ (194)	$a = 4.122$ $c = 5.470$	1.327	[97]
HT-$Cu_{1.7}Al$	Ni_2In, $P6_3/mmc$ (194)	$a = 4.146(1)$ $c = 5.063(3)$	1.221	[98]
CuAl	CuAl, $C12/m1$ (12)	$a = 12.066$ $b = 4.105$ $b = 6.913$ $\beta = 55.04°$		[98]
$Cu_{4.8}Al_{3.6}$	$Cu_{4.8}Al_{3.6}$, $Fmm2$ (42)	$a = 8.1267(3)$ $b = 14.1985(5)$ $c = 9.9928(3)$	1.230	[99]
Cu_7In_3	Cu_7In_3, $P\bar{1}$ (2)	$a = 6.733(2)$	1.219	[58]

Compound	structure type, space group	lattice parameters, Å	c/a	reference
		$b = 9.134(3)$		
		$c = 10.074(3)$		
		$\alpha = 73.20(2)^\circ$		
		$\beta = 82.77(2)^\circ$		
		$\gamma = 89.76(2)^\circ$		
A,B-Cu_7In_4	A,B-Cu_7In_4	$a = 4.2607(6)$	1.231	[79]
	$P6_3/m(\alpha,\beta,0)(-\alpha-\beta,\alpha,0)00$	$c = 5.2463(7)$		
	(176.2.80.1)	$\alpha = 0.301(1)$		
		$\beta = 0.301(1)$		
C-Cu_7In_4	C-Cu_7In_4,	$a = 38.391(5)$	1.229	[77]
	not determined	$b = 7.388(1)$		
		$c = 20.972(3)$		
$Cu_{11}In_9$	$Cu_{11}In_9$, $C1m1$ (8)	$a = 12.8212(6)$	1.21	PaperV
		$b = 4.3548(5)$		
		$c = 7.3574(3)$		
		$\beta = 125.523(1)^\circ$		
η^8-Cu_5Sn_4	Cu_5Sn_4, $P12_1/c1$ (14)	$a = 9.84$	1.249	[85]
		$b = 7.27$		
		$c = 9.84$		
		$\beta = 62.5^\circ$		
η^6-Cu_5Sn_4	Cu_5Sn_4, $C121$ (5)	$a = 12.60$	1.214	[85]
		$b = 7.27$		
		$c = 10.20$		
		$\beta = 90^\circ$		
Cu_6Sn_5	Cu_6Sn_5, $\mathbf{C}12/c1$ (15)	$a = 11.022(5)$	1.202	[44]
		$b = 7.282(4)$		
		$c = 9.827(2)$		
		$\beta = 98.84(4)^\circ$		
HT-$Cu_{1.27}Sn$	Ni_2In, $P6_3/mmc$ (194)	$a = 4.219(5)$	1.211	[100]
		$c = 5.108(6)$		
Dy_2In	Ni_2In, $P6_3/mmc$ (194)	$a = 5.346$	1.247	[94]
		$c = 6.6677$		
Dy_2Tl	Ni_2In, $P6_3/mmc$ (194)	$a = 5.301$	1.255	[101]
		$c = 6.652$		
Er_2In	Ni_2In, $P6_3/mmc$ (194)	$a = 5.297$	1.254	[94]
		$c = 6.641$		
$Fe_{13}Ge_8$	$Fe_{13}Ge_8$, $P6_3/mmc$ (194)	$a = 7.976(5)$	1.252	[102]
		$c = 4.993(5)$		
$Fe_{1.6}Ge$	Ni_2In, $P6_3/mmc$ (194)	$a = 3.998(5)$	1.253	[102]
		$c = 5.010(5)$		
$Fe_{1.38}Sb$	Ni_2In, $P6_3/mmc$ (194)	$a = 4.140$	1.252	[97]

Compound	structure type, space group	lattice parameters, Å	c/a	reference
		$c = 5.183$		
FeSb	AuSn, $P6_3/mmc$ (194)	$a = 4.06$	1.264	[49]
		$c = 5.13$		
Fe_2Si	Ni_2Al, $P\bar{3}m1$ (164)	$a = 4.052$	1.255	[103]
		$c = 5.0855$		
$Fe_{1.67}Sn$ (HT)	Ni_2In, $P6_3/mmc$ (194)	$a = 4.225(2)$	1.240	[104]
		$c = 5.241(2)$		
Gd_2In	Ni_2In, $P6_3/mmc$ (194)	$a = 5.413$	1.248	[94]
		$c = 6.756$		
Gd_2Tl	Ni_2In, $P6_3/mmc$ (194)	$a = 5.360$	1.250	[105]
		$c = 6.700$		
Ho_2In	Ni_2In, $P6_3/mmc$ (194)	$a = 5.3216(10)$	1.253	[106]
		$c = 6.6667(9)$		
Ir_3Si_2	Ni_2In, $P6_3/mmc$ (194)	$a = 3.963$	1.293	[107]
		$c = 5.126$		
La_2In	Ni_2In, $P6_3/mmc$ (194)	$a = 5.636$	1.254	[94]
		$c = 7.065$		
Lu_2In	Ni_2In, $P6_3/mmc$ (194)	$a = 5.240$	1.257	[108]
		$c = 6.588$		
Mn_2Ge	Ni_2In, $P6_3/mmc$ (194)	$a = 4.171(1)$	1.265	[109]
		$c = 5.278(2)$		
HT-Mn_2Sn	Ni_2In, $P6_3/mmc$ (194)	$a = 4.3735(10)$	1.261	[110]
		$c = 5.5148(11)$		
Mn_8Sn_5	Mn_8Sn_5, $Pnma$ (62)	$a = 7.6003(5)$	1.261	[111]
		$b = 5.5247(5)$		
		$c = 21.9114(4)$		
Mn_8Sn_5	Mn_8Sn_5, $Pmmn$ (59)	$a = 5.5247(5)$	1.261	[111]
		$b = 21.9114(4)$		
		$c = 7.6003(5)$		
Mn_3Sn_2	Ni_3Sn_2, $Pnma$ (62)	$a = 7.5547(2)$	1.282	[110]
		$b = 5.4994(2)$		
		$c = 8.5842(2)$		
NbSb	AuSn, $P6_3/mmc$ (194)	$a = 4.270$	1.276	[112]
		$c = 5.447$		
Nd_2In	Ni_2In, $P6_3/mmc$ (194)	$a = 5.505$	1.248	[94]
		$c = 6.868$		
Nd_2Tl	Ni_2In, $P6_3/mmc$ (194)	$a = 5.520$	1.235	[113]
		$c = 6.816$		
NiBi	NiBi, $F12/m1$ (12)	$a = 14.124(1)$	1.313	[114]
		$b = 8.1621(6)$		
		$c = 21.429(2)$		

Compound	structure type, space group	lattice parameters, Å	c/a	reference
		$\beta = 90°$		
$Ni_{0.92}Bi$	$Ni_{0.92}Bi$, $Pmcm(0,0,\gamma)s00$ (51.1.9.10)	$a = 8.1527$ $b = 14.1204$ $c = 5.3243$ $\gamma = 0.26$	1.306	[115]
$Ni_{1.22}Bi$	Ni_2In, $P6_3/mmc$ (194)	$a = 4.072$ $c = 5.345$	1.313	[116]
$Ni_{13}Ga_9$	$Ni_{13}Ga_9$, $C12/m1$ (12)	$a = 13.822$ $b = 7.894$ $c = 8.478$ $\beta = 35.88°$	1.280	[117]
$Ni_{1.78}Ga$	Ni_2In, $P6_3/mmc$ (194)	$a = 3.992(5)$ $c = 4.973(5)$	1.246	[118]
HT-Ni_3Ge_2	Ni_3Ge_2, $P6\bar{6}/m2$ (187)	$a = 3.864$ $c = 5.042$	1.301	[119]
$Ni_{19}Ge_{12}$	$Ni_{19}Ge_{12}$, $C121$ (5)	$a = 11.631$ $b = 6.715$ $c = 10.048$ $\beta = 90°$	1.299	[119]
Ni_5Ge_3	Ni_5Ge_3, $C121$ (5)	$a = 11.682(6)$ $b = 6.737(3)$ $c = 6.264(3)$ $\beta = 52.11°$	1.292	[75]
LT-Ni_7Ge_4	Ni_7Ge_4, $C12/m1$ (No.12)	$a = 10.13$ $b = 7.80$ $c = 6.83$	1.299	[75;120]
$Ni_{13}In_9$	$Ni_{13}Ga_9$, $C12/m1$ (12)	$a = 14.7417(2)$ $b = 8.3905(4)$ $c = 9.0376(3)$ $\beta = 36.375°$		[121]
$Ni_{13}In_9$	$Ni_{13}Ga_9$, $C12/m1$ (12)	$a = 10.4585(9)$ $b = 8.3952(4)$ $c = 9.0309(4)$ $\beta = 125.38(1)°$	1.238	this study
Ni_2In	Ni_2In, $P6_3/mmc$ (194)	$a = 4.187(1)$ $c = 5.132(1)$	1.226	[14]
Ni_7In_3	Cu_7In_3, $P\bar{1}$ (2)	$a = 11.1000(16)$, $b = 11.0951(19)$, $c = 6.5697(13)$ $\alpha = 126.593(11)°$ $\beta = 61.121(12)°$	1.209	[121]

Compound	structure type, space group	lattice parameters, Å	c/a	reference
		$\gamma = 119.589(8)°$		
Ni_7In_3	Ni_7In_3, $P\bar{1}(\alpha\beta\gamma)000$ (2.1.1.1)	$a = 4.197(2)$ $b = 4.237(3)$ $c = 5.092(3)$ $\alpha = 90.7(1)°$ $\beta = 89.7(1)°$ $\gamma = 119.9(1)°$ $\alpha = 0.1428$ $\beta = 0.2857$ $\gamma = 0.1438$	1.209	this study
NiSb	AuSn, $P6_3/mmc$ (194)	$a = 3.94532(6)$ $c = 5.14257(9)$	1.303	[95]
HT-Ni_2Si	Ni_2In, $P6_3/mmc$ (194)	$a = 3.805$ $c = 4.890$	1.285	[122;123]
HT-Ni_3Sn_2	Ni_2In, $P6_3/mmc$ (194)	$a = 4.1373(3)$ $c = 5.2050(4)$	1.258	[124]
RT-Ni_3Sn_2	Ni_3Sn_2, $Pnma$ (62)	$a = 7.1240(9)$ $b = 5.1970(4)$ $c = 8.1562(7)$	1.274	[96]
RT-$Ni_{1.41}Sn_2$	UPt_2, $Cmcm$ (63)	$a = 4.0606$ $b = 7.087$ $c = 5.1683$	1.273	[124]
HT-$Pd_{1.44}Pb$	Ni_2In, $P6_3/mmc$ (194)	$a = 4.493(2)$ $c = 5.762(3)$	1.282	[125]
RT-$Pd_{13}Pb_9$	$Pd_{13}Pb_9$, $C12/c1$ (15)	$a = 15.6027(9)$ $b = 9.0599(5)$ $c = 13.911(1)$ $\beta = 55.875(5)°$	1.282	[125]
RT-Pd_5Pb_3	Ni_5Ge_3, $C121$ (5)	$a = 13.331(4)$ $b = 7.667(4)$ $c = 7.258(2)$ $\beta = 52.227°$	1.283	[126]
$Pd_{1.67}Pb$	Ni_2In, $P6_3/mmc$ (194)	$a = 4.463(1)$ $c = 5.728(2)$	1.283	[126]
$Pd_{13}Sn_9$	$Pd_{13}Sn_9$, $P3_121$ (152)	$a = 8.7985(11)$ $c = 16.9837(34)$	1.287	[127]
$Pd_{13}Tl_9$	$Pd_{13}Tl_9$ $P\bar{3}m1$ (164)	$a = 8.958$ $c = 5.623$	1.255	[128]
Pr_2In	Ni_2In, $P6_3/mmc$ (194)	$a = 5.534$ $c = 6.893$	1.246	[94]
PtBi	AuSn, $P6_3/mmc$ (194)	$a = 4.324(1)$	1.272	[129]

Compound	structure type, space group	lattice parameters, Å	c/a	reference
PtIn	CuAl, $C12/m1$ (12)	$c = 5.501(2)$ $a = 13.572(1)$ $b = 4.4299(2)$ $c = 7.5797(3)$ $\beta = 54.198(3)°$	1.277	[130]
$Pt_{13}In_9$	$Ni_{13}Ga_9$, $C12/m1$ (12)	$a = 15.344$ $b = 8.792$ $c = 9.500$ $\beta = 35.79°$	1.277	[117]
HT-Pt_3In_2	Ni_2In, $P6_3/mmc$ (194)	$a = 4.35$ $c = 5.55$	1.276	[131]
PtPb	AuSn, $P6_3/mmc$ (194)	$a = 4.24$ $= 5.48$	1.292	[132]
PtSb	AuSn, $P6_3/mmc$ (194)	$a = 4.126$ $c = 5.481$	1.328	[97]
PtSn	AuSn, $P6_3/mmc$ (194)	$a = 4.1014(2)$ $c = 5.4405(2)$	1.326	[133]
HT-Pd_3Sn_2	Ni_2In, $P6_3/mmc$ (194)	$a = 4.389$ $c = 5.703$	1.299	[134]
Rh_3Pb_2	Ni_2In, $P6_3/mmc$ (194)	$a = 4.330(7)$ $c = 5.639(8)$	1.302	[135]
Rh_3Si_2	Ni_2Al_3, $P\bar{3}m1$ (164)	$a = 3.965$ $c = 5.051$	1.274	[136]
HT-$Rh_{20}Si_{13}$	Ni_2In, $P6_3/mmc$ (194)	$a = 3.949$ $c = 5.047$	1.278	[107]
Rh_3Sn_2	Ni_2In, $P6_3/mmc$ (194)	$a = 4.331$ $c = 5.542$	1.280	[137]
Sc_2Al	Ni_2In, $P6_3/mmc$ (194)	$a = 4.8813$ $c = 6.167$	1.263	[138]
Sc_2In	Ni_2In, $P6_3/mmc$ (194)	$a = 5.024$ $c = 6.276$	1.249	[139]
Sm_2In	Ni_2In, $P6_3/mmc$ (194)	$a = 5.450$ $c = 6.785$	1.245	[94]
Sm_2Tl	Ni_2In, $P6_3/mmc$ (194)	$a = 5.44$ $c = 6.77$	1.244	[140]
Tb_2In	Ni_2In, $P6_3/mmc$ (194)	$a = 5.367$ $c = 6.707$	1.250	[94]
Tb_2Tl	Ni_2In, $P6_3/mmc$ (194)	$a = 5.362$ $c = 6.663$	1.243	[101]
Ti_2Ga	Ni_2In, $P6_3/mmc$ (194)	$a = 4.51$ $c = 5.50$	1.220	[141]

Compound	structure type, space group	lattice parameters, Å	c/a	reference
Tm_2In	Ni_2In, $P6_3/mmc$ (194)	$a = 5.274$ $c = 6.621$	1.255	[94]
VSb	AuSn, $P6_3/mmc$ (194)	$a = 4.270$ $c = 5.447$	1.276	[50]
HT-V_3Sb_2	Ni_2In, $P6_3/mmc$ (194)	$a = 4.28$ $c = 5.11$	1.194	[142]
Y_2In	Ni_2In, $P6_3/mmc$ (194)	$a = 5.365$ $c = 6.778$	1.263	[143]
Yb_2Sn	Ni_2In, $P6_3/mmc$ (194)	$a = 5.371$ $c = 7.066$	1.316	[144]
RT-Zr_2Al	Ni_2In, $P6_3/mmc$ (194)	$a = 4.8939(5)$ $c = 5.9283(5)$	1.21	[145]

B.3. Ternary Compounds TM1-TM2-P with Ni_2In Type Structures

Table B.2.: Literature Overview for ternary compounds TM1-TM2-P with Ni_2In type superstructures. High pressure modifications are not included. Superspace groups and their numbers are given in accordance with the lists by *van Smaalen and Stokes*[92;93]. Axial ratios c/a are given for the underlying Ni_2In aristotype lattice.

Compound	structure type, space group	lattice parameters, Å	c/a	reference
$Ag_2Pd_{12}Pb_8$	$Ni_{13}Ga_3Ge_6$, $P3_121$ (152)	$a = 8.9713(16)$ $c = 17.2900(43)$	1.285	[127]
$Au_{0.76}Co_{0.24}Sn$	AuSn, $P6_3/mmc$ (194)	$a = 4.20$ $c = 5.42$	1.290	[146]
$Au_{0.58}Co_{0.92}Sn$	Ni_2In, $P6_3/mmc$ (194)	$a = 4.16$ $c = 5.40$	1.298	[146]
$Au_2Cu\text{-}In_2$	Ni_2In, $P6_3/mmc$ (194)	$a = 4.3842(1)$ $c = 5.5710(2)$	1.271	this study
$Au_2Cu\text{-}In_2$	Ni_2In, $P6_3/mmc$ (194)	$a = 4.3754(1)$ $c = 5.5554(2)$	1.270	this study
$AuCu_2In_2$	Ni_2In, $P6_3/mmc$ (194)	$a = 4.3462(2)$ $c = 5.3804(2)$	1.238	this study
$AuCu_2In_2$	Ni_2In, $P6_3/mmc$ (194)	$a = 4.3475(1)$ $c = 5.3816(2)$	1.238	this study
$Au_{1.5}Cu_{1.5}In_2$	Ni_2In, $P6_3/mmc$ (194)	$a = 4.3670(1)$ $c = 5.4681(2)$	1.252	this study
$Au_{1.5}Cu_{1.5}In_2$	Ni_2In, $P6_3/mmc$ (194)	$a = 4.3804(4)$ $c = 5.4854(5)$	1.252	this study
$Au_{0.56}Cu_{0.56}Sn$	Ni_2In, $P6_3/mmc$ (194)	$a = 4.288$ $c = 5.313$	1.239	[100]
$AuCuSn_2$	$CuAuSn_2$, $P\bar{3}m1$ (164)	$a = 4.2597(17)$ $c = 5.2688(15)$	1.237	[80]
Au-Ni-In	average cell	$a = 4.3426(10)$ $c = 5.4785(16)$	1.262 1.262	this study this study
$Au_{3.895}Ni_{9.283}In_{8.812}$	$Ni_{13}Ga_9$, $C12/m1$ (12)	$a = 10.6828(8)$ $b = 8.4779(8)$ $c = 9.0739(5)$ $\beta = 126.06(0)$ °	1.261	this study
$AuNiSn_2$	$AuNiSn_2$, $P\bar{3}m1$ (164)	$a = 4.1241(14)$ $c = 5.2924(11)$	1.283	[80]
$Au_{0.8}Pt_{0.2}Sn$	AuSn, $P6_3/mmc$ (194)	$a = 4.2625$ $c = 5.5375$	1.299	[147]

Compound	structure type, space group	lattice parameters, Å	c/a	reference
AuTiAl	Ni_2In, $P6_3/mmc$ (194)	$a = 4.4075(8)$ $c = 5.829(1)$	1.323	[148]
$Co_{0.53}Cr_{0.47}Sb_{0.93}$	AuSn, $P6_3/mmc$ (194)	$a = 4.05$ $c = 5.32$	1.314	[149]
$Co_{0.9}Fe_{0.9}Ge$	Ni_2In, $P6_3/mmc$ (194)	$a = 3.989$ $c = 5.035$	1.262	[150]
CoFeSn	Ni_2In, $P6_3/mmc$ (194)	$a = 4.175$ $c = 5.278$	1.264	[151]
$Co_{0.833}Ni_{0.833}Ge$	Ni_2In, $P6_3/mmc$ (194)	$a = 3.892$ $c = 5.008$	1.287	[152]
$Co_{0.81}Ni_{1.08}Ge_{1.11}$	Ni_2In, $P6_3/mmc$ (194)	$a = 3.905(1)$ $c = 5.020(1)$	1.286	[153]
$Co_{0.5}Ni_{0.5}Sb$	AuSn, $P6_3/mmc$ (194)	$a = 3.9215(3)$ $c = 5.1424(4)$	1.311	[95]
CoNiSn	Ni_2In, $P6_3/mmc$ (194)	$a = 4.120$ $c = 5.208$	1.264	[151]
$Cr_{0.64}Fe_{0.59}Sb$	Ni_2In, $P6_3/mmc$ (194)	$a = 4.158(2)$ $c = 5.365(3)$	1.290	[154]
$Cr_{0.366}Fe_{0.854}Sb$	Ni_2In, $P6_3/mmc$ (194)	$a = 4.156(2)$ $c = 5.272(2)$ $c = 5.16$	1.269	[154]
$Cr_{0.8}Ni_{0.2}Sb$	AuSn, $P6_3/mmc$ (194)	$a = 4.103$ $c = 5.432$	1.324	[155]
$Cr_{0.41}Ni_{0.59}Sb$	AuSn, $P6_3/mmc$ (194)	$a = 4.11$ $c = 5.28$	1.285	[156]
$Cr_{0.2}Ni_{0.8}Sb$	AuSn, $P6_3/mmc$ (194)	$a = 3.943$ $c = 5.144$	1.305	[155]
$Cu_{0.62}Mn_{1.38}Ga$	Ni_2In, $P6_3/mmc$ (194)	$a = 4.202$ $c = 5.353$	1.274	[157]
$Cu_{0.81}Ni_{0.97}In$	Ni_2In, $P6_3/mmc$ (194)	$a = 4.232$ $c = 5.195$	1.228	[158]
$(Cu,Ni)_7In_3$ [1]	Ni_7In_3, $P\bar{1}(\alpha\beta\gamma)0$ (2.1.1.1)	$a = 4.2253(14)$ $c = 5.2142(17)$ $\alpha = 0.1428(8)$ $\beta = 0.2860(6)$ $\gamma = 0.1433(8)$		this study
$Ni_{0.747}CuIn$	$(Cu,Ni)_2In$, $Pnam(0\beta0)s00$ (62.1.9.1)	$a = 5.159(7)$ $b = 7.383(15)$ $c = 4.222(7)$	1.222	this study

[1] incommensurate structure model, $Ni_4Cu_3In_3$

Compound	structure type, space group	lattice parameters, Å	c/a	reference
		$\beta = 0.320(2)$		
$CuNiSb_2$	$AuNiSn_2$, $P\bar{3}m1$ (164)	$a = 4.0510(2)$	1.268	[81]
		$c = 5.1382(4)$		
$Cu_{0.43}Ni_{1.43}Si$	Ni_2In, $P6_3/mmc$ (194)	$a = 3.86$	1.282	[159]
		$c = 4.95$		
$Cu_4Ni_2Sn_5$	Cu_6Sn_5, $C12/c1$ (15)	$a = 10.902$		[160]
		$b = 7.038$		
		$c = 9.538$		
		$\beta = 99.142°$		
HT-$Cu_{0.84}Ni_{0.66}Sn$	Ni_2In, $P6_3/mmc$ (194)	$a = 4.16608(7)$	1.238	[55]
		$c = 5.1565(1)$		
HT-$Cu_{0.67}Ni_{0.53}Sn$	Ni_2In, $P6_3/mmc$ (194)	$a = 4.13441(4)$	1.240	[55]
		$c = 5.12471(6)$		
HT-$Cu_{0.20}Ni_{1.20}Sn$	Ni_2In, $P6_3/mmc$ (194)	$a = 4.053$	1.268	[161]
		$c = 5.14$		
$Cu_{0.34}Ni_{2.56}Sn_{2.1}$	Ni_3Sn_2, $Pnma$ (62)	$a = 7.1184(3)$	1.264	[55]
		$b = 5.1734(2)$		
		$c = 8.1793(5)$		
$Cu_{1.84}Pt_{3.09}In_3$[2]	Ni_2In, $P6_3/mmc$ (194)	$a = 4.2468(3)$	1.303	this study
		$c = 5.5351(5)$		
$Fe_{.9}Ni_{0.9}Ge$	Ni_2In, $P6_3/mmc$ (194)	$a = 3.976$	1.260	[150]
		$c = 5.009$		
$Fe_{0.833}Ni_{0.833}Ge$	Ni_2In, $P6_3/mmc$ (194)	$a = 3.957$	1.273	[162]
		$c = 5.036$		
FeNiIn	Ni_2In, $P6_3/mmc$ (194)	$a = 4.377$	1.214	[151]
		$c = 5.313$		
$Fe_{0.36}Ni_{0.84}Sb$	Ni_2In, $P6_3/mmc$ (194)	$a = 4.036$	1.284	[163]
		$c = 5.184$		
$Fe_{0.5}Pt_{0.5}Sn$	AuSn, $P6_3/mmc$ (194)	$a = 4.115$	1.316	[164]
		$c = 5.416$		
HT-MnCoGe	Ni_2In, $P6_3/mmc$ (194)	a =4.101(2)	1.286	[165]
		$c = 5.273(2)$		
HT-MnCoSi	Ni_2In, $P6_3/mmc$ (194)	$a = 4.03$	1.313	[166]
		$c = 5.29$		
MnCoSn	Ni_2In, $P6_3/mmc$ (194)	$a = 4.280$	1.260	[151]
		$c = 5.394$		
MnFeGe	Ni_2In, $P6_3/mmc$ (194)	$a = 4.112$	1.275	[151]
		$c = 5.242$		
$Mn_{0.67}FeGe$	Ni_2In, $P6_3/mmc$ (194)	$a = 4.064(2)$	1.272	[167]

[2] average basic lattice

Compound	structure type, space group	lattice parameters, Å	c/a	reference
		$c = 5.168(2)$		
MnFeIn	Ni_2In, $P6_3/mmc$ (194)	$a = 4.302$	1.245	[151]
		$c = 5.356$		
MnPtAl	Ni_2In, $P6_3/mmc$ (194)	$a = 4.336$	1.269	[151]
		$c = 5.501$		
MnPtGa	Ni_2In, $P6_3/mmc$ (194)	$a = 4.336$	1.289	[151]
		$c = 5.590$		
$Ni_{12}PdGa_9$	$Pd_{13}Tl_9$, $P\bar{3}m1$ (164)	$a = 7.978(4)$	1.260	[168]
		$c = 5.025(4)$		
$Ni_{0.45}PtIn$ (773 K)	Ni_3Sn_2, $Pmnb$ (62)	$a = 5.5272(3)$	1.317	this study
		$b = 7.3592(4)$		
		$c = 8.3910(6)$		
$Ni_{7.642}Pt_{5.498}In_{8.86}$	$Ni_{13}Ga_9$, $C12/m1$ (12)	$a = 10.6755(9)$	1.255	this study
		$b = 8.5048(11)$		
		$c = 9.130(2)$		
		$\beta = 125.77(1)^\circ$		
$Pd_{2-x}Cu_xSn$	Ni_2In, $P6_3/mmc$ (194)	$a = 4.23$-4.37		[169]
		$c = 5.22$-5.68		
$Pt_{0.5}Co_{0.5}Sn_{0.5}$	AuSn, $P6_3/mmc$ (194)	$a = 4.144$	1.306	[164]
		$c = 5.410$		
$Pt_{0.5}Cr_{0.5}Sn_{0.5}$	AuSn, $P6_3/mmc$ (194)	$a = 4.106$	1.325	[164]
		$c = 5.441$		
$Pt_{0.67}Ni_{0.67}Sn_{0.67}$	AuSn, $P6_3/mmc$ (194)	$a = 4.205$	1.281	[164]
		$c = 5.388$		
$Pt_{0.7}Pd_{0.3}Bi$	AuSn, $P6_3/mmc$ (194)	$a = 4.30$	1.302	[129]
		$c = 5.60$		
$Pd_{0.9}Pt_{0.9}Sn$	Ni_2In, $P6_3/mmc$ (194)	$a = 4.435(4)$	1.285	[170]
		$c = 5.699(4)$		
$Pt_{0.84}Pd_{0.16}Sn$	AuSn, $P6_3/mmc$ (194)	$a = 4.104(2)$	1.325	[170]
		$c = 5.436(2)$		
TiMnSb	Ni_2In, $P6_3/mmc$ (194)	$a = 4.386$	1.327	[171]
		$c = 5.820$		
TiPtAl	Ni_2In, $P6_3/mmc$ (194)	$a = 4.3964(2)$	1.248	[172]
		$c = 5.4868(3)$		
TiPtGa	Ni_2In, $P6_3/mmc$ (194)	$a = 4.3733(1)$	1.263	[173]
		$c = 5.5226(2)$		
$Ti_{1.94}Zr_{0.06}Sn$	Ni_2In, $P6_3/mmc$ (194)	$a = 4.639(3)$	1.205	[174]
		$c = 5.589(6)$		
$V_2Cu_3Sb_4$	$V_2Cu_3Sb_4$, $P6_3/mmc$ (194)	$a = 8.52905(5)$	1.242	[175]
		$c = 5.29456(4)$		
$V_{0.5}Fe_{0.5}Sb$	AuSn, $P6_3/mmc$ (194)	$a = 4.238(5)$	1.274	[176]

Compound	structure type, space group	lattice parameters, Å	c/a	reference
		$c = 5.399(6)$		
$V_{0.5}MnSb$	Ni_2In, $P6_3/mmc$ (194)	$a = 4.280$	1.324	[177]
		$c = 5.668$		
$V_{0.07}NiSb_{0.95}$	AuSn, $P6_3/mmc$ (194)	$a = 3.9333(5)$	1.307	[178]
		$c = 5.1402(6)$		
$V_{0.5}Ni_{0.5}Sb$	AuSn, $P6_3/mmc$ (194)	$a = 4.217(3)$	1.280	[176]
		$c = 5.398(4)$		
$V_{0.07}Ni_{0.93}Sb$	AuSn, $P6_3/mmc$ (194)	$a = 3.9398(4)$	1.305	[178]
		$c = 5.1408(6)$		
$V_{0.88}Ni_{0.12}Sb$	AuSn, $P6_3/mmc$ (194)	$a = 4.244(2)$	1.264	[178]
		$c = 5.366(4)$		
$VNi_{0.35}Sb$	Ni_2In, $P6_3/mmc$ (194)	$a = 4.2134(6)$	1.287	[178]
		$c = 5.4225(8)$		
$Zr_{0.1}Ni_{0.9}Sb$	AuSn, $P6_3/mmc$ (194)	$a = 3.959(1)$	1.299	[179]
		$c = 5.141(2)$		

B.4. Ternary Compounds TM-P1-P2 with Ni_2In Type Structures

Table B.3.: Literature Overview for ternary compounds TM-P1-P2 with Ni_2In type superstructures. High pressure modifications are not included. $Au_{10}In_7Sb_3$ [41] was excluded as the phase was inaccessible within this study. Superspace groups and their numbers are given in accordance with the lists by *van Smaalen and Stokes* [92;93]. Axial ratios c/a are given for the underlying Ni_2In aristotype lattice.

Compound	structure type, space group	lattice parameters, Å	c/a	reference
Au_3InSn_2	AuSn, $P6_3/mmc$ (194)	$a = 4.2852(2)$ $c = 5.5403(1)$	1.293	PaperIV
$Au_{1.1}In_{0.25}Sn_{0.75}$	AuSn, $P6_3/mmc$ (194)	$a = 4.2949(2)$ $c = 5.5329(1)$	1.288	PaperIV
$Au_{0.98}In_{0.14}Sn_{0.86}$	AuSn, $P6_3/mmc$ (194)	$a = 4.3088(2)$ $c = 5.5380(1)$	1.285	PaperIV
Au_6Sn_5Sb	AuSn, $P6_3/mmc$ (194)	$a = 4.3396(6)$ $c = 5.5127(4)$	1.270	PaperIV
$Co_3Ga_{0.5}As_{1.5}$	Ni_2In, $P6_3/mmc$ (194)	$a = 3.8177(4)$ $c = 5.0951(7)$	1.335	[180]
$Co_{1.80}Ga_{0.5}As_{0.5}$	Ni_2In, $P6_3/mmc$ (194)	$a = 3.968(1)$ $c = 5.021(1)$	1.265	[181]
HT-Co_7GaGe_3	$Fe_{6.5}Ge_4$, $P6_3/mmc$ (194)	$a = 7.853(5)$ $c = 4.999(5)$	1.273	[102]
$Co_{13}Ga_{2.17}Ge_{6.5}$	$Pd_{13}Tl_9$, $P\bar{3}m1$ (164)	$a = 7.83$ $c = 4.96$	1.265	[128]
HT-$Co_2Ge_{0.7}Si_{0.3}$	Ni_2In, $P6_3/mmc$ (194)	$a = 3.887$ $c = 4.989$	1.284	[182]
$Cu_7In_{4-x}Ge_x$	A-Cu_7In_4, $P6_3/m(\alpha,\beta,0)(-\alpha-\beta,\alpha,0)00$ (176.2.80.1)	$a = 4.2523(15)$ $c = 5.2001(18)$ $\alpha = 0.2907$ $\beta = 0.2907$	1.223	this study
HT-$Cu_{2-x}In_2Sb_2$ [3]	Ni_2In, $P6_3/mmc$ (194)	$a = 4.2477(3)$ $c = 5.1117(4)$	1.203	this study
HT-$Cu_5In_2Sb_2$	$Cu_5In_2Sb_2$, $Xm2m(\alpha00)000$ (38.1.16.13)	$a = 4.249(1)$ $b = 7.360(2)$ $c = 10.219(2)$ $\alpha = 0.33(1)$	1.203	PaperIII
LT-$Cu_5In_2Sb_2$	$Cu_5In_2Sb_2$, $Cmc2_1$ (36)	$a = 10.1813(4)$	1.204	PaperI

[3] diffuse scattering, average cell

Compound	structure type, space group	lattice parameters, Å	c/a	reference
		$b = 8.4562(4)$		
		$c = 7.3774(2)$		
$Cu_2In_{0.75}Sb_{0.25}$	$Cu_2In_{0.75}Sb_{0.25}$, *Pmnm* (59)	$a = 5.1770(2)$	1.208	PaperVI
		$b = 7.4093(4)$		
		$c = 8.5659(4)$		
$Cu_7In_{2.5}Sb_{0.5}$	$Cu_7In_{2.5}Sb_{0.5}$, $P\bar{1}$ (2)	$a = 6.7427(8)$	1.209	PaperVI
		$b = 9.074(1)$		
		$c = 10.047(2)$		
		$\alpha = 107.28(1)°$		
		$\beta = 97.12(1)°$		
		$\gamma = 90.56(1)°$		
$Cu_7In_{4-x}Sn_x$	A-Cu_7In_4,	$a = 4.2341(1)$	1.232	this study
	$P6_3/m(\alpha,\beta,0)(-\alpha-\beta,\alpha,0)00$	$c = 5.2159(2)$		
	(176.2.80.1)	$\alpha = 0.284(1)$		
		$\beta = 0.284(1)$		
Cu_7In_2Sn	average cell	$a = 4.2984(6)$	1.208	this study
	Ni_2In, $P6_3/mmc$ (194)	$c = 5.1941(5)$		
		$c =$		
LT1-$Cu_{7.8}In_{1.7}Sn_3$	$Cu_{7.8}In_{1.7}Sn_3$	$a = 5.1517(7)$	1.209	this study
	$P2_1nb(\alpha00)0ss$	$b = 7.296(1)$		
	(33.1.9.2)	$c = 8.519(1)$		
		$\alpha = 0.3813(4)$		
LT2-$Cu_7In_{1.55}Sn_{2.45}$	$Cu_7In_{1.55}Sn_{2.45}$, *Pnma* (62)	$a = 7.3732(2)$	1.213	this study
		$b = 5.1657(4)$		
		$c = 8.5157(4)$		
HT$Cu_{7.8}In_{1.8}Sn_3$	Ni_2In, $P6_3/mmc$ (194)	$a = 4.2445(4)$	1.212	this study
		$c = 5.1452(4)$		
$Cu_{4.8}Sn_{3.84}Sb_{0.16}$	Cu_5Sn_4, $P12_1/c1$ (14)	$a = 9.921(8)$	1.214	[43]
		$b = 7.352(10)$		
		$c = 9.921(12)$		
		$\beta = 62.5416°$		
Fe_3GaAs	Ni_2In, $P6_3/mmc$ (194)	$a = 4.015$	1.255	[183]
		$c = 5.040$		
$Fe_6Ga_{3.4}As_{0.6}$	$Fe_{6.5}Ge_4$, $P6_3/mmc$ (194)	$a = 8.156$	1.228	[183]
		$c = 5.006$		
HT-MnCoGe	Ni_2In, $P6_3/mmc$ (194)	$a = 4.087(1)$	1.301	[184]
		$c = 5.316(3)$		
$Fe_{1.45}Ga_{0.59}Sb_{0.46}$	Ni_2In, $P6_3/mmc$ (194)	$a = 4.0943(4)$	1.242	[185]
		$c = 5.0843(2)$		
$Fe_{1.59}Ga_{0.62}Sb_{0.38}$	Ni_2In, $P6_3/mmc$ (194)	$a = 4.107$	1.240	[186]
		$c = 5.094$		

Compound	structure type, space group	lattice parameters, Å	c/a	reference
$FeGe_{0.3}Sb_{0.7}$	AuSn, $P6_3/mmc$ (194)	$a = 4.025(2)$ $c = 5.090(3)$	1.265	[187]
$Fe_{1.45}Sn_{0.5}Sb_{0.5}$	Ni_2In, $P6_3/mmc$ (194)	$a = 4.165$ $c = 5.19$	1.246	[188]
$FeSn_{0.20}Sb_{0.80}$	AuSn, $P6_3/mmc$ (194)	$a = 4.105(3)$ $c = 5.146(5)$	1.254	[189]
$Mn_2Ga_{0.5}As_{0.5}$	Ni_2In, $P6_3/mmc$ (194)	a =4.062(3) $c = 5.048(6)$	1.243	[181]
$Mn_{1.5}Sn_{0.5}Sb_{0.5}$	Ni_2In, $P6_3/mmc$ (194)	$a = 4.32$ $c = 5.55$	1.285	[190]
$Ni_{1.75}Al_{0.5}As_{0.5}$	Ni_2In, $P6_3/mmc$ (194)	$a = 3.959(2)$ $c = 5.064(7)$	1.279	[191]
$Ni_{1.5}Al_{0.2}As_{0.8}$	Ni_2In, $P6_3/mmc$ (194)	$a = 3.836(1)$ $c = 5.115(2)$	1.333	[191]
$Ni_{1.5}Al_{0.5}Sb_{0.5}$	Ni_2In, $P6_3/mmc$ (194)	$a = 4.03(1)$ $c = 5.13(1)$	1.273	[192]
HT-$Ni_{12.5}Al_{0.9}Si_{8.1}$	$Ni_{13}Ga_3Ge_6$, $P3_121$ (152)	$a = 7.653(1)$ $c = 14.665(3)$	1.277	[193]
$NiBi_{0.4}Sb_{0.6}$	AuSn, $P6_3/mmc$ (194)	$a = 4.000$ $c = 5.200$	1.300	[129]
$Ni_{1.5}Ga_{0.25}As_{0.75}$	Ni_2In, $P6_3/mmc$ (194)	$a = 3.826(2)$ $c = 5.109$	1.335	[194]
$Ni_{1.5}Ga_{0.5}As_{0.5}$	Ni_2In, $P6_3/mmc$ (194)	$a = 3.90(1)$ $c = 5.01(2)$	1.285	[195]
$Ni_{1.78}Ga_{0.5}As_{0.5}$	Ni_2In, $P6_3/mmc$ (194)	$a = 3.941(2)$ $c = 5.060(2)$	1.284	[194]
$Ni_{1.7}Ga_{0.46}Ge_{0.54}$	Ni_2In, $P6_3/mmc$ (194)	$a = 3.951(1)$ $c = 5.002(2)$	1.266	[14]
$Ni_{13}Ga_3Ge_6$	$Ni_{13}Ga_3Ge_6$, $P3_121$ (152)	$a = 7.8487(4)$ $c = 15.036(1)$	1.277	[196]
$Ni_{1.5}Ga_{0.5}Sb_{0.5}$	Ni_2In, $P6_3/mmc$ (194)	$a = 4.00(1)$ $c = 5.09(1)$	1.273	[192]
$NiGa_{0.125}Sb_{0.875}$	AuSn, $P6_3/mmc$ (194)	$a = 3.935(1)$ $c = 5.130(1)$	1.304	[197]
$NiGa_{0.51}Si_{0.08}$	AuSn, $P6_3/mmc$ (194)	$a = 3.955(1)$ $c = 4.960(1)$	1.254	[198]
$Ni_{13\pm x}Ge_{9-y}Al_y$	$Ni_{13}Ga_3Ge_6$, $P3_121$ (152)	$a = 7.871(2)$ $c = 15.018(1)$	1.272	[199]
$Ni_{1.68}In_{0.33}Sn_{0.67}$	$Ni_{1.68}In_{0.33}Sn_{0.67}$, $R32$ (155)	$a = 7.1969(7)$ $c = 15.554(2)$	1.248	this study
Ni_5In_2Sn	Ni_5In_2Sn, $Cmcm$ (63)	$a = 12.4576(2)$	1.256	this study

Compound	structure type, space group	lattice parameters, Å	c/a	reference
		$b = 7.1774(3)$		
		$c = 5.2168(2)$		
Ni_3InSb	Ni_2In, $P6_3/mmc$ (194)	$a = 4.11(1)$	1.263	[192]
		$c = 5.19(1)$		
$Ni_{1.25}Sn_{0.5}As_{0.5}$	Ni_2In, $P6_3/mmc$ (194)	$a = 3.88(1)$	1.33	[200]
		$c = 5.16$		
$NiSn_{0.08}Sb_{0.92}$	AuSn, $P6_3/mmc$ (194)	$a = 3.9244(1)$	1.309	[201]
		$c = 5.1372(6)$		
$Ni_{1.25}Sn_{0.5}Sb_{0.5}$	Ni_2In, $P6_3/mmc$ (194)	$a = 4.040$	1.275	[51]
		$c = 5.151$		
$Ni_{13}ZnGe_8$	$Ni_{13}Ga_3Ge_6$, $P3_121$ (152)	$a = 7.8394(13)$	1.288	[127]
		$c = 15.1405(30)$		
$Pd_{13}In_{5.25}Sb_{3.75}$	$Pd_{13}Pb_9$, $C12_1/c1$ (15)	$a = 15.189(2)$	1.284	[202]
		$b = 8.799(1)$		
		$c = 13.602(2)$		
		$\beta = 123.83(1)$		
$Pd_{13}In_{2.4}Sn_{6.6}$	$Ni_{13}Ga_3Ge_6$, $P3_121$ (152)	$a = 8.7845$	1.287	[203]
		$b = 16.963$		
$PtBi_{0.5}Sb_{0.5}$	AuSn, $P6_3/mmc$ (194)	$a = 4.225$	1.298	[129]
		$c = 5.485$		
$PtPb_{0.5}Bi_{0.5}$	AuSn, $P6_3/mmc$ (194)	$a = 4.300$	1.274	[129]
		$c = 5.480$		
$Ti_2Ga_{0.92}Si_{0.08}$	Ni_2In, $P6_3/mmc$ (194)	$a = 4.527(1)$	1.220	[204]
		$c = 5.524(3)$		
$Zn_{0.5}Fe_{0.5}Sb$	AuSn, $P6_3/mmc$ (194)	$a = 4.380(2)$	1.307	[205]
		$c = 5.725(5)$		

B.5. Compounds with Different Type Structures

Table B.4.: Crystallographic data of compounds adopting structures with different aristotypes that were studied within this project. Superspace groups and their numbers are given in accordance with the lists by *van Smaalen and Stokes*[92;93].

Compound	structure type, space group	lattice parameters, Å	reference
$Ag_{9-x}Au_xIn_4$	Cu_9Al_4, $P\bar{4}3m$ (215)	$a = 9.8602(6)$	this study
$Au_9In_{4-x}Ga_x$	Cu_9Al_4, $P\bar{4}3m$ (215)	$a = 9.7954(2)$	[206]
$Au_{3.5}Cu_{3.5}In_3$	Cu_9Al_4, $P\bar{4}3m$ (215)	$a = 9.4799(6)$	this study
$Au_{4.7}Cu_{2.3}In_3$	Cu_9Al_4, $P\bar{4}3m$ (215)	$a = 9.61383(7)$	this study
$Cu_9In_{4-x}Ga_x$	Cu_9Al_4, $P\bar{4}3m$ (215)	$a = 9.0178(5)$	this study
$Cu_{3+x}In_ySb_{1-y}$	Mg_3Cd, $P6_3/mmc$ (194)	$a = 5.5482(3)$	this study
		$c = 4.3239(2)$	
$Cu_{11}In_2Sn$	$Cu_{11}In_2Sn$, $Ia\bar{3}d$ (230)	$a = 24.1095(3)$	this study
$Cu_3In_{0.17}Sn_{0.83}$	Cu_3Sn,	$a = 5.5190(11)$	this study
	$Xmcm(0\beta0)000$	$b = 4.7884(7)$	
	(51.1.10.11)	$c = 4.3411(9)$	
		$\beta = 0.1663(4)$	
$Cu_3In_{0.08}Sn_{0.92}$	Cu_3Sn,	$a = 5.513(6)$	this study
	$Xmcm(0\beta0)000$	$b = 4.765(3)$	
	(51.1.10.11)	$c = 4.337(4)$	
		$\beta = 0.1247(4)$	
$Cu_3In_{0.33}Sn_{0.67}$	Mg_3Cd, $P6_3/mmc$ (194)	$a = 5.5099(9)$	this study
		$c = 4.3214(5)$	
$Cu_3Sn_{0.2}Sb_{0.8}$	Cu_3Ti, $Pmmn$ (59)	$a = 4.3489(2)$	this study
		$b = 4.7833(2)$	
		$c = 5.5326(2)$	
$Cu_{3+x}Sn_{1-y}Sb_y$	Cu_3Sn,	$a = 5.5489(16)$	this study
	$Xmcm(0\beta0)000$	$b = 4.8019(12)$	
	(51.1.10.11)	$c = 4.3507(11)$	
		$\beta = 0.1662(12)$	